THESE

Pour obtenir le grade de
DOCTEUR de l'université Paul-Cézanne - Aix-Marseille III

préparée au laboratoire : **URFM – UR629 - INRA Avignon**

dans le cadre de l'Ecole Doctorale Sciences de l'Environnement

Spécialité : *Ecologie*

Par

Maxime Cailleret

Causes fonctionnelles du dépérissement et de la mortalité du sapin pectiné en Provence

ANNEXES

Table des matières

Annexe 1 ………………………………………………………………………….................... **5**

Effects of climate on diameter growth of co-occurring *Fagus sylvatica* and *Abies alba* along an altitudinal gradient.

Annexe 2 ………………………………………………………………………….................... **41**

Comparison of drought-induced decline and mortality processes on silver fir among three sites in Provence, south-east France.

Annexe 3 ………………………………………………………………………….................... **77**

Global change induces contradictory age effects on tree-ring growth sensitivity to climate.

Annexe 4 ………………………………………………………………………….................. **105**

How to predict drought-induced tree mortality from radial growth data?

Annexe 5 ………………………………………………………………………….................. **137**

Regulation of silver fir (*Abies alba* Mill.) transpiration during drought in relation to soil characteristics.

Annexe 6 ………………………………………………………………………….................. **175**

Partitioning of silver fir Leaf Mass Area (LMA) and Leaf Area (LA) variations, from organs to populations.

Annexe 7 ………………………………………………………………………….................. **205**

Modélisation du fonctionnement des sapins du Mont Ventoux.

Annexe 1

Effects of climate on diameter growth of co-occurring *Fagus sylvatica* and *Abies alba* along an altitudinal gradient

Cailleret M, Davi H.

INRA, URFM, UR 629, Domaine Saint Paul, Site Agroparc, F-84914 Avignon Cedex 9.

Publié dans *Trees, Structure and Functions*

Cailleret M, Davi H (2011)
Trees, 25, 265-276. DOI 10.1007/s00468-010-0503-0

Abstract

In high-elevation forests, growth is limited by low temperatures, while in Mediterranean climates drought and high temperatures are the main limiting factors. Consequently, the climate-growth relationships on Mont Ventoux, a mountain in the Mediterranean area, are influenced by both factors. Two co-occurring species were studied: silver fir (*Abies alba* Mill.) and common beech (*Fagus sylvatica* L.), whose geographical distribution depends on their low tolerance to summer drought at low altitude/latitude, and low temperatures (late frost and short length of the growing season) at high altitude/latitude. Firs and beeches distributed along an elevational gradient were investigated using dendroecological methods. Silver fir growth was found to be more sensitive to summer water stress than beech. On the other hand, beech growth was more impacted by extreme events such as the 2003 heat wave, and negatively related to earlier budburst, which suggests a higher sensitivity to late frost. These results are confirmed by the different altitudinal effects observed in both species. Beech growth decreases with altitude whereas an optimum of growth potential was observed at intermediate elevations for silver fir. Recent global warming has caused a significant upward shift of these optima. As found for the period 2000-2006, rising temperatures and decreasing rainfall may restrain growth of silver fir. If these trends continue in the future beech might be favored at low altitudes. The species will have a reduced capacity to migrate to higher altitudes due to its sensitivity to late frosts, although an upward shift of silver fir is likely.

Keywords: Growth; Altitude; *Abies alba*; *Fagus sylvatica*; Climate change; Drought

Introduction

Tree growth will be modified in response to climate change. It is now well established that warmer temperatures (Christensen et al. 2007) would increase tree growth, due to a lengthening of the growing season (e.g., Menzel and Fabian 1999; Bronson et al. 2009; Delpierre et al. 2009) and higher metabolic rates during winter and spring (Paulsen et al. 2000), especially at high altitudes/latitudes (Theurillat and Guisan 2002). A positive impact of elevated CO_2 on tree growth is also expected due to higher photosynthesis rates (Hyvönen et al. 2007), even if some experimental studies did not confirm this hypothesis (Handa et al. 2006). On the other hand, these positive effects may be moderated by the likely increase in autotrophic respiration due to higher temperatures, and by the predicted decline in summer precipitation in the south of Europe (Christensen et al. 2007). First, tree water deficit negatively affects tree-ring formation by inhibiting cell division and enlargement (Zweifel et al. 2006). Second, it reduces carbon assimilation via a stomatal control of photosynthesis and transpiration (Breda et al. 2006). In addition, an earlier budburst may increase the probability of late frost impact in temperate, boreal or mountainous zones (Hanninen 2006). All these phenomena impact physiological processes and thus stem radial growth and tree vigor (Dobbertin 2005). But as some contradictory effects are expected, co-occurring species with different functional strategies can exhibit different responses to global change (Büntgen et al. 2007; Green 2007).

Silver fir (*Abies alba* Mill.) and common beech (*Fagus sylvatica* L.) often co-occur in the mountain vegetation belt. In this paper we studied both species at their Southern Alps margin: on Mont Ventoux, a French mountain located in the Mediterranean area. In this ecosystem, silver fir and beech are recolonizing planted pine stands (Chauchard et al. 2007) and are undergoing rapid environmental changes because both warming and drought trends were considerable. During the twentieth century, warmer temperatures and nitrogen deposition has led to an increase in radial growth of silver fir (Bert 1992; Pinto et al. 2007) and beech (Badeau 1995). However, in the Mediterranean region, with the accumulation of summer droughts, new forest decline have also been observed (Jump et al. 2006; Sarris et al. 2007; Piovesan et al. 2008). On Mont Ventoux observed trends could be the consequence of the contradictory effects of both reduced frost and increased drought. Consequently, a better understanding of the species-specific effects of climate is needed to determine costs and benefits for beech and silver fir in this context and to predict future competitive ability.

The assessment of climate-growth relationships provides understanding of the effect of averaged climate and extreme events. To our knowledge, climatic responses of silver fir and beech have been analyzed many times, but separately (Bert 1992; Badeau 1995; Desplanque et al. 1998; Rolland et al. 2000; Dittmar et al. 2003; Lebourgeois et al. 2005; Manetti and Cutini 2006; Di Filippo et al. 2007; Lebourgeois 2007). The impact of extreme events has also been studied alone, for example by focusing on the consequences of the summer 2003, which impacted forest productivity throughout Europe (Ciais et al. 2005; Granier et al. 2007; Pichler and Oberhuber 2007). Assessing the variability of tree-ring components of silver fir and beech along an elevational gradient can consequently be useful to reveal different growth responses to climate, and their sensitivity to frost and drought (Guehl 1985; Badeau 1995; Dittmar et al. 2006; Geßler et al. 2007). With increasing altitude, reduced temperatures, shorter growing season, increased exposure to wind and reduced nutrient supply should negatively impact growth rates (Coomes and Allen 2007; Körner 2007). However, in the Mediterranean region where summer drought is the main limiting factor, low elevation sites may also be affected by declining precipitation.

The aims of this study were: (1) to describe if these co-occurring species are impacted in a same way by monthly-averaged climate and climatic events, by respectively analyzing climate-growth relationships and the effects of the 2003 heat wave for both species; (2) to examine the different altitudinal effects on tree growth and if the conclusion agrees with the first analysis; and (3) to investigate if recent climate change has differently impacted growth of both species according to altitude.

Materials and methods

Study site

The study was conducted on Mont Ventoux (44°11’N; 5°17’E), a calcareous mountain located in the southwestern Alps, 1909 m above sea level (a.s.l.). Originally forested, Mont Ventoux suffered massive deforestation from the 12th century onwards as the wood from the trees was used to serve the demands for shipbuilding, firewood and charcoal and because of grazing. In 1850, it was almost entirely deforested and mixed *Abies alba – Fagus sylvatica* forests were reduced to small forest islands. A decrease in grazing combined with reforestation efforts undertaken in the 20th century (using pines) made it possible for post-pioneers (*e.g. Sorbus aria*, *Acer opalus*) and shade-tolerant species (such as silver fir and beech*)* to gradually recolonize the planted stands. Substrates range between limestone lithosol to one meter deep colluvium. However, soil water content is probably low considering the percentage of coarse material (between 50 and 80%), high slope (25° on average) and water infiltration into the calcareous bedrock. On the north-facing slope of Mont Ventoux (weather station of Mont Serein, 1445 m a.s.l., 1993-2006), mean annual temperature has been 6.8°C. The distribution of rainfall (1300 mm on average) is characteristic of a Mediterranean climate: the driest season is summer and rainfall occurs mostly in autumn. The elevational effect on temperature on the studied gradient was assessed in 2007 and 2008 by five HOBO Pro V2 microloggers located at 995m, 1117m, 1225m, 1340m and 1485m. The number of late frost days was calculated from April to June. As the altitudinal effect on rainfall varies between years, we used longer data (2000-2005) from seven meteorological stations distributed throughout Mont Ventoux (100m, 300m, 430m, 792m, 1100m, 1445m, 1455m).

Study species

Silver fir *(Abies alba* Mill.) and common beech (*Fagus sylvatica* L.) are two shade-tolerant species which need high atmospheric humidity due to their weak tolerance to summer drought (Geßler et al. 2007; Lebourgeois 2007). In France, both species are distributed in mountainous regions (Pyrenees, Vosges, Jura, Massif-Central, Alps) while beech is found in plain in northern regions as well. Their ranges are currently expanding in mountainous regions due to pastoral abandonment and forest maturation (Chauchard et al. 2007). On Mont Ventoux, beech is present in the form of coppice or high forest, between 950 to 1500m a.s.l. on the north- and south- facing slopes (Ladier et al. 2007). On the northern slope fir is generally associated with beech. This affinity reveals that both species are generally influenced in the same way by environmental conditions. However, their wood production mechanisms belong to two different functional groups, and silver fir needles persist seven to nine years on the twig in contrast to deciduous beech. Concerning phenology, beech budburst on the study site generally begins two weeks earlier than silver fir.

Tree-ring processing

73 firs and 77 beeches were sampled along a continuous elevational transect from 970 to 1530m (a.s.l.) on the north-facing slope of Mont Ventoux. The continuous transect followed the same slope orientation (NNW) and was chosen to minimize non-climatic variations, such as soil heterogeneity and management. For the same goal, and to have a reasonable sample size for the dendroclimatic analysis, dominant and codominant trees were sampled, explaining

the variability in ages (Table 1). Suppressed trees were excluded from the study because of their high sensitivity to competition. For the analysis the individuals were ranged in five classes of increasing altitudes (F1-F5 for silver fir and B1-B5 for beech). Cores were extracted in autumn 2006 and 2007 with an increment borer, 1.3m above the ground and perpendicular to the slope to avoid compression wood (for silver fir) and tension wood (for beech). After preparation with a razor blade, cores were scanned at 1200dpi. Ring limits were pointed using the semi-automatical software CooRecorder v5.3 and coordinates were transcribed into the nearest 0.01mm ring-width using CDendro v5.3 (CDendro 5.3 & CooRecorder 5.3; Larsson L.A. et al. 2006; Cybis Elektronik & Data AB. Sweden). Individual series were checked for missing rings and dating errors and mean chronologies were calculated using CDendro v5.3. Classical dendrochronological parameters were respectively computed for all the individual series and for the mean chronologies (Fritts 1976). Mean sensitivity (MS) was calculated to characterize relative intensity of year-to-year changes in growth. Calculation of the first autocorrelation coefficient (A1) was made for each tree to assess the influence of the previous year's growth upon the current year.

To study growth trends, basal area increments (BAI, mm²) were calculated from ring widths (RW, mm) assuming a circular outline of stem cross-sections. When a core did not reach the pith, the total missing width was estimated using the curvature of the innermost rings of the sample. The number of years estimated to the pith is based on the growth rate after the missing segment (Esper et al. 2003). Age effect was removed using the mean regional age curve (RC) of BAI of both species. This theoretical growth curve is exclusively dependent on the cambial age of the tree and is assumed to be correct for a given species in a given area (Bert 1992; Esper et al. 2003). In addition to the study sampling, 227 firs cored in 2008 (Cailleret et al. submitted) and 84 beeches cored in 2007 close to the study site were used to process these curves. A mean radial growth index (GI) was calculated for each tree

$$GI = \sum_{t=1}^{t=n} \frac{BAI_{(x,t)}}{BAI_{(RC,t)}}$$

where $BAI_{(x,t)}$ and $BAI_{(RC,t)}$ are the BAI of the tree x at the cambial age t, and the corresponding theoretical value of BAI given by the regional curve. A GI superior to 1 indicates that the tree had a better growth than the average. The date effect, i.e. the effect of recent environmental changes, was also removed because RC was performed using both old and young trees, which have grown under different conditions, and not using old trees alone. This procedure makes it possible to test the effect of altitude but not to compare growth of both species.

Recent change of growth optima along the altitudinal gradient with date was assessed by comparing GI for the whole period (all years) and GI for the 2000-2006 period. Linear regressions between BAI and years were fitted for each individual and for the master chronology of both species to identify significant temporal growth trends between 2000 and 2006. Even though the regression included only seven points, a significant negative trend ($p<0.1$) is a sound indication of decline in tree growth (Pedersen 1998; Dobbertin 2005; Piovesan et al. 2008).

Climate-growth relationships

Analyses of the climate-growth responses were conducted using detrended series. Ring widths were first detrended with a negative exponential or linear function and then with a cubic spline with 50% frequency response for 75 years using the ARSTAN software (Cook 1985). Autoregressive modelling of residuals (ARMA) and bi-weight robust estimation of the mean were used to calculate chronology indices for each ring component. Pearson correlation coefficients between annual growth indices and monthly precipitation and temperatures were then calculated separately using the statistical software R (R for Windows version 2.8.0; R

Development Core Team 2008). Climate-growth relationships were calculated using meteorological data from Carpentras (99m a.s.l.), the closest station with long-term meteorological time series (1964-2006). Carpentras and Mont Ventoux differ in altitude but they belong to the same climate sub-unit according to monthly precipitation patterns as defined by Guiot (1986). Each growth index was related to monthly mean, maximum and minimum temperatures and monthly rainfall from the previous July to August of the growth year (i.e 14*4 variables). Consequently, current climate and climate feedback due to the previous year were taken into account.

Effect of budburst date on growth was studied by matching spring phenological data with the increment index for the year 2006. First, as spring phenology varies with altitude (Dittmar and Elling 2006), a potential budburst date for each elevational level was estimated as the average of observed dates for trees located at this level. Secondly, a "phenological discrepancy" (ΔBd) was calculated for each tree based on the difference between potential and observed date to determine which trees had an early budburst ($\Delta Bd<0$) and which had a delayed one ($\Delta Bd>0$). Finally, the difference between individual growth index and the average of indices of trees situated at the same level was calculated for each tree to extract elevational and current climate effects on growth. A growth index ratio superior to 0 indicated that this tree proportionally had a better increment in 2006 than its neighbours at the same elevational level. We then analysed if differences in growth between individuals are linked to differences in budburst dates and altitude using generalized linear models.

Results

Characteristics of the tree-ring chronologies

Numerical features of tree-ring chronologies are summarized in Table 1. Elevational levels were slightly different between silver fir and beech. For example, the range of F1 (silver fir of the lowest altitude class) was from 970 to 1040m a.s.l. whereas B1 (beech of the lowest altitude class) was from 1000 to 1100m a.s.l.. These differences do not reflect a differential distribution of each species on Mont Ventoux, but rather differences along the transect where trees were sampled. Ages were also heterogeneous, although beeches sampled were on average older than firs (88.2 to 72.6; $p=0.001$; unpaired t-test). Mean sensitivity (MS) was lower for silver fir (0.20 ± 0.04) than for beech (0.30 ± 0.05) and no statistical differences between elevational levels were found ($p>0.1$; unpaired t-test). First-order autocorrelation coefficients were high, not statistically different between silver fir and beech (0.63 and 0.67 respectively; $p=0.19$; $df=115$), and were also positively correlated with age ($r^2=0.47$ and $r^2=0.22$; $p<0.001$). The well-synchronization between chronologies of both species (RW; $r^2=0.41$), and the high mean series correlation ($r^2=0.58$ for silver fir; $r^2=0.52$ for common beech) indicated a common growth forcing.

Contrasting radial growth-climate relationships

Growth responses to climate showed species-specific differences (Table 2). While silver fir was only negatively affected by high temperatures during September of the previous year, negative correlations between beech growth and temperatures were significant for July and August. Moreover, a weak positive effect of rainfall was only found for beech at low altitudes, indicating a negative impact of previous summer drought. Winter conditions seemed to have no clear explanatory impact, except for beech with a negative effect of November temperatures at high altitude (B4 and B5), and a positive one at low altitude (B1). A positive effect of temperature was also found for silver fir in February of the current year. The effect of maximum temperatures in April on radial growth differed between the two species. Particularly at high elevation and for codominant trees (data not shown), positive responses were observed for silver fir in contrast to beech, which was negatively influenced by high temperatures in April. This effect can be linked to budburst, which largely depends on spring meteorological conditions. In 2006, differences in radial growth between trees were related to differences in budburst date. Beech trees with delayed leaf-out had better growth than those whose budburst was earlier whatever altitude, ($p<0.05$; Table 3). For silver fir, radial increment was slightly negatively related with a positive budburst discrepancy. This trend seemed to be stronger at low altitude (Table 3).

During the beginning of summer (May-June) beech radial growth was observed to be independent of rainfall except in B2; whereas a positive impact of May temperatures appeared at high altitude. For silver fir, growth was more dependent on summer drought, indicated by the positive correlations between growth indices and rainfall in June, July, and even in May for trees at low elevations. Silver fir growth was also negatively correlated with temperature, especially at low altitudinal sites.

Altitudinal effect on growth

In the years 2007 and 2008 mean temperatures decreased on the north-facing slope by 0.71°C for every 100m rise in altitude, and the mean number of spring frost days increased exponentially with up to 9.5 frost days per year at 1500m (a.s.l.) (Fig. 1a). For the period 2000-2005 spring and summer rainfall (March to August) increased in average 14mm per 100m (Fig. 1b). GI was used to analyze the altitudinal effect. Elevational effects on radial growth were different between species. For silver fir the maximum value was observed at an intermediate altitudinal level (F3) (mean GI = 1.60; Fig. 2a). Minima were observed for the low-elevational (F1) (0.74) and for the high-elevational level group (F5) (0.72). Growth indices of beech trees located at B2 were significantly different from those growing at higher altitude (B3, B4 and B5), but not to those located at B1 (Fig. 2b) indicating a global negative relationship between altitude and tree-ring growth.

Climate change and growth trends

Since 1964 there was a clear warming trend in mean annual temperatures ($r^2=0.60$, $p<0.001$), which corresponds to an increase of 0.4°C per decade and was more pronounced during summer (0.6 to 0.7°C by decade; Fig. 3). Since the 1980s this warming has been associated with a decrease in summer rainfall (Fig. 4).

The effects of altitude on growth (GI) in the 2000-2006 period differed from the period studied as a whole (Fig. 2a-2b). When comparing present and past growth (grey and black lines), an upward shift of growth potentials appears. For beech, lower GI values were found for trees at level B1, while differences between B2 and B3, B4 and B5 were not significant anymore (Fig. 2b). The upward shift was more obvious for silver fir (Fig. 2a). Growth optimum was still located at F3. Even if not significant, trees located at higher altitudes (F4 and F5) seemed to show higher GI values compared with those at lower altitudes (F1 and F2).

As in most of Europe, weather conditions in the 2003 summer on Mont Ventoux were exceptional. At the weather station of Mont Serein (1445m a.s.l.) temperatures during June till August were 3.3°C above average (19.3°C compared to 16°C). Rainfall corresponded to 67% of the mean (92.8mm compared to 138.8mm) but could have been partly counterbalanced by high rainfall in April (172.4mm compared to 124.1mm). However, in 2003 BAI of beech and silver fir was close to the average of the 2000-2006 period (respectively 102% and 104% compared to the mean; Fig. 4). Nevertheless, an important decrease in BAI was found in 2004, where silver fir and beech growth were 16% and 29% respectively below average compared to the reference period. A negative relationship between altitude and 2004 increment was observed for silver fir ($p<0.001$; $r=-0.43$) but not for beech ($p>0.1$). This growth decline does not only depend on a post-effect of 2003 drought, since meteorological conditions during the 2004 growing period were also particular. A dry period was recorded at the beginning of summer, with only 7.3mm of rainfall during June and July, instead of 86.7mm on average, but with normal temperatures.

Since the beginning of the 21th century there has been a significant decrease in BAI: 38 of the 73 firs (52%) had a negative slope over time, whereas only 5 trees had a positive slope (Table 4). This trend was also found for the master chronology whose slope was negative (BAI; -65.5mm^2/year; $p=0.006$). No significant trend was observed for the growth of 70% of the beeches (54 of 77), and 25% had a negative slope. The non-significant slope of the average chronology ($p=0.43$) emphasized these results.

Discussion

Growth of both co-occurring species

Values of mean sensitivity and of mean series correlation were high and in agreement with previous studies (Desplanque et al. 1998; Dittmar et al. 2003; Lebourgeois et al. 2005; Lebourgeois 2007), which demonstrated a high suitability for dendroclimatic analysis for both species (Table 1). Silver fir was observed to be less sensitive to environmental changes than beech, which is likely due to the persistence of needles in winter and to a higher maximal root depth (Stokes et al. 2007), yielding higher growth inertia.

High autocorrelation values indicated that the tree-ring width of both species was influenced by growth conditions of previous years (Table 1). High temperatures during July to

September of the previous year negatively impact wood production of the next year (Table 2), and more precisely earlywood production (Desplanque et al. 1998; Lebourgeois et al. 2005; Di Filippo et al. 2007), by changing the dynamic of carbohydrate storage, decreasing the root elongation and inducing leaf fall. Other mechanisms can also be envisaged such as delayed bud differentiation or abnormal losses of hydraulic conductivity (Selås et al. 2002; Lebourgeois 2007). No strong influence of winter conditions (January to March) was observed. Silver fir resists winter frosts well (Guehl 1985; Aussenac 2002), whereas beech develops mechanisms to recover hydraulic conductivity after winter cavitation (Cochard et al. 2001).

During the growing period, meteorological conditions differently impact the radial growth of both species. It is commonly accepted that high temperatures in April positively influence tree growth by causing earlier budburst and cambium activation, which lengthen the growing season and increase carbon assimilation (Davi et al. 2006; Delpierre et al. 2009). In this study, the same trend was observed for silver fir as in other dendroclimatic studies (Bert 1992; Manetti and Cutini 2006). However, for beech, whose budburst began two weeks before silver fir, a significant negative effect of maximal temperatures in April was observed for trees growing at high altitude. This report should not be attributed to different evolutionary adaptation along the altitudinal gradient due to the historical context of forests of Mont Ventoux. As silver fir and beech trees were reduced to small forest islands in 1850, due to large deforestation, genetic diversity should be reduced such as the adaptation processes since this period. The most convincing hypothesis to explain this result is that an earlier budburst increases the risk of late frost damage on open buds and young leaves. These spring frosts can kill leaves blocking carbon assimilation and thus provoking a decrease in radial growth (Dittmar et al. 2006; Awaya et al. 2009). Budburst could also be advanced due to high temperatures in autumn. According to Chuine and Cour (1999), the more chilling units are cumulated, the less forcing units are subsequently needed for budburst, which can also explain the negative relationship between November temperatures and beech growth at high altitude. This explanation is confirmed by the results obtained by comparing radial growth of trees with different budburst date (Table 3). In 2006, beeches whose leaf-out was earlier had lower growth than those whose budburst was later. Analysis of minimal temperatures at the meteorological station located at 1445m strengthens this conclusion. Negative temperatures were indeed recorded during 2006 beech budburst: six in April, four in May and one in June. To conclude, beech seems to be more sensitive to spring frost than silver fir.

The beginning of the current summer (May-July) differently affects wood production of both species. Drought during the first half of summer (May-July) negatively influenced ring-width of silver fir, particularly latewood (Lebourgeois 2007). These results can be explained by a high vulnerability to drought-induced cavitation, which involves a rapid and complete stomatal closure to avoid xylem embolism (Guicherd 1994; Aussenac 2002), and by an inhibition of cell division and enlargement (Zweifel et al. 2006). In contrast, beech growth indices were not related to summer rainfall and a positive effect of May temperatures was found at high altitude. This correlation with temperature shows that the conditions at the beginning of the growing season are important for cambial activity and wood production (Skomarkova et al. 2006; Čufar et al. 2008).

Mean radial increment variations with altitude were consistent with previous dendroclimatic results. Until the end of the 20th century, silver fir growth optimum was at intermediate altitudes (between 1140 and 1240m a.s.l.) with lower values at lower and higher elevation. For beech, growth changes along the elevational gradient were less clear. Tree-ring growth analysis seemed to indicate that the optimum was between 1100 and 1230m a.s.l., with a mean radial growth between 1000 and 1100m not significantly different from the optimum, while height growth patterns seemed more confused. Below 1000m, beech trees are very scattered. This under representation at lower elevations was probably due to low recolonization rates from upper refuge sites. Presence of beech down to an altitude of 800m is possible (Fig. 5). Coomes and Allen (2007) have recently reported a decrease in potential growth rate with altitude caused by reduced temperatures and shorter growing season. However, in their study water limitation at low elevations was not as important as on Mont Ventoux. In the Mediterranean region, where summer drought is the main growth limiting factor, trees located on low elevational sites may be more constrained than those on upper sites because of the positive effect of altitude on water availability: less evaporation and more precipitation (Fig. 1b).

Climate change effects

Climate in south-eastern France showed an increase in mean annual and especially summer temperatures since the 1960s, which was associated with a decrease in summer rainfall since the 1980s (Fig. 3). It is well known that global warming and nitrogen deposition have increased tree radial growth (Hyvönen et al. 2007). Constant age methods have demonstrated this increase for both species (Bert 1992; Badeau 1995). However, our results also show that the effect of altitude on radial growth has changed. For the 2000-2006 period, trees growing in high altitudinal sites showed a high increase in radial growth, whereas trees at lower elevations did not grow better. This shift in growth optima to higher altitudes is consistent with the upward shift of species range recently observed and attributed to global change (Beckage et al. 2008; Lenoir et al. 2008; Jump et al. 2009). The intensity of factors limiting growth at low elevation (drought) has increased, whereas those which restrict carbon assimilation at upper elevation sites (low temperatures) have decreased. However, this upward shift can be mitigated by species-specific effects. For example, at high elevations, changes in budburst date could be connected with changes in late frosts damage probabilities and in competitiveness, which could alter beech vitality

Since the beginning of 21^{st} century, with the increase in summer drought frequency and intensity, most of the silver firs showed a decline of their growth (Table 4) and vitality. In the worst cases this led to mortality. For beech no significant trend was evident in this study. Even if several authors have already found a decrease in beech growth at its southern range edge (Peñuelas and Boada 2003; Jump et al. 2006; Piovesan et al. 2008), beech is able to survive periods of reduced water availability (Dittmar et al. 2003), which also explains why other authors have found an increasing growth potential for beech (Geßler et al. 2007).

It is predicted that climate change will cause an increase in the frequency of extreme events, such as heat waves (Meehl and Tebaldi 2004). The 2003 summer was exceptional due to the intensity and duration of high temperatures (Schar et al. 2004; Rebetez et al. 2006). In France, the South-East was the region with the highest rainfall deficit (50 to 70% below average; Landmann et al. 2003). Nevertheless, no significant growth decrease was observed that year for both study species on Mont Ventoux. This result does not agree with studies on beech in Catalonia (Jump et al. 2006) or in north-eastern France (Granier et al. 2007) where tree growth was significantly reduced. The study of vegetative response to 2003 heat wave in the Swiss Alps revealed that trees located in the mountain zone (700m–1400m) showed a decrease in growth, whereas an increase was observed in the subalpine zone (1400m–2100m; Jolly et al. 2005). This demonstrates that the impact of these extreme events on radial growth depends on the site- and species-specific responses to climatic factors (Pichler and Oberhuber 2007). Lag-effects of this heat wave cannot be deduced in this study due to the occurrence of severe drought in spring 2004, in summer 2005 and 2006. Moreover post-drought growth reductions occurring the following year (2004) were more detectable in beech.

Probable modification of species' range

The elevational gradient can be schematized as a curve where the two major limiting factors progress exponentially with altitude (Fig. 5). The number of frost days and their intensity increase exponentially with the upward shift in altitude (Fig. 1a). As elevation decreases, the frequency, intensity and duration of summer drought increase exponentially due to the combination of rising temperatures and decreased rainfall (Fig. 1a and Fig. 1b). Therefore, the future distribution of both species can change. In Mediterranean area, rising temperatures and decreasing rainfall (4-27%) are predicted (Christensen et al. 2007). Along with these trends a growth decline is expected for silver fir, and the species could disappear at the lowest altitudes and on soils with low water content, replaced by more drought tolerant species such as *Fagus sylvatica, Quercus pubescens* or *Acer opalus* (Fig. 5). Beech vitality would probably be less effected, except if the expected increase in intensity, frequency and duration of heat-waves occur (Meehl and Tebaldi 2004). It is commonly accepted that both warming and a decrease in anthropogenic pressure may favor the upward expansion of species distribution. Although a rise of 70m in altitude has already been observed for beech in the Montseny Mountains (Peñuelas and Boada 2003), an upward shift of beech would be limited by the likely increase in late frost damage (Hanninen 2006; Augspurger 2009). At higher altitude silver fir could completely take advantage of higher carbon assimilation due to rising temperatures and lengthening of the growing season (winter and summer photosynthesis). Factors limiting its shift would be mainly seed dispersion, along with edaphic and topographic conditions. If climatic events are not taken into account silver fir is predicted to face higher risks than common beech (Ohlemüller et al. 2006). However, the probable increase in late frost and heat-wave frequency and intensity would put beech at a disadvantage. These results need to be completed by considering other dynamic processes (regeneration, herbivory, intra-and interspecific competition, seed production and dispersion), and can be mitigated in some sites by changes in soil with altitude.

Co-occurring species can show quite divergent responses to climate despite occupying nearby niches and can be differently impacted by environmental changes such as those induced by global change. Using tree rings as proxy of tree growth give interesting results but further research is needed to investigate these relationships for different-aged trees, and under others environmental conditions (with different growth-limiting factors).

Acknowledgements

The authors wish to thank Nicolas Mariotte, William Brunetto and Florence Courdier for their support in the field. We would also like to thank Philippe Dreyfus and Bruno Fady for reading and comments on the paper. We are very grateful to Julia Fady-Welterlen and May Myklebust for the English revision of the whole manuscript. Thanks are also due to anonymous reviewers for their useful comments. This study was supported by the French National Institute for Agronomical Research (ECOGER Project).

References

Augspurger CK (2009) Spring 2007 warmth and frost: phenology, damage and refoliation in a temperate deciduous forest. Funct Eco 23:1031-1039. doi: 10.1111/j.1365-2435.2009.01587.x

Aussenac G (2002) Ecology and ecophysiology of circum-Mediterranean firs in the context of climate change. Ann For Sci 59:823-832

Awaya Y, Tanaka K, Kodani E, Nishizono T (2009) Responses of beech (*Fagus crenata* Blume) stand to late spring frost damage in Morioka, Japan. For Ecol Manag 257:2359-2369. doi:10.1016/j.foreco.2009.03.028

Badeau V (1995) Etude dendroécologique du hêtre (Fagus sylvatica L.) sur les plateaux calcaires de Lorraine. Influence de la gestion sylvicole. PhD Thesis. Université de Nancy I Henry Poincaré. France.

Beckage B, Osborne B, Gavin DG, Pucko C, Siccama T, Perkins T (2008) A rapid upward shift of a forest ecotone during 40 years of warming in the Green Mountains of Vermont. PNAS 105:4197-4202

Bert GD (1992) Influence du climat, des facteurs stationnels et de la pollution sur la croissance et l'état sanitaire du sapin pectiné (*Abies alba* Mill.) dans le Jura. Etude phytoécologique et dendrochronologique. PhD Thesis. Université de Nancy I Henry Poincaré. France

Breda N, Huc R, Granier A, Dreyer E (2006) Temperate forests trees and stands under severe drought: a review of ecophysiological responses, adaptations processes and long-term consequences. Ann For Sci 63:625-644. doi:10.1051/forest:2006042

Bronson DR, Gower ST, Tanner M, Van Herk I (2009) Effect of ecosystem warming on boreal black spruce bud burst and shoot growth. Glob Change Biol 15:1534–1543. doi: 10.1111/j.1365-2486.2009.01845.x

Büntgen U, Franck CD, Kaczka RJ, Verstege A, Zwijacz-Kozica T, Esper J (2007) Growth responses to climate in a multi-species tree-ring network in the Western Carpathian Tatra Mountains, Poland and Slovakia. Tree Physiol 27:689-702

Cailleret M, Bert D, Davi H (submitted in Trees) Global change induces contradictory age effects on tree-ring growth sensitivity to climate.

Chauchard S, Carcaillet C, Guibal F (2007) Patterns of land-use abandonment control tree-recruitment and forest dynamics in Mediterranean mountains. Ecosystems 10:936-948

Christensen JH, Hewitson B, Busuioc A, Chen A, Gao X, Held I, Jones R, Kolli RK, Kwon WT, Laprise R, Magaña Rueda V, Mearns L, Menéndez CG, Räisänen J, Rinke A, Sarr A, Whetton P (2007) Regional Climate Projections. In : Solomon S, Qin D, Manning M et al. (ed) Climate Change 2007: The Physical Science Basis. Contribution of Working Group I to the Fourth Assessment Report of the Intergovernmental Panel on Climate Change Cambridge University Press, Cambridge, United Kingdom and New York, NY, USA.

Chuine I, Cour P (1999) Climatic determinants of budburst seasonality in four temperate-zone tree species. New Phytol 143:339-349

Ciais P, Reichstein M, Viovy N, Granier A, Ogee J, Allard V, Aubinet M, Buchmann N, Bernhofer C, Carrara A, Chevallier F, De Noblet N, Friend AD, Friedlingstein P, Grunwald T, Heinesch B, Keronen P, Knohl A, Krinner G, Loustau D, Manca G, Matteucci G, Miglietta F, Ourcival JM, Papale D, Pilegaard K, Rambal S, Seufert G, Soussana JF, Sanz MJ, Schulze ED, Vesala T, Valentini R (2005). Europe-wide reduction in primary productivity caused by the heat and drought in 2003. Nature 437:529-533

Cochard H, Lemoine D, Améglio T, Granier A (2001) Mechanisms of xylem recovery from winter embolism in *Fagus sylvatica*. Tree Physiol 21:27-33

Cook E (1985) A time series analysis approach to tree-ring standardization. PhD dissertation, University of Arizona, Tucson.

Coomes DA, Allen RB (2007) Effects of size, competition and altitude on tree growth. J Ecol 95:1084-1097

Čufar K, Prislan P, De Luis M, Gricar J (2008) Tree-ring variation, wood formation and phenology of beech (*Fagus sylvatica*) from a representative site in Slovenia, SE Central Europe. Trees 22:749–758. doi: 10.1007/s00468-008-0235-6

Davi H, Dufrêne E, Francois C, Le Maire G, Loustau d, Bosc A, Rambal S, Granier A, Moors E (2006) Sensitivity of water and carbon fluxes to climate changes from 1960 to 2100 in European forest ecosystems. Agric For Meteorol 141:35-56. doi:10.1016/j.agrformet.2006.09.003

Delpierre N, Dufrêne E, Soudani K, Ulrich E, Cecchini S, Boé J, François C (2009) Modelling interannual and spatial variability of leaf senescence for three deciduous species in France. Agric For Meteorol 149:938-948. doi:10.1016/j.agrformet.2008.11.014

Desplanque C, Rolland C, Michalet R (1998) Dendroécologie comparée du sapin blanc (*Abies alba*) et de l'épicéa commun (*Picea abies*) dans une vallée alpine de France. Can J For Res 28:737-748

Di Filippo A, Biondi F, Čufar K, de Luis M, Grabner M, Maugeri M, Saba EP, Schirone B, Piovesan G (2007) Bioclimatology of beech (*Fagus sylvatica* L.) in the Eastern Alps: spatial and altitudinal climatic signals identified through a tree-ring network. J Biogeogr 34:1873-1892. doi:10.1111/j.1365-2699.2007.01747.x

Dittmar C, Elling W (2006) Phenological phases of common beech (*Fagus sylvatica* L.) and their dependence on region and altitude in Southern Germany. Eur J For Res 125:181-188

Dittmar C, Fricke W, Elling W (2006) Impact of late frost events on radial growth of common beech (*Fagus sylvatica* L.) in Southern Germany. Eur J For Res 125:249-259

Dittmar C, Zech W, Elling W (2003) Growth variations of common beech (*Fagus sylvatica* L.) under different climatic and environmental conditions in Europe – a dendroecological study. For Ecol Manag 173:63-78

Dobbertin M (2005) Tree growth as indicator of tree vitality and if tree reaction to environmental stress: a review. Eur J For Res 124:319-333. doi:10.1007/s10342-005-0085-3

Fritts HC (1976) Tree-ring and climate, Academic, London.

Geßler A, Keitel C, Kreuzwieser J, Matyssek R, Seiler W, Rennenberg H (2007) Potential risks for European beech (*Fagus sylvatica* L.) in a changing climate. Trees 21:1-11. doi :10.1007/s00468-006-0107-x

Granier A, Reichstein M, Bréda N, Janssens IA, Falge E, Ciais P, Grünwald T, Aubinet M, Berbigier P, Bernhofer C, Buchmann N, Facini O, Grassi G, Heinesch B, Ilvesniemi H, Keronen P, Knohl A, Köstner B, Lagergren F, Lindroth A, Longdoz B, Loustau D, Mateus J, Montagnani L, Nys C, Moors E, Papale D, Peiffer M, Pilegaard K, Pita G, Pumpanen J, Rambal S, Rebmann C, Rodrigues C, Seufert G, Tenhunen J, Vesala T, Wang Q (2007) Evidence for soil water control on carbon and water dynamics in European forests during the extremely dry year: 2003. Agric For Meteorol 143:123-145. doi:10.1016/j.agrformet.2006.12.004

Green DS (2007) Controls of growth phenology vary in seedlings of three, co-occurring ecologically distinct northern conifers. Tree Physiol 27:1197-1205. doi:10.1093/treephys/27.8.1197

Guehl JM (1985) Etude comparée des potentialités hivernales d'assimilation carbonée de trois conifères de la zone tempérée (*Pseudotsuga menziesii* Mirb., *Abies alba* Mill. et *Picea excelsa* Link.). Ann For Sci 42:23-38

Guicherd P (1994) Water relations of European silver fir (*Abies alba* Mill.) in 2 natural stands in the French Alps subject to contrasting climatic conditions. Ann For Sci 51:599-611

Guoit J. (1986) Sur la détermination de régions climatiques quasi-homogènes. Revue de Statistiques Appliquées. 34:15-34

Handa T, Körner C, Hättenschwiler S (2006) Conifer stem growth at the altitudinal treeline in response to four years of CO2 enrichment. Glob Change Biol 12:2417-2430. doi:10.1111/j.1365-2486.2006.01258.x

Hanninen H (2006) Climate warming and the risk of frost damage to boreal forest trees: identification of critical ecophysiological traits. Tree Physiol 26:889-898

Hyvönen R, Ågren GI, Linder S, Persson T, Cotrufo MF, Ekblad A, Freeman M, Grelle A, Janssens IA, Jarvis PG, Kellomäki S, Lindroth A, Loustau D, Lundmark T, Norby RJ, Oren R, Pilegaard K, Ryan MG, Sigurdsson BD, Strömgren M, van Oijen M, Wallin G (2007) The likely impact of elevated [CO_2], nitrogen deposition, increased temperature and management on carbon sequestration in temperate and boreal forest ecosystems: a literature review. New Phytol 173:463-480

Jolly WM, Dobbertin M, Zimmermann NE, Reichstein M (2005) Divergent vegetation growth responses to the 2003 heat wave in the Swiss Alps. Geophys Res Lett 32:L18409. doi:10.1029/2005GL023252

Jump AS, Hunt JM, Peñuelas J (2006) Rapid climate change-related growth decline at the southern range edge of *Fagus sylvatica*. Glob Change Biol 12:2163-2174. doi:10.1111/j.1365-2486.2006.01250.x

Jump AS, Mátyas C, Peñuelas J (2009) The altitude-for-latitude disparity in the range retractions of woody species. Trends Ecol Evol 24:694-701. doi:10.1016/j.tree.2009.06.007

Körner C (2007) The use of 'altitude' in ecological research. Trends Ecol Evol 22:569-574

Ladier J, Dreyfus P, Reboul D (2007) La place du hêtre en région méditerranéenne. RDV techniques ONF HS (2):105-111

Landmann G, Bréda N, Houllier F, Dreyer E, Flot JL (2003) Sécheresse et canicule de l'été 2003 : quelles conséquences pour les forêts françaises ? Rev For Fra LV-4:299–308

Lebourgeois F (2007) Climatic signal in annual growth variation of silver fir (*Abies alba* Mill.) and spruce (*Picea abies* Karst.) from the French Permanent Plot Network (RENECOFOR). Ann For Sci 64:333-343

Lebourgeois F, Bréda N, Ulrich E, Granier A (2005) Climate-tree-growth relationships of European beech (*Fagus sylvatica* L.) in the French Permanent Plot Network (RENECOFOR). Trees 19:385-401

Lenoir J, Gégout JC, Marquet PA, de Ruffray P, Brisse H (2008) A significant upward shift in plant species optimum elevation during the 20th century. Science 320:1768-1771

Manetti MC, Cutini A (2006) Tree-ring growth of silver fir (*Abies alba* Mill.) in two stands under different silvicultural systems in central Italy. Dendrochronologia 23:145-150

Meehl GA, Tebaldi C (2004) More intense, more frequent, and longer lasting heat waves in the 21st century. Science 305:994-997

Menzel A, Fabian P (1999) Growing season extended in Europe. Nature 397:659-659

Ohlemüller R, Gritti ES, Sykes MT, Thomas CD (2006) Quantifying components of risk for European woody species under climate change. Glob Change Biol 12:1788-1799. doi: 10.1111/j.1365-2486.2006.01231.x

Paulsen J, Weber UM, Körner C (2000) Tree growth near treeline: abrupt or gradual reduction with altitude? Arc Ant Alpine Res 32:14-20

Pedersen BS (1998) The role of stress in the mortality of Midwestern oaks as indicated by growth prior to death. Ecology 79:79-93

Peñuelas J, Boada M (2003) A global change-induced biome shift in the Montseny mountains (NE Spain). Glob Change Biol 9:131-140. doi:10.1046/j.1365-2486.2003.00566.x

Pichler P, Oberhuber W (2007) Radial growth response of coniferous forest trees in an inner Alpine environment to heat-wave in 2003. For Ecol Manag 242:688-699. doi:10.1016/j.foreco.2007.02.007

Pinto PE, Gégout JC, Hervé JC, Dhôte JF (2007) Changes in environmental controls on the growth of *Abies alba* Mill. in the Vosges Mountains, north-eastern France, during the 20th century. Glob Ecol Biogeogr 16:472-484

Piovesan G, Biondi F, Di Filippo A, Alessandrini A, Maugeri M (2008) Drought-driven growth reduction in old beech (*Fagus sylvatica*) forests of the central Apennines, Italy. Glob Change Biol 14:1265-1281

Rebetez M, Mayer H, Dupont O, Schindler D, Gartner K, Kropp JP, Menzel A (2006) Heat and drought 2003 in Europe : a climate synthesis. Ann For Sci 63:569-577. doi:10.1051/forest:2006043

Rolland C, Desplanque C, Michalet R, Schweingruber FH (2000) Extreme tree-rings in Spruce (*Picea abies* Karst.) and Fir (*Abies alba* Mill.) stands in relation to climate, site, and space in the southern French and Italian Alps. Arct Ant Alpine Res 32:1-13

Sarris D, Christodoulakis D, Körner C (2007) Recent decline in precipitation and tree growth in the eastern Mediterranean. Glob Change Biol 13:1187-1200. doi: 10.1111/j.1365-2486.2007.01348.x

Schär C, Vidale PL, Lüthi D, Frei C, Häberli C, Liniger MA, Appenzeller C (2004) The role of increasing temperature variability in European summer heatwaves. Nature 427:332-336

Selås V, Piovesan G, Adams JM, Bernabei M (2002) Climatic factors controlling reproduction and growth of Norway spruce in southern Norway. Can J For Res 32:217-225

Skomarkova MV, Vaganov EA, Mund M, Knohl A, Linke P, Boerner A, Schulze ED (2006) Inter-annual and seasonal variability of radial growth, wood density and carbon isotope ratios in tree rings of beech (*Fagus sylvatica*) growing in Germany and Italy. Trees 20:571-586

Stokes A, Ghani MA, Salin F, Danjon F, Jeannin H, Berthier S, Kokutse AD, Frochot H (2007). Root morphology and strain distribution during tree failure on mountain slopes. In: Stokes A (ed) Eco- and ground bio-engineering: The use of vegetation to improve slope stability. Development in Plant and Soil Sciences. Springer, Netherlands, pp165-173

Theurillat JP, Guisan A (2002) Potential impact of climate change on vegetation in the European Alps: a review. Climatic Change 50:77-109

Zweifel R, Zimmermann L, Zeugin F, Newbery DM (2006) Intra-annual radial growth and water relations of trees: implications towards a growth mechanism. J Exp Bot 57:1445-1459. doi:10.1093/jxb/erj125

Figures

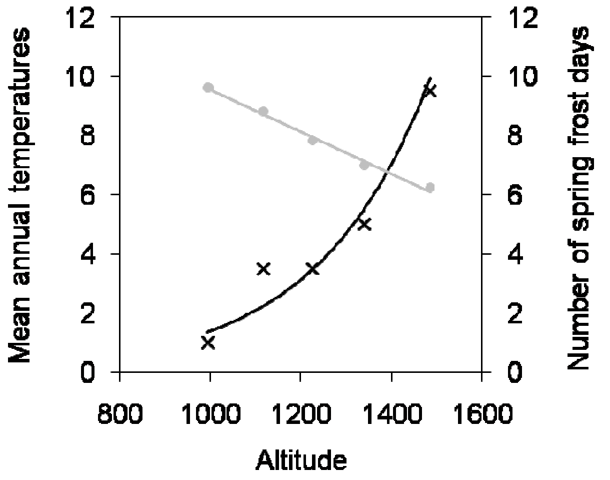

Fig. 1a: Altitudinal effect on mean annual temperature (grey circles) and on the number of spring frost days (black crosses) in 2007 and 2008 along the gradient studied on the north-facing slope of Mont Ventoux. The number of spring frost days was calculated as the average of the number of frost days between April and June for the years 2007 and 2008. The slope of the linear regression between mean temperature and altitude is –0.71°C/100m.

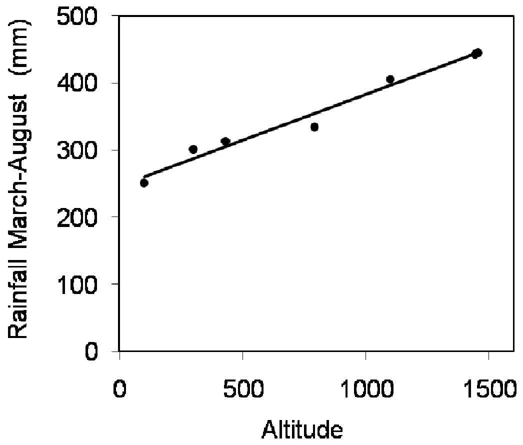

Fig. 1b: Elevational effect on spring and summer (March to August) rainfall on the Mont Ventoux for the period 2000-2005. The slope of the linear regression between rainfall and altitude is +14mm/100m.

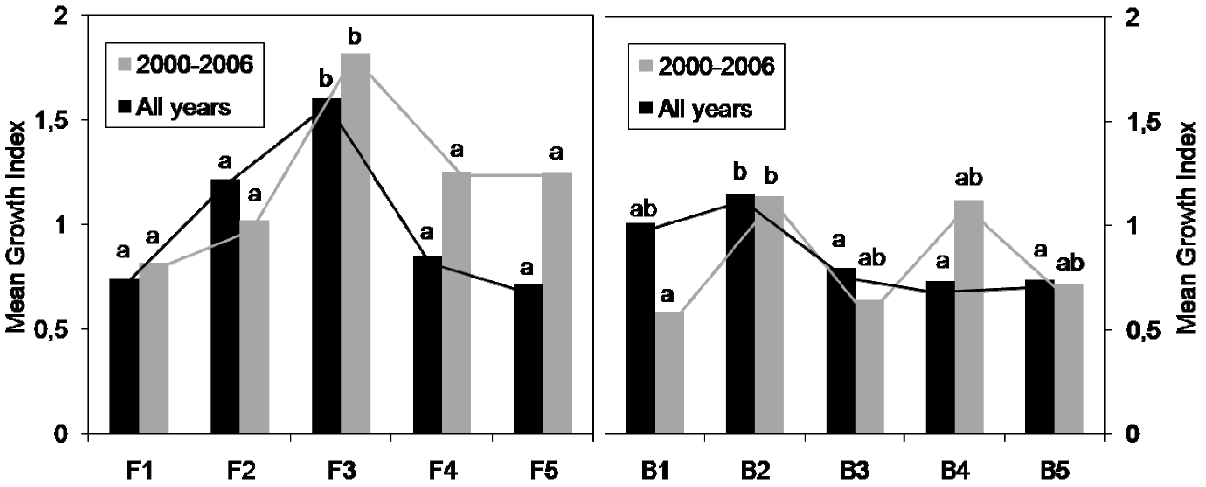

Fig. 2: Altitudinal effect on predicted mean annual growth index of *Abies alba* (a) and *Fagus sylvatica* (b) for the whole period studied (black histogram) and for the period 2000-2006 (grey histogram). Elevational levels are abbreviated as in Table 1. Different letters indicate significant differences between means for the same period (p<0.1, Tukey's HSD).

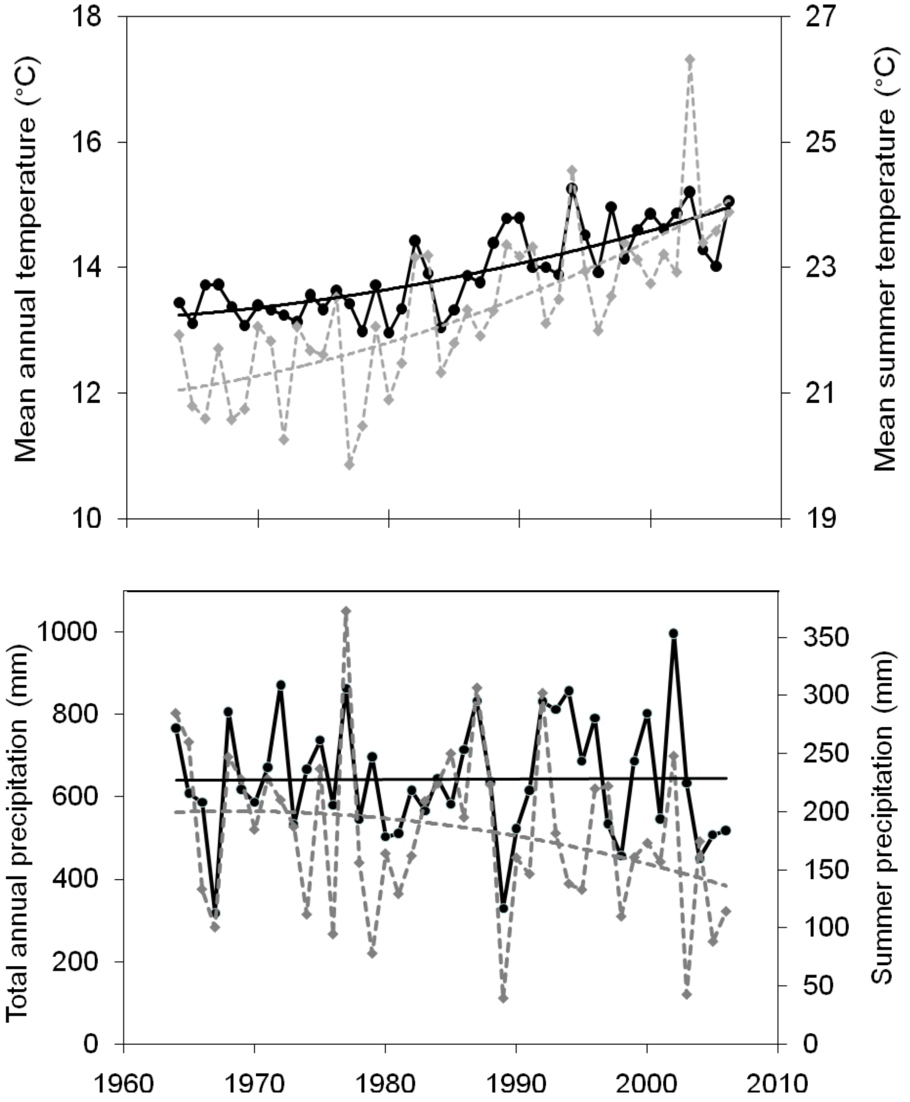

Fig. 3: Climate trends in the studied area (measured at the Carpentras meteorological station at 99 m) between 1964 and 2006. Mean annual (in black) and mean summer (June to August; in grey) temperature increases were statistically significant (p<0.1). The decrease in summer rainfall (in grey) was significant at the p<0.1, while no trend appeared for annual rainfall (in black).

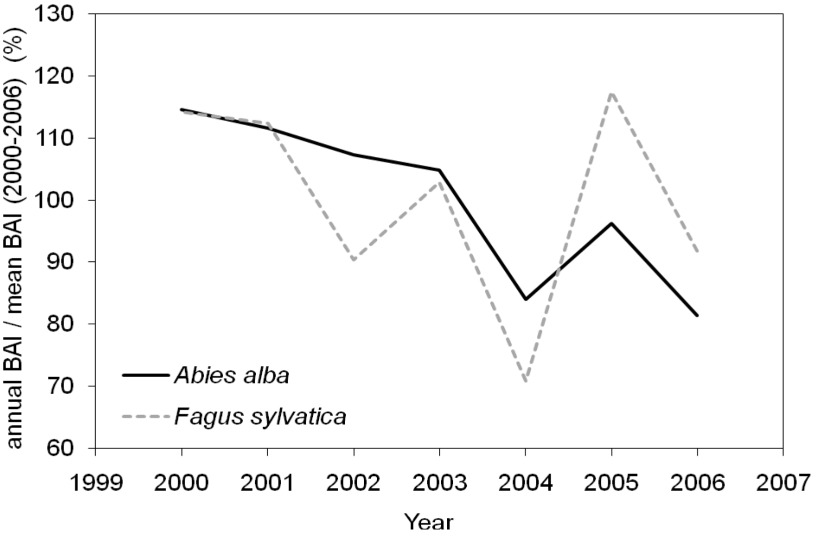

Fig. 4: Temporal trend in mean annual growth for *Abies alba* (solid line) and *Fagus sylvatica* (grey dashed line) between 2000 and 2006. To compare both species, basal area increment values were standardized by dividing them by mean basal area increment during this period.

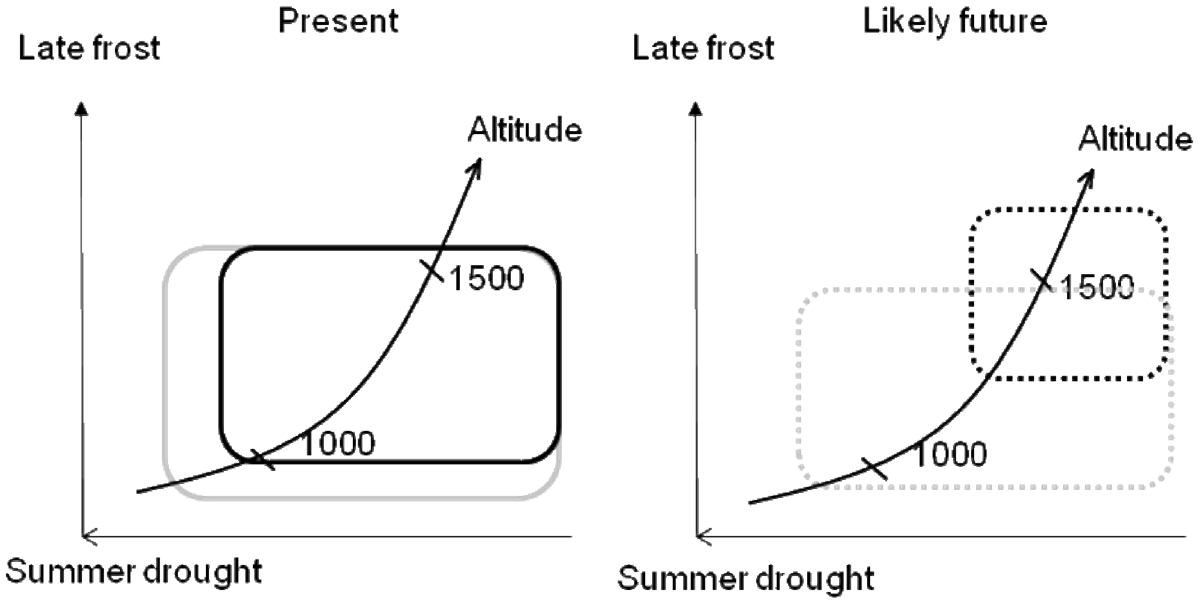

Fig. 5: Present (left: continuous rectangle) and likely future (right: dashed rectangle) distribution range of silver fir (black) and common beech (grey). The two major limiting factors are late frost (number and/or intensity), and summer drought (frequency, intensity and/or duration). The curve is the elevational gradient studied.

Table 1

Characteristics of selected elevational levels (F1 and B1: low-altitude to F5 and B5: high altitude) and statistics for tree-ring chronologies (mean followed by standard deviation in parentheses).

		Altitude (m)	Mean Altitude (m)	N	Age (years)	Height (m)	MS	A1	RW (mm)	BAI (mm²)	GI
Silver fir ***Abies alba***	**TOTAL**	**970-1530**	**1214.5 (152.4)**	**73**	**72.6 (35.3)**	**13.1 (3.5)**	**0.20**	**0.63**	**1.84 (0.66)**	**767.4 (493.0)**	**1.06 (0.65)**
	F1	970-1040	1005.8 (26.9)	13	56.1 (22.5)	10.9 (2.9)	0.21	0.54	1.71 (0.48)	511.4 (259.2)	0.74 (0.40)
	F2	1040-1140	1096.7 (28.2)	14	57.8 (13.0)	12.0 (2.5)	0.20	0.61	1.91 (0.55)	744.8 (378.2)	1.22 (0.66)
	F3	1140-1240	1193.2 (28.2)	13	54.5 (22.2)	14.9 (3.2)	0.19	0.56	2.59 (0.79)	1185.9 (724.1)	1.60 (0.83)
	F4	1240-1350	1285.9 (34.9)	16	80.5 (36.5)	14.1 (3.3)	0.20	0.63	1.76 (0.55)	787.9 (459.1)	0.85 (0.36)
	F5	1350-1530	1428.4 (50.2)	17	105 (41.2)	13.2 (4.3)	0.20	0.77	1.36 (0.26)	633.3 (340.7)	0.72 (0.30)
Common beech ***Fagus sylvatica***	**TOTAL**	**1000-1520**	**1260.7 (149.5)**	**77**	**88.2 (19.1)**	**12.2 (2.2)**	**0.30**	**0.67**	**1.01 (0.32)**	**295.7 (154.1)**	**0.90 (0.42)**
	B1	1000-1100	1042.4 (30.0)	15	97.3 (8.1)	12.1 (1.2)	0.31	0.72	0.99 (0.24)	333.5 (157.8)	1.01 (0.43)
	B2	1100-1230	1177.1 (37.0)	18	68.2 (28.8)	10.7 (2.0)	0.30	0.58	1.32 (0.36)	360.8 (171.3)	1.15 (0.44)
	B3	1230-1330	1278.2 (26.5)	16	93.9 (8.1)	12.5 (2.9)	0.30	0.68	0.89 (0.29)	268.2 (157.3)	0.79 (0.42)
	B4	1330-1420	1375.1 (31.4)	13	94.1 (6.8)	13.3 (1.5)	0.30	0.68	0.89 (0.24)	265.9 (135.1)	0.73 (0.37)
	B5	1420-1520	1461.3 (38.6)	15	91.7 (10.6)	12.9 (1.9)	0.32	0.69	0.89 (0.24)	253.7 (112.4)	0.74 (0.31)

N: Number of trees selected; **MS** : Mean Sensitivity; **RW**: Mean Ring-Width; **BAI**: Mean Basal Area Increment; **GI**: Mean Radial Growth Index; **A1**: First-order Autocorrelation coefficient.

Table 2

Summary of the significant correlation between monthly meteorological data and annual growth index of the five elevational level chronologies. + expresses a positive relation; – indicates an inverse relation. Grey and white boxes indicate that the corresponding correlation coefficient attains 95% and 90% of probability respectively. N1 corresponds to the lowest elevational level, and N5 to the highest altitudinal level.

		Abies alba														*Fagus sylvatica*													
		Year n-1						Year n								Year n-1						Year n							
		J	A	S	O	N	D	J	F	M	A	M	J	J	A	J	A	S	O	N	D	J	F	M	A	M	J	J	A
P	N5					+			-					+										+					
	N4					+							+	+										+					
	N3												+	+										+					
	N2					+						+	+	+		+				+							+		
	N1											+	+	+		+				+									
Tmean	N5			-					+		+					-	-			-					-	+			
	N4			-					+		+			-		-	-			-									
	N3			-					+					-			-												
	N2												-	-			-												
	N1			-									-	-		-	-			+				-					
Tmax	N5			-					+		+					-	-	+		-					-				
	N4			-					+		+			-		-	-			-					-				
	N3			-							+		-	-			-								-				
	N2			-									-	-			-										-		
	N1			-									-	-		-	-							-					
Tmin	N5		-	-				-								-	-			-						+			
	N4			-					+							-	-									+			
	N3			-										-			-												
	N2		-											-															
	N1													-						+	+								

Table 3

Coefficients of the best generalized linear models chosen by AIC in a stepwise algorithm. Models were fitted on individual Growth Index Difference for *Abies alba* and *Fagus sylvatica*.

Species	**Variables**	**Estimate**	**Error**	**t value**	**Pr(>|t|)**
	Intercept	-6.37e-2	0.268	-0.251	0.802
Abies alba	ΔBd	-0.131	7.12e-2	-1.842	0.071
AIC=20.31	Altitude	4.97e-5	2.17e-4	0.228	0.820
	ΔBd*Altitude	1.13e-4	6.19e-5	1.823	0.074
Fagus sylvatica	Intercept	-7.55e-17	2.77e-2	-2.73e-15	1.000
AIC=-9.06	ΔBd	2.32e-2	1.04e-2	2.224	0.030

Table 4

Comparison of linear Basal Area Increment trend for the 2000-2006 period.

	Individual chronologies		Master chronology	
Species	Range of slopes	Direction	Slope	P (linear regression)
Abies alba	-355 to +136	38 (-), 30 (=), 5 (+)	-65.5	0.006
Fagus sylvatica	-69 to +145	19 (-), 54 (=), 4 (+)	-10.7	0.43

Slope values are in mm²/year.

Direction of slopes: (-) / (+), significant negative / positive trend ($p<0.1$); (=), no significant trend.

Supplementary material

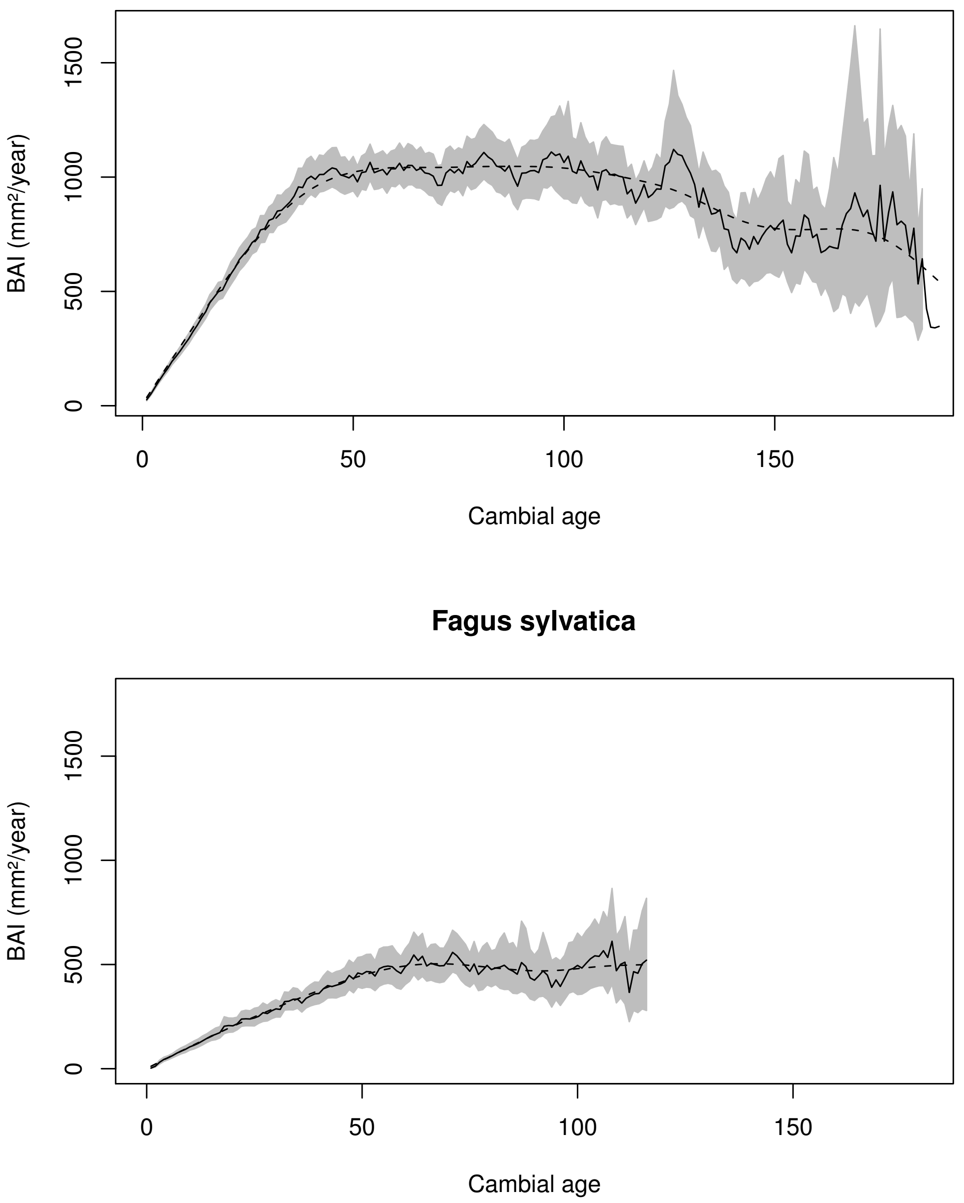

Figure S1: Mean regional age curve of silver fir (up; *Abies alba* Mill.) and common beech (bottom; *Fagus sylvatica* L.) on Mont Ventoux. The area in grey corresponds to the 95% confidence interval calculated with bootstrap methods.

Annexe 2

Comparison of drought-induced decline and mortality processes on silver fir among three sites in Provence, south-east France.

Cailleret M[1], Nourtier M[2], Amm A[1], Gillmann M[1], Davi H[1]

[1]INRA, URFM, UR 629, Domaine Saint Paul, Site Agroparc, F-84914 Avignon Cedex 9.

[2]INRA, EMMAH, UMR 114 Domaine Saint Paul, Site Agroparc, F-84914 Avignon Cedex 9.

En préparation pour *Annals of Forest Science*

Abstract

Tree decline and mortality are ones of the main processes which affect forest functioning and dynamics that explain their increasing interest in ecological studies. In the Mediterranean area many dieback phenomena were reported during last decades. They are likely due to increases in summer drought severity, and thus especially concern drought-sensitive species such as silver fir (*Abies alba* Mill.). Factors involved in determining this mortality were examined at plot and tree level using altitudinal gradients localized on three sites in the south-eastern part of France. Radial growth trends of dead and healthy trees and of trees with crown damages were compared by dendrochronological analysis.

At the tree scale, individuals with higher inter-annual variability in growth were more prone to die. On two sites, dead trees had lower growth rates all their life time. However, on the other site, their juvenile growth rate was higher on average. In the same way, trees with crown damages showed different trends in radial growth than dead trees and may had higher rates than healthy trees.

These results showed that tree mortality probability was not always related with crown damages and low growth rates, indicating a trade-off between vulnerability and growth. The patchy mortality and the slight effect of altitude on tree vulnerability underscore the importance of edaphic and topographic conditions on the mortality process, and highlight the need to use tree structural traits as indicators of vitality.

Introduction

Tree decline and mortality are main processes in forest functioning and dynamics. As it impacts forest regeneration, timber production, carbon sequestration and biodiversity, an increasing number of studies were done on this topic, but our knowledge on the processes leading to tree mortality is still limited (Allen *et al.* 2010). Decline in tree vitality can be reversible but in the worst cases, when the stress is too long, intense, or occurs too frequently, the process becomes irreversible leading to tree death. Natural tree mortality can be split into two categories: regular and irregular mortality (Hawkes 2000). The regular mortality results either from competition for light, water and soil nutrients; or from a decrease in hydraulic conductance due to tree height. In contrast, irregular mortality is caused by random events or hazards such as insect attacks, fire, wind, snow, rock falls, browsing and severe drought, all of them being able to interact. A strong increase in the number of mortality reports was observed since 40 years (Allen et al. 2010) which is mainly due to changes in climatic conditions. The increase in background mortality was recently assigned to temperatures rising (van Mantgem et al. 2009), but massive diebacks were usually directly or indirectly induced by drought (Peñuelas et al., 2001; Bréda et al., 2006).

As climatic change might increase the frequency and intensity of drought, water-limited areas were expected to be concerned by decline in tree vitality, and mortality events. Dry zones of North-America already experienced high mortality rates (Adams et al. 2009; Mc Dowell et al. 2008). Similarly, die-off and decline of forests were reported after severe droughts in European Mediterranean bioclimate (Carnicer et al. 2011) linked with tree growth decrease (Jump et al. 2006; Sarris et al., 2007; Cailleret and Davi, 2010). As climate is predicted to be hotter and dryer in the future (Somot et al., 2008), we can expect that massive diebacks would occur more frequently and would affect more species and larger forest areas.

This decrease in water availability during the growing period strongly affects drought-sensitive species. The *Abies genus* is an interesting study case for mortality since this keystone species, economically important, is especially sensitive to drought. Since the beginning of the 21th century, high rates of mortality and crown defoliation have already been observed for this *genus* on the southernmost European forests. In Spain, the relict *A. pinsapo* species was declining (Linares et al. 2009b), while many *A. cephalonica* died in Greece due to a severe drought in 2000 (Tsopelas et al. 2004). Concerning silver fir (*Abies alba* Mill.), all its xeric range was concerned by the phenomenon (Macias et al. 2006; Oliva and Colinas 2009; Ficko et al. 2010).

To better understand how interacts all the factors leading to decline and death, a first step is to achieve a reliable indicator of tree vitality. Radial growth was commonly used as it is very well related with carbon assimilation and the drought level experienced by the tree (Dobbertin 2005). As an example, tree mortality can be predicted by models using radial growth data with a respectable performance (Cailleret and Davi submitted, Wunder et al. 2006). Diameter increment was easily assessed with surveys of tree diameter or tree-ring width measurements. Considering radial growth as a reliable indicator, we compared the performance of two other variables commonly used: the sapwood area and the crown condition. Sapwood area (SA) can approximates tree vitality because it is the area of living wood which contains carbohydrates reserves, and the area of functional xylem conducting the sapflow. Higher is the SA, higher is the hydraulic conductance within the tree, and we commonly assumed that higher is the leaf area. Tree vigour can also be estimated by assessing crown damage (De Vries 2000; Zierl 2004). Defoliation, low needle retention and chlorosis were usually reported as common decline symptoms in coniferous trees (Breda et al. 2006). To our knowledge no comparative analysis was made between these three vitality indicators by gathering both spatial and temporal analysis. If sapwood area was very well related with growth trends for studies with long-term growth decline (Becker 1987; Bert and Becker 1990), the relationship can changed for a quick decline in tree vitality due to multi-year droughts. Concerning crown condition, temporal surveys of defoliation gave suitable indications on changes in tree vitality (temporal analysis); but few studies compared the growth of trees with different crown damages (spatial analysis).

A second task is to use these indicators to get information on which areas or trees are more prone to decline or to die. Different biotic and abiotic factors predispose a tree to mortality. For drought-induced dieback, we commonly accept that higher risk was observed on dry stations, i.e. at low latitude, low altitude, on shallow or karstic soils, with high slope or located on south-facing slopes (Manion 1981). In the same way, depending on the infestation degree, a decrease in tree vitality can be provoked by pathogens such as fungi which induced a decrease in water uptake, by bark beetle which amplified hydraulic failure when water transport is interrupted by symbiotic fungi inoculated into trees and which fed phloem, or mistletoe which used tree sap flow for its own photosynthesis. Different relationships can be found between tree size and mortality rates. It was negative in an undisturbed environment (Coomes and Allen 2007), while big trees can be more affected by extreme events such as storms. In the same way, it is commonly accepted that tree survival probability increase with large diameter increment (Cailleret and Davi submitted), but some studies recently showed a trade-off between tree growth rate and longevity (Black et al. 2008; Bigler et al. 2009). This trade-off is commonly found on coniferous species and is likely due to differences in tree structure (e.g. total leaf area; Kaufmann 1996) induced by current and previous spatial heterogeneity in water and light availabilities. Consequently, all these factors require being studied and organized into a hierarchy that strongly depends on the scale of interest. Indeed, different spatial scales can be studied: from the region to the grove, and a high issue concerned how and why there is a large spatial variability in tree vitality in the case of a patchy mortality.

Experiments carrying out tree mortality at several spatial scales will contribute in a better understanding of the complexion of causes determining tree decline. This knowledge might be useful to decide between the two main hypotheses in explaining the tree mortality: the carbon starvation versus hydraulic failure (see Mc Dowell 2011 for a review). It can also help for improving adapted management at stand (to decide which tree should be thinned) and at watershed levels (to choice where a species or a provenance might be planted).

In this paper we compared the decline and mortality processes of silver firs on three Mediterranean mountains located in Provence, south-eastern France, to assess: (1) what kind of indicator should be used to characterize tree vitality?, (2) which factors predispose and incite trees to decline or die?, (3) if mortality and decline processes are directly related.

Material and Methods

This study was conducted on three Mediterranean mountains in Provence, south-eastern France: Mont Ventoux, Issole forest and Vésubie (Fig 1). Sites were selected to represent contrasted climatic and edaphic conditions in order to study different temporal declining processes. At comparable altitudes, mean annual temperatures in Vésubie (1242m above sea level) were respectively above 1.2°C and 1.4°C than temperatures in Issole (1281m a.s.l.) and on Mont Ventoux (1225m a.s.l.) for the period 1964-2009. Even if the magnitude differed, this trend was constant whatever the season. Concerning annual rainfalls, climate was wetter on Mont Ventoux (1126mm) following by Vésubie (954mm) and Issole (856mm). But this order was reversed when considering summer rainfalls: 243mm for Mont Ventoux, 217mm in Issole and 194mm on Vésubie. In the same way, strong differences in soil properties induced inter-sites changes in the amount of water available during the growing season. In Vésubie the mother bedrock was a sandstone schist, while it was calcareous clay in Issole and entirely calcareous on Mont Ventoux. Soils on the last site were karstic, leading in a likely higher water infiltration than in Issole and Vésubie which was intensified by the high slope (between 23% and 47%).

On each site, respectively five, five and six plots located along an altitudinal gradient were studied considering that a downward shift in altitude approximates climate change, i.e. decreases in rainfalls and rising temperatures (Korner 2007; Cailleret and Davi 2011). Elevational transects were located on the northern slopes of the mountains following the same northern exposure (between ENE and WNW). The plots were installed to cover all the distribution range of silver fir from low (Dvx1, Diss1, Dves1) to high altitudes (Dvx5, Diss5, Dves5). Hobos meteorological stations were installed on the plots in 2008 and 2009, to assess the elevational effect on temperatures. On Mont Ventoux, two others stations were also used at 1225m and 1485m a.s.l. Firstly, Dvx2 and Diss1 were cooler than expected by linear regression models. Differences in topographic situations explained this inversion in thermal gradient (Cailleret 2011). Thus, these both measurements were not used to calculate the relationship between temperature and altitude. Dves3 was hotter than expected, but data from this plot were used as it had a slight impact on the slope of the relationship. Mean annual temperatures decrease in the order of 0.72°C/100m (R^2=0.99), 0.51°C/100m (R^2=0.98) and 0.71°C/100m (R^2=0.94) with the upward shift in altitude respectively for Mont Ventoux, Issole and Vésubie (Fig 2), but with a high temporal instability (Cailleret 2011). Thermal gradients were stronger at midday than during the night, and during spring. The impact of local edaphic variations was also studied using 16 plots distributed along a transect in contour line between 1100 and 1140m on Mont Ventoux. Four hobos meteorological stations were installed from September 2007 to October 2009 at the top of trees to assess climate variations along this transect. Slight differences in mean temperatures (-0.25°C) and relative humidity (+0.65%) were observed between the crest (TC1) and the valley (TC15) of this transect.

At each site a study plot was established (20×20m) and all the trees with a diameter breast height (dbh, diameter at 1.30m) of more than 10cm were identified, mapped and measured for dbh. Soil water storage capacity was assessed by measuring soil depth and the percentage of coarse elements on one pedological pit situated at the centre of the plot. As karstic soils are very variable in space, soil depth was also measured on the four corners of the plot using a heal bar. The impact of competition on radial growth was calculated for all the studied trees. As the forest inventory made within the 400m² plot is not sufficient to correctly assess impact of tree density, all the trees and stumps with dbh of more than 10cm were measured and mapped within a radius 20m around each studied tree. On Mont Ventoux, Issole and Vésubie, a previous study reveals that the highest determination coefficient between radial growth rate and competition was obtained using a distance dependent index (equation of Martin-Ek 1984), and considering all neighbouring trees respectively located within a radius of 9m, 15m and 14m around the tree as competitors (Cailleret 2011).

Climatic conditions

Long-term evolution of climatic conditions on study sites were reconstructed using closest long-term meteorological stations and hobos stations localised on the plots. Meteorological data was gathered from stations of the French National Climatic Network (Météo-France). On Mont Ventoux, Issole and Vésubie, stations in Carpentras (1964-2009; 99m a.s.l.), St André (1964-2009; 890m a.s.l), and Moulinet (1961-2009; 780m a.s.l) were respectively used. To compare climate between sites, reconstruction was made for plots with close altitudes between sites: hobo stations located at 1225m on Mont Ventoux, 1281m on Issole and 1242m on Vésubie. A strong increase in temperatures was found since the 1960s on each site, especially during the summer, and was respectively in the order of +4.6°C, +5.9°C and +3.4°C per century on Mont Ventoux, Issole and Vésubie (Cailleret 2011). No significant trends were found for annual rainfalls but the amount of water during summer was slightly reduced on Mont Ventoux (-177mm per century; $p<0.1$), while changes in Issole (-37mm per century) and Vésubie (-69mm per century) were not significant.

Measurements were done in 2008 and 2009 and monthly climatic data were related with long-term data using linear regression models. Relationships between both data were reliable concerning temperatures (R^2 ranged between 0.95 and 0.99) and summer rainfalls ($R^2 = 0.93$ to 0.98) but not for winter rainfalls ($R^2=0.77$ on Mont Ventoux, 0.28 in Issole, and 0.84 in Vésubie). These discrepancies were caused by the amount of snow which falls on the site. However as the amount of water which falls during the winter did not impact silver fir growth (Cailleret and Davi 2011), we can support that this climatic reconstruction is reliable in the case of tree-ring growth analysis.

Growth analysis

A total of 561 dominant or codominant firs were studied. Inter-annual and inter-tree variability of radial growth was analysed using classical tree-ring width analysis. Trees were sampled with an increment borer at dbh and the cores were then planned with a razor blade. Ring-widths (RW, mm/year) were measured at the precision of 0.01 mm using the softwares CDendro v5.3 & CooRecorder 5.3 (Larsson L.A. et al. 2006; Cybis Elektronik & Data AB. Sweden). When a core did not reach the pith, the total missing width was estimated using the curvature of the innermost rings of the sample which allow to calculate basal area increments (BAI, mm²/year) assuming a circular outline of stem cross-sections. The number of years estimated to the pith is based on the growth rate after the missing segment (Esper et al. 2003).

To analyze the impact of climate on inter-annual growth variability, individual RW series were standardized in a two-step procedure using the ARSTAN software (Holmes 1994). First, the best model between a negative exponential curve or a linear regression line was fitted to remove long-term trend. Second, a more flexible detrending was made by a cubic smoothing line with a 50% frequency response over 75 years. To obtain residual chronologies, autocorrelation was removed using autoregressive models for each individual series. Individual residual chronologies were introduced into principal component analysis (PCA) to elucidate the impact of climatic conditions on tree radial growth inter-annual variability and an ecological structure between trees. Relationships between climatic variables of current and previous year and interannual changes in PC scores for the first (PC1) and the second axes (PC2) were analyzed using linear models. Following results of a previous dendroclimatic analysis carried out on Mont Ventoux (Cailleret and Davi 2011), the selected input variables were the sum of rainfalls, maximum, and minimum temperatures of previous end of summer (August-September), current winter (October to February), current spring (March and April) and current summer (May to July). The effect of tree age, size and altitude on inter-tree changes in PC1 and PC2 scores was also assessed. The sensitivity of each tree to environmental changes was assessed by calculating Gini indices (Biondi and Qaedan 2008). The package ade4 of the statistical software R (R for Windows version 2.8.0; R Development Core Team 2008) was used for PCA analysis, MASS for the selection of models by AIC in a stepwise algorithm (stepAIC), and dplR for dendrochronological analyses (Bunn 2008).

The analysis of radial growth trends during 20th and 21st century was made after removing the age effect by using the RCS method (Esper et al. 2003). The mean regional age curve (RC) of BAI of the species (RC_{BAI}) was commonly used as reference. This theoretical growth curve is exclusively dependent on the cambial age of the tree and is assumed to be correct for a given species in a given area (Bert 1992; Esper et al. 2003). However, medium frequencies variations can emerge from RC_{BAI} curves when the sampling effort is not enough important (Cailleret 2011). These changes in growth are only due to a sampling effect, not to aging, and are therefore included in smoothing splines fitted on RC_{BAI} curves. Finally, an important bias is transmitted to annual growth indices calculated with this method. For these reasons, BA (cumulative BAI, in mm²) curves were preferred considering that they included less medium frequencies changes (Cailleret 2011). As the effect of tree age on radial growth strongly differs between altitudes, different mean plot age curves BA (PC_{BA}) were used. Gompertz functions were fitted on each PC_{BA} curve considering that the increase in BA is less and less important when the tree is very old. Finally, annual growth indices were calculated as:

$$GI_{i,t} = BAI_{i,t} / (BA_{PC,t} - BA_{PC,t-1})$$

With $GI_{i,t}$ the growth index of a tree i at the cambial age t, and $BA_{PC,t}$ and $BA_{PC,t-1}$ the Basal Area predicted by the plot curve (PC_{BA}) during current and previous age. A GI superior to 1 indicates that the tree had a better growth than the average at same age. The mean growth index ($GI_{i,mean}$) was calculated as the ratio $BA_{i,u} / BA_{PC,u}$ with u the age when the tree die or was cored.

Tree health status

Tree vitality was evaluated in 2008 using different methods. First, crown vitality was evaluated through the analysis of crown defoliation and chlorosis rates. Crown defoliation was preferred to crown transparency as trees with high shoot elongation rates usually showed high transparency level while they are vigorous. In this way, defoliation rate only depends on unexpected branch death and needle loss. Four vitality classes were used: healthy trees with crown defoliation and chlorosis less than 20% (class 0); moderately declining trees with crown defoliation and/or chlorosis between 20% and 40% (class 1); severely declining trees with crown defoliation and/or chlorosis above 40%, typically with a large number dead branches in the crown (class 2); and dead trees (class 3).

Sapwood area was assessed on 281 trees by differentiating heartwood and sapwood on each core using perchloric acid. This chemical reagent identified living wood by reacting with chemical compounds in the heartwood and is the most adapted for firs (Kutscha and Sachs 1962, Becker 1987). For this study, sapwood area was analysed as it is, but we also used an index of sapwood area (ResSA) where tree age, size, altitude and competition effects were removed (Tab S1; Cailleret 2011). To compare GI trends of trees with different sapwood area, the “plot” effect should also be removed as GI was performed at the intra-plot scale. ResSA were calculated as individual ResSA divided by the mean sapwood area of the neighboring trees.

Results

Inter-annual variability of growth

The Principal Component analysis revealed that the inter-annual variability of tree-ring width was mostly explained by climatic conditions. PCA axes 1 and 2 explained more than 60% of the total variance of the growth indices (Table 2). The first axis differentiates years with high growth (positive PC1 scores) to those with low growth (negative PC1 scores) (Fig 3). On each site PC1 scores were negatively related with previous PC1 scores indicating that an increase in tree GI was mostly followed by a decrease in GI (Table 3). This inter-annual evolution was not due to biological changes but to the standardisation method which removed medium frequencies in order to highlight interannual growth variability. Summer rainfalls positively impacted current radial growth (Table 3). The amount of rainfalls in April and May seemed also to be positively related growth in Issole. Annual decrease in the growth rates also occurred due to particular climatic conditions during previous end of summer. High maximum temperatures negatively affect growth of the following year on Mont Ventoux and in Issole, while a lack of water during this period was slightly related with low growth rates in Vésubie. For some years low growth rate on Mont Ventoux was explained by low minimum temperatures during spring. On all sites, high ring-widths reductions were observed in 1942, 1974, 1986 (dry summers), and 2004 (dry spring and dry summer during previous year). To the contrary, 1995 and 1996 were reported as “good” years for growth due to a high amount of water during spring and the beginning of summer (Fig 3). PC scores along the first axis (PC1) increased with tree size but decreased with tree age, and were not related with altitude (Table 2; Fig 3). The second axis discriminates years when growth trends strongly differed among altitudes. Positive PC2 scores indicated that trees at high altitude showed increases in growth rate during these years and the reverse at low altitude. Negative PC2 scores indicated increase in growth rate at low altitude but not at high altitude. PC2 scores were slightly related to climatic conditions. A negative impact of maximum temperatures in spring and a positive one of winter temperatures was observed on PC2 scores in Issole, and a positive impact of maximum temperatures during summer on Mont Ventoux.

Indicators of tree decline

The comparison of growth levels of trees with different sapwood area (ResSA = observed SA / theoretical SA given by the generalized linear model; Tab S1) indicated that differences in ResSA were related with differences in GI. Between trees, higher ResSA were mostly positively related with higher radial growth rates (GI). This trend was reported on on Mont Ventoux during the period 1950-2000 (Fig 4a, 4c), but was less clear in Issole where GI of trees with ResSA>1.2 was higher than GI of the others, and not significant in Vésubie (Fig 4b).

Sapwood area of dead trees was not significantly different to the one of living trees (Fig 7c; $p>0.1$). On Issole declining trees had larger sapwood than healthy trees but this trend was attributed to a tree size effect as declining trees are the biggest ones on this site.

Relationships between crown condition and current radial growth differed between sites (Fig 5). On Mont Ventoux and Vésubie, dead trees and severely damaged trees had lower growth rates than healthy and moderately damaged trees. Trees with severely crown damages (class 2) showed the lowest growth rates since many years while growth rate of dead trees was lower than the one of healthy trees twenty years before their death. Different patterns were observed in Issole. Dead trees had the lowest growth rates but unexpectedly trees with crown damages had higher growth than trees with a healthy crown.

Characteristics of declining trees

Silver fir mortality rate was important on Mont Ventoux (20% on average, until 54% on some plots). All tree sizes were affected but medium-size trees were more predisposed to die (Chi-square test: $p<0.001$; Tab 1; Fig 6). On the other sites, the dieback process affected less than 10% of the firs which were principally small on Issole (Chi-square test: $p<0.01$), while mortality rate was equally distributed with tree size in Vésubie (Chi-square test: $p>0.1$). Our sampling was representative of this pattern, except a lack of big dead trees in Vésubie (Fig 6). Concerning tree crown condition, about 10%, 50% and 30% of the trees sampled in Ventoux, Issole and Vésubie had a crown whose defoliation rate and/or discoloration rate was superior to 20%. All sizes were affected by this phenomenon on Ventoux and Vésubie while the probability for a tree to have a damaged crown in Issole increased with its size (Fig 5).

No impact of the degree of competition on tree vitality was found on Mont Ventoux and Vésubie (Fig 7a). In Issole, dead trees experienced a higher competition degree than healthy trees, and declining trees showed the lowest competition indices. These differences were due to unequal distributions in declining and dead trees with tree size which biased the comparison of CI: for a same density, smaller is the tree, higher is CI.

Trees showed different growth trends during their juvenile phase according to their vitality assessed by crown condition and to the study site (Fig 8). On Ventoux, dead trees showed higher growth during the juvenile ages ($p<0.05$ until 35 years old; unpaired t.test), while the reverse pattern was found in Issole ($p<0.05$ since 12 years old) and Vésubie ($p<0.05$ between 17 and 36 years old). On the contrary, differences in juvenile growth between living trees with different crown damages (healthy – declining – severely declining) were not important, except lower growth levels for severely declining trees on Mont Ventoux compared with the others. Tree sensitivity to inter-annual environmental changes was revealed by Gini index. On each site Gini indices were higher for dead trees than living trees (Fig 7b). This relationship was not biased by other explained variables such as altitude, tree age and size as the same result was obtained when removing all other effects (not shown).

On Mont Ventoux, mortality rate clearly increased with the downward shift in altitude (Table 1). But a high variability was also explained by variations in local edaphic conditions. The sixteen plots located on the transect in contour line on Mont Ventoux revealed that mortality rate ranged between 0 to 54% at same altitude, which was not related with the slope and with soil depth of the central pit of the plot (linear regression model; $p>0.1$). On Vésubie, 25% of the firs located in Dves3 died while this rate is below 5% on the other sites (Table 1).

Growth trends during last century

Temporal drops between GI curves of trees with different ResSA were observed in Fig 4. On Mont Ventoux it occurred in 1942. Afterwards, differences in GI increased until the end of 90s where growth curves of trees with ResSA inferior to 1.2 began to converge (Fig 4a).

Whichever ResSA, a strong decrease in radial growth was observed during last decade. In Issole and Vésubie a drop seemed to occur during the first part of the 60s. If the divergence is clear in Issole (especially in 1965), the differences between trees of different sapwood class were not significant (Fig 4b, 4c).

Results were different when comparing growth trends of trees with different crown damage. On Mont Ventoux, growth of severely declining trees (class 2) is very low since the 30s (Fig 5a). Growth curves of dead and healthy trees converged in 1965. Previously, GI of dead trees was at a higher level than healthy trees. Two slight divergences occurred in 1979 and 1989 when decreases in GI of dead trees were stronger than for the other trees. In Issole, growth curves of dead and healthy trees converged in 1942 and then diverged in 1958 (Fig 5b) and since this date dead trees had a lower GI. In Vésubie, dead trees exhibited lower GI since the beginning of measurements although severely declining trees showed equivalent GI until 1974, after they strongly decline during the six following years and since 1980, became equal to those of dead trees.

These years were the strong negative pointer years revealed by PCA (Fig 3). On Mont Ventoux divergences between curves occurred in 1942, 1965, 1979 and 1989 whose PC1 scores were respectively the 8th, 3rd, 16th and 11th lowest values of the 20th and 21st century. In Issole, the years 1942, 1965 (2nd and 4th rank on PC1) and 1958 (2nd lowest value on PC2) emerged of the analysis, while the years 1965, 1974, 1979 (5th, 2nd, 13th on PC1) seemed to have an impact on tree decline on Vésubie.

Discussion

Main factors limiting growth

Optimized neighbouring radius used for the determination of competitors ranged between 9 and 15m, which is quite high comparing with several studies (e.g. 8m to 10m on *Pinus sylvestris*; Garcia-Abril *et al.* 2007). Linares et al. (2009b) recently showed on *Abies pinsapo* that maximum correlation between $\sigma 13C_{wood}$ and the degree of competition were obtained at short spatial scale (2-5m) was and this competition effect was attributed to competition for light. Competition for light arises between trees with overlapped crown. Silver fir of Mont Ventoux exhibits in average a diameter of crown projection near 5m (Nourtier et al., submitted). Consequently, a larger radius, from 9 to 15m and a strong relationship between competition index and growth as in our case (R>0.45), reveals a stronger importance of competition for water than for light on tree growth. High radius values were also probably due to high slope. At same distance, neighbouring trees located above the studied trees (south azimuth) may have a stronger importance than those located below.

Results of the Principal Components Analysis also showed that drought is the main growth limiting factor. Inter-annual variability in radial growth was mainly explained by water availability during the vegetation period. This relationship was commonly found on silver fir, especially at its xeric range (Andreu 2007; Cailleret and Davi 2011; Lebourgeois 2007; Macias et al. 2006) and affects trees whatever their altitude. These results can be explained by high vulnerability to drought-induced cavitation which is counterbalanced by a rapid and complete stomatal closure when soil water potential decrease to avoid cavitation (Aussenac 2002; Nourtier et al. submitted), and by an inhibition of cell division and enlargement (Zweifel et al. 2006). Moreover, a lack of water during summer also negatively impacts growth of the following years by reducing the quantity of carbohydrates stored on the tree, by reducing fine root turnover and by inducing needle loss (Breda et al. 2006).

Variability in temperatures also induced changes in growth as indicated by PCA. On Mont Ventoux, increases in temperatures in spring lead to an increase in carbon assimilation by the tree due to an earlier budburst and higher photosynthesis rates (Davi et al. 2006; Delpierre et al. 2009) and an earlier cambium activation (ref). High maximum temperatures induced increase in growth increment at high altitude, but a decrease at low altitude, which was likely due to the thermal gradient. However these trends were not found on the other sites.

Indicators of tree vitality

Recent tree radial growth is commonly used as indicator of tree vitality and to predict tree mortality (Dobbertin 2005). On Mont Ventoux we recently showed that the performance of tree mortality models based on dendrochronological data was above 80% (Cailleret and Davi submitted). As the prediction of mortality models was improved using relative growth values, GIs were studied instead of BAI to remove the age effect. GIs before death were at lower levels than GIs of living trees but differences appeared concerning the periods since growth curves diverge. On Mont Ventoux, growth differences were observed since about 30 years while it was about 60 and 70 years in Issole and Vésubie. Moreover, even if growth levels were very low, silver fir can survive. This report was often made under dense canopies where young seedlings acclimate needle traits to tolerate shade (Robakowski et al. 2004), and is likely when a tree grows on a very shallow soil.

Tree vitality can also be approximated using sapwood area (SA) as it is the area of living wood which contains carbohydrates reserves, and the area of functional xylem conducting the sapflow. SA well discriminates tree with different current and past growth levels. But surprisingly, there were no differences in SA between dead and living trees, and between healthy and declining trees. As perchloric acid reveals heartwood, its use is reliable when the wood transformed in heartwood really contains carbohydrates and is conducting sap. However, in the case of rapid decline of carbon reserves and large xylem embolism, heartwood formation is maybe not enough important, and the sapwood area can have been overestimated by perchloric acid. If this method can be used in the case of long-term growth declines (Becker 1987), other methods can be preferred when rapid tree dieback occurred, depending on the aim of the study. For such as sapflow analysis, sapwood length i.e. the length of functional xylem should be measured using physical methods or visually. The area of wood which contains carbohydrates should be analyzed using specific reagents such as lugol for testing starch.

Crown damage was also commonly assessed to estimate tree vigour (De Vries 2000; Zierl 2004) and is often related with tree mortality probability (Dobbertin and Brang 2001). Two visible symptoms were recorded: chlorosis and defoliation. Needle chlorosis can be caused by several factors such as nutrient deficiency, atmospheric pollution (e.g. ozone), pathogens and drought (Landmann et al. 1995), and reduced the photosynthetic capacities of the leaves (Dreyer et al. 1994). Defoliation had a stronger impact on tree functioning especially for coniferous because needles act as storage organs for carbon and nitrogen (Hoch et al. 2003). Needle loss and branch mortality were usually due to pathogens such as budworm or to drought. Firstly, premature leaf shedding can occur during drought while leaves were still green likely, due to petiole cavitation (Breda et al. 2006). Secondly, the number and viability of leaf buds can also be reduced to limit water use but to the detriment of a quick recovering an efficient crown development after complete refilling of water resources (Le Dantec et al. 2000; Limousin et al. 2009). In our study, crown condition was not clearly related with tree radial growth. If GI decreases with increasing crown damages on Mont Ventoux, declining trees had higher GI than healthy trees on Vésubie, while GI curves of declining and severely declining trees were largely above GI curves of healthy trees in Issole. In the same way, dates of GI curves drops were changed when using different crown condition classes or different sapwood area classes.

Tree crown condition can be assumed as a good indicator of the evolution of tree vigour with time (temporal analysis). However, comparing trees with different crown damages did not reveal differences in tree vitality and vulnerability to dieback (spatial analysis).However, crown damage assessment can be improved by focusing on the active part of the crown (1/3 upper part).

To conclude, as severely declining trees showed different GI evolution with time than dead trees what indicates that decline and mortality processes were dissociated. Dead trees would not be necessarily those which had highest crown damages. This hypothesis can be supported by the study of Kaufmann (1996) where *Pinus ponderosa* trees with the higher leaf areas had generally smaller growth efficiencies (per m² total leaf area), but should be confirmed by a temporal monitoring of the health of the studied trees.

Moreover, absolute growth rates were commonly used as indicator of tree vitality and predictor of mortality but relative ones should be preferred as they are closer to tree functioning (Chao et al. 2008; Cailleret et al. submitted). Tree size and juvenile growth rate can be used as references because they approximate the quantity of carbon needed to maintain metabolism. Tree vulnerability to decline and death should be assessed using structural functional traits such as xylem embolism vulnerability, ratio between leaf area and roots area, ratio between the carbon available and demand. For this aim, more experimental data is needed to better understand the functional processes during drought, by coupling whole-tree hydraulic and carbohydrate measurements (Ryan 2011).

Factors predisposing decline and mortality

Large areas of silver fir forests showed declining and dieback symptoms, but mortality was extremely patchy. The high heterogeneity in mortality rates within a site and within a plot was explained by a combination of numerous stress factors which predispose tree to dieback. Firstly, the process did not affect all size distribution of the trees. Smaller trees were affected in Issole which corresponds to a common trend in forest stands. On Mont Ventoux, medium-size trees seemed to be the most vulnerable. To our knowledge, this pattern was not yet observed, while Coomes and Allen (2007) showed the reverse in disturbed stands, where trees more prone to die are small and big ones. These differences can be due to changes in tree sensitivity to climate with tree size. Individuals with variable growth were more prone to die from drought than tree with more regular growth (Cailleret et al. submitted; Suarez et al. 2004).

Long-term stress factors are often expressed as reduced tree growth rates contributing to an increase in tree vulnerability to dieback (Manion 1981, Pedersen 1998). This pattern was found on Issole and Vésubie where dead trees showed very low growth rates. This trend can be explained by higher competition degree experienced by dead trees in Issole, but not in Vésubie. It is commonly accepted that competition acts as a long-term predisposing mortality factor (Bigler and Bugmann 2003) due to the decrease in light availability which lead to a decrease in carbon assimilation. This effect can be important for pioneer species but lesser for shade-tolerant species such as silver fir.

In the Mediterranean area, the main predisposing factor is the water availability. Our study shows that silver fir at low altitude on Mont Ventoux or in high xeric condition due to specific topographic position in Vésubie (Dves3) are more prone to die. At a large spatial scale analysis, Quesney (2008) also revealed that silver fir mortality on south-east part of France was more important on dry plots, i.e. at low altitude, on south-facing slopes, and on dry edaphic conditions due to particular topographic conditions (high slope, convex).

In Issole and Vésubie, dead trees are those with the lowest growth rates since their birth which confirm previous results. However, we also found on Mont Ventoux that dead trees averaged higher growth rates during the juvenile phase than living trees (Cailleret et al. submitted). This trade-off between longevity and juvenile growth rates was already observed within a species (Black et al. 2008; Bigler and Veblen 2009). Fast growth rates during young ages can increase tree vulnerability to mortality as it is related with high ratios of above- to below-ground biomass, reduced investment in secondary carbon compounds used for defence against pathogens (Loehle 1988), and higher respiration and transpiration rates. It leads in higher water, carbon and nutrient needs which will cause troubles when these supplies fall short (McDowell et al. 2008). High differences in juvenile growth rates were found at the distribution range scale but also at same altitude which can be explained by differences in the water availability in the first layers of the soil (Nourtier et al. submitted). Herbivorous insects and pathogens may also contribute to loss of vigour and increase tree susceptibility to subsequent stress (e.g. drought). If no herbivorous insects were reported on study sites during last decade, infestations by mistletoe (*Viscum album*) and bark beetles were important especially on Mont Ventoux (Gillmann et al. submitted)

The concept of predisposing factors as described by Manion (1981) might be revised as they differ between sites and even within a site by assessing soil heterogeneity in depth using geophysical methods (Nourtier et al. submitted). Structural traits of the trees should also be integrated using allometric variables (total leaf area measurements using hemispherical photography, sapwood area) and xylem anatomy. Predisposing factors induced higher tree vulnerability to drought events which not necessarily include its weakening.

Impact of extreme events during last century

Estimating the climatic conditions during the years when the divergence of growth curves began allow determining the inciting factors (Becker 1987; Bigler et al. 2006). As revealed by the PCA analysis, these years were negative pointer years mainly characterized by a severe drought during the vegetation period. 1965 was identified as an important date, because most of the growth trajectories of trees with different vitality diverged on all sites. In Issole, temporal drops occurred in 1958 which was a strong negative year for trees located at low altitude, and this decrease was amplified by droughts during the beginning of the 1960s.

The negative impact of single drought years on the onset of declining growth was observed for a wide range of species (Pedersen 1998, Ogle et al. 2000). However an increasing number of studies showed that multi-year droughts had more adverse and decisive effects on tree growth (LeBlanc 1998; Bigler et al. 2006) which is supported by our study. Several drought events occurred during last decade (summer 2003, spring 2004, and summer 2006) in connection with a recent decline in tree radial growth (Cailleret and Davi 2011). At the same time, first dead trees were reported at the end of the year 2002 on Mont Ventoux and 2003 in Issole and Vésubie. The accumulation of summer drought between 2003 and 2006 seemed to be the main contributing stress factor.

To conclude, mortality and decline processes should be separated. As there was a huge of causes inducing mortality, many interactions between them, and which differ between sites, different vitality indicators should be used. Relative radial growth trends, crown damages and sapwood area should be analyzed as it allow to assess spatio-temporal changes in tree vitality, but were not sufficient to assess differences in tree vulnerability to dieback. An integration of functional processes is needed to understand the complexion of causes for example by assessing the sensitivity of different carbon allocation rules to fine roots, growth, reproduction and defences, and of different hydraulic parameters on tree mortality probability (Davi et al. in prep).

References

Aussenac G (2002) Ecology and ecophysiology of circum-Mediterranean firs in the context of climate change. Ann For Sci 59:823–832

Becker M (1987) Bilan de santé actuel et rétrospectif du sapin (Abies alba Mill.) dans les Vosges. Etude écologique et dendrochronologique. Ann. For. Sci., 44, 379-402

Bigler C, Bräker OU, Bugmann H, Dobbertin M, Rigling A (2006) Drought as an inciting factor mortality factor in scots pine stands of the Valais, Switzerland. Ecosystems, 9, 330-343. DOI: 10.1007/s10021-005-0126-2

Bigler C, Bugmann H (2003) Growth-dependent tree mortality models based on tree rings. Can J For Res 33:210–21.

Bigler C, Veblen TT (2009) Increased early growth rates decrease longevities of conifers in subalpine forests. *Oikos*, 118 (8), 1130-1138. DOI: 10.1111/j.1600-0706.2009.17592.x

Biondi F, Qeadan F (2008) Inequality in Paleorecords. Ecology, 89, 1056-1067

Black BA, Colbert JJ, Pederson N (2008) Relationships between radial growth rates and lifespan within North American tree species. Ecoscience, 15, 349-357

Breda N, Huc R, Granier A, Dreyer E (2006). Temperate forest trees and stands under severe drought: a review of ecophysiological responses, adaptation processes and long-term consequences. Annals of Forest Science, 63, 625-644. doi:10.1051/forest:2006042

Bunn A (2008) A dendrochronology program library in R (dplR). *Dendrochronologia*, 26, 115-124. doi:10.1016/j.dendro.2008.01.002

Bussotti F, Ferretti M (2009) Visible injury, crown condition, and growth responses of selected Italian forests in relation to ozone exposure. Environmental Pollution, 157, 1427-1437. doi:10.1016/j.envpol.2008.09.034

Cailleret M (2011) Causes fonctionnelles du dépérissement et de la mortalité du sapin pectiné en Provence. Thèse de doctorat de l'Université d'Aix-Marseille III.

Cailleret M, Davi H (2011) Effects of climate on diameter growth of co-occurring *Fagus sylvatica* and *Abies alba* along an altitudinal gradient. Trees, 25, 265-276. DOI 10.1007/s00468-010-0503-0

Cailleret M, Davi H (submitted) How to predict tree drought-induced tree mortality from radial growth data. Journal of Ecology.

Canham CD, LePage PT, Coates KD (2004) A neighborhood analysis of canopy tree competition: effects of shading versus crowding. *Can J For Res*, 34, 778-787. doi: 10.1139/X03-232

Chao KJ, Phillips OL, Gloor E, Monteagudo A, Torres-Lezama A, Vasquez-Martinez R (2008) Growth and wood density predict tree mortality in Amazon forests. J Ecol, 96, 281-292. doi: 10.1111/j.1365-2745.2007.01343.x

Coomes DA, Allen R (2007) Mortality and tree-size distributions in natural mixed-age forests. Journal of Ecology, 95, 27-40

Davi H, Simioni G, Marie G, Cailleret M, Delpierre N, Dufrêne E (in prep) Modelling forest functioning under climate change.

Davi H, Dufrëne E, Francois C, Le Maire G, Loustau D, Bosc A, Rambal S, Granier A, Moors E (2006) Sensitivity of water an carbon fluxes to climate changes from 1960 to 2100 in Europea forest ecosystems. Agric For Meteorol 141:35–56. doi:10.1016/j.agrformet.2006.09.003

Delpierre N, Dufrêne E, Soudani K, Ulrich E, Cecchini S, Boé J, Franc¸ois C (2009) Modelling interannual and spatial variability of leaf senescence for three deciduous species in France. Agric For Meteorol 149:938–948. doi:10.1016/j.agrformet.2008. 11.014

De Vries, W., Klap, J.M., Erisman, J.W., 2000. Effects of environmental stress on forest crown condition in Europe. Part I. Hypotheses and approach to the study. Water Air Soil Pollut. 119, 317–333.

Dobbertin M, Brang P. (2001) Crown defoliation improves tree mortality models. For. Eco. Manage., 141, 271-284

Dobbertin M (2005) Tree growth as indicator of tree vitality and tree reaction to environmental stress: a review. *Eur J For Res*, 124, 319-333. doi:10.1007/s10342-005-0085-3

Dreyer E., Fichter J., Bonneau M., (1994) Nutrient content and photosynthesis of young yellowing Norway spruce trees (*Picea abies* L. Karst.) following calcium and magnesium fertilisation, Plant Soil 160 67–78.

Esper J, Cook ER, Krusic PJ, Peters K, Schweingruber FH (2003) Tests of the RCS method for preserving low-frequency variations in long tree-ring chronologies. Tree Ring Res 59:81–98

Ficko A, Poljanec A, Boncina A (2011) Do changes in spatial distribution, structure and abundance of silver fir (*Abies alba* Mill.) indicate its decline? For. Eco. Manage. 261, 844-854. doi:10.1016/j.foreco.2010.12.014

Garcia-Abril A, Martin-Fernandez S, Grande MA, Manzanera JA (2007) Stand structure, competition and growth of Scots pine (Pinus sylvestris L.) in a Mediterranean mountainous environment. Ann For Sci., 64, 825-830. DOI: 10.1051/forest:2007069.

Gillmann et al. (submitted)

Granier A (1981) Etude des relations entre la section du bois d'aubier et la masse foliaire chez le Douglas (Pseudotsuga menziesii Mirb. Franco). Ann. For. Sci., 38, 503-512

Hoch G, Richter A, and Körner C, (2003) Non-structural carbon compounds in temperate forest trees. Plant Cell Environ. 26: 1067–1081.

Holmes RL (1994) Dendrochronology program manual. Laboratory of Tree-Ring Research. Tucson, Arizona, U.S.A.

Kaufmann MR (1996) To live fast or not: growth, vigor, longevity of old-growth ponderosa pine and lodgepole pines. Tree Physiology, 16, 139-144

Knapic S and Pereira H (2005) Within-tree variation of heartwood and ring-width in maritime pine (*Pinus pinaster* Ait.) Forest Ecology and Management, 210, 81-89

Kutscha NP, Sachs IB (1962) Color tests for differentiating heartwood and sapwood in certain softwood tree species. Report 2246, Forest Products Laboratory, Madison, WI, pp. 16.

Landmann G., Bonneau M., Bouhot-Delduc L., Fromard F., Chéret V., Dagnac J., Souchier B., Crown damage in Norway Spruce and Silver Fir: relation to nutritional status and soil chemical characteristics in the French mountains, in: Landmann G., Bonneau M. (Eds.), Forest decline and atmospheric deposition effects in the French Mountains, Springer, Berlin Heidelberg, New York, 1995, pp. 41–81.

LeBlanc DC. 1998. Interactive effects of acidic deposition, drought, and insect attack on oak populations in the midwestern United States. Can J Forest Res 28:1184–97.

Lebourgeois F (2007) Climatic signal in annual growth variation of silver fir (Abies alba Mill) and spruce (Picea abies Karst.) from the French Permanent Plot Network (RENECOFOR). Ann. For. Sci., 64, 333-343. DOI: 10.1051/forest:2007010

Le Dantec V, Dufrêne E, Saugier B (2000) Interannual and spatial variation in maximum leaf area index of temperate deciduous stands, For. Ecol. Manage. 134 71–81.

Leuzinger, S. et al. 2005. Responses of deciduous forest trees to severe drought in Central Europe. Tree Physiol. 25: 641_650.

Limousin J.M., Rambal S., Ourcival J.M., Rocheteau A., Joffre R. and Rodriguez-Cortina R., (2009). Long-term transpiration change with rainfall decline in a Mediterranean *Quercus ilex* forest. Global Change Biol. DOI: 10.1111/j.1365-2486.2009.01852.x.

Linares JC, Camarero JJ, Carreira JA (2009a) Interacting effects of changes in climate and forest cover on mortality and growth of the southernmost European fir forests. Global Ecol. Biogeogr. 18, 485-497. DOI: 10.1111/j.1466-8238.2009.00465.x

Linares JC, Delgado-Huertas A, Camarero JJ, Merino J, Carreira JA (2009b) Competition and drought limit the response of water-use efficiency to rising atmospheric carbon dioxide in the Mediterranean fir Abies pinsapo. Oecologia, 161, 611-624. DOI 10.1007/s00442-009-1409-7

Loehle C. 1988. Tree life history strategies: the role of defenses. Can J For Res 18:209–22.

Macias M, Andreu L, Bosch O, Camarero JJ, Gutie´rrez E (2006) Increasing aridity is enhancing silver fir Abies alba (Mill.) water stress in its south-western distribution limit. Clim Change 79:289–313

Manion PD (1981) Tree disease concepts. Prentice-Hall, Inc. Englewood Cliffs, New Jersey, 399p.

Martin GL, Ek AR (1984) A comparison of competition measures and growth models for predicting plantation red pine diameter and height growth, For. Sci, 30, 731–743.

Martinez-Vilalta J, Cochard H, Mencuccini M, Sterck F, Herreo A, Korhonen JFJ, Llorens P, Nikinmaa E, Nolè A, Poyatos R, Ripullone F, Sass-Klaassen U, Zweifel R (2009) Hydraulic adjustment of Scots pine across Europe. New Phytol. 184, 353-364. doi: 10.1111/j.1469-8137.2009.02954.x

McDowell NG, Pockman W, Allen C, Breshears D, Cobb N, Kolb T, Plaut J, Sperry J, West A, Williams D et al. (2008). Mechanisms of plant survival and mortality during drought: why do some plants survive while others succumb? *New Phytologist* 178: 719–739.

Mc Dowell N (2011) Mechanisms linking drought, hydraulics, carbon metabolism, and vegetation mortality. Plant Phjysiology, 155, 1051-1059

Nourtier M, Cailleret M, Yingge X, Chanzy A, Davi H (submitted) Regulation of silver fir (Abies alba Mill.) transpiration during drought in relation to soil characteristics.

Pedersen BS. 1998. The role of stress in the mortality of Midwestern oaks as indicated by growth prior to death. Ecology 79:79–93.

Ogle K, Whitham TG, Cobb NS. 2000. Tree-ring variation in pinyon predicts likelihood of death following severe drought. Ecology 81:3237–43.

Quesney T (2008) Observatoire dépérissement des forêts des Alpes-Maritimes ; rapport 2008-11-25, ONF DT Méditerranée, pôle RDSA

Robakowski P, Wyka T, Samardakiewicz S, Kierzkowski D (2004) Growth, photosynthesis, and needle structure of silver fir (*Abies alba* Mill.) under different canopies. For. Eco. Manage., 201, 211-227. doi:10.1016/j.foreco.2004.06.029

Ryan MG (2011) Tree responses to drought. Tree Physiology, 31, 237-239. doi:10.1093/treephys/tpr022

Suarez ML, Ghermandi L, Kitzeberger (2004) Factros predisposing episodic drought-induced tree mortality in Nothofagus – site, climatic sensitivity and growth trends. Journal of Ecol., 92, 954-966

Tsopelas P, Angelopoulos A, Economou A, Soulioti N (2004) Misteltoe (*Viscum album*) in the forest of Mount Parnis, Greece. Forest Ecology and Management, 202, 59-65

Zierl B (2004) A simulation study to analyse the relations between crown condition and drought in Switzerland. Forest Ecology Management, 188, 25-38

Zweifel R, Zimmermann L, Zeugin F, Newbery DM (2006) Intraannual radial growth and water relations of trees: implications towards a growth mechanism. J Exp Bot 57:1445–1459. doi:10.1093/jxb/erj125

Table 1: Sampling

Plot	Altitude (m a.s.l.)	Slope (°)	Soil depth (cm)	Coarse elements (%)	BA (m^2/ha)	Fir proportion	Mortality rate	Number of trees cored	Mean age	Mean Circ (mm)	Mean Gini index
Dvx1	995	25	35	50.0	42.5	0.11	0.39	20	75.4	497.8	0.120
Dvx2	1020	36	20	80.0	53.6	0.46	0.26	30	63.3	542.6	0.127
Dvx3	1117	22	65	82.5	50.8	0.28	0.13	25	62.9	428.0	0.119
Dvx4	1247	29	32	48.0	44.2	0.82	0.25	16	160.8	591.4	0.130
Dvx5	1340	27	60	58.3	32.6	0.62	0.07	25	156.0	626.8	0.120
TC1	1138	35	62	86.5	34	0.40	0.13	9	65.4	496.1	0.106
TC2	1108	37	67	81.9	19.5	0.27	0	7	57.1	312.8	0.095
TC3	1125	41	62	76.1	35.5	0.57	0.33	18	65.9	493.3	0.120
TC4	1110	41	72	72.8	28.4	0.34	0.20	11	73.7	519.1	0.124
TC5	1122	37	65	80.8	32.2	0.56	0.48	19	75.9	483.3	0.121
TC6	1128	39	67	61.2	40.2	0.53	0.54	22	75.0	496.9	0.130
TC7	1128	42	60	61.3	41.9	0.53	0.16	13	83.5	474.4	0.143
TC8	1123	45	20	60.0	31.1	0.66	0.23	15	73.7	405.0	0.136
TC9	1131	44	43	83.0	35.9	0.52	0.21	15	82.3	421.7	0.124
TC10	1124	47	45	40.0	40.2	0.48	0.46	12	104.9	595.4	0.134
TC11	1121	45	25	65.0	49.2	0.51	0.36	16	107.9	524.9	0.143
TC12	1134	42	58	79.7	35.3	0.36	0.12	11	108.6	614.9	0.136
TC13	1143	40	20	75.0	54.7	0.59	0.05	16	148.4	610.4	0.124
TC14	1137	47	16	40.0	29.0	0.67	0.06	10	102.9	551.7	0.131
TC15	1132	46	34	75.0	61.1	0.70	0.11	17	142.1	677.7	0.132
TC16	1128	45	50	71.0	48.3	0.55	0.16	16	106.3	598.4	0.131
Diss1	1108	38	34	30.0	54.6	0.95	0	15	167.1	658.1	0.144
Diss2	1196	39	30	43.5	56.9	0.93	0.08	27	101.3	492.0	0.165
Diss3	1281	23	33	52.4	65.5	0.94	0.01	22	91.5	507.5	0.121
Diss4	1468	25	36	56.9	44.7	0.79	0.06	21	79.8	578.7	0.130
Diss5	1585	35	67	57.1	63.6	0.83	0.09	19	74.4	759.2	0.125
Dves1	1078	43	NA	NA	55.9	0.23	0.01	17	78.6	699.4	0.112
Dves2	1130	42	NA	NA	45.4	0.44	0.03	19	77.8	688.8	0.114
Dves3	1242	47	NA	NA	43.9	0.52	0.25	26	96.8	637.9	0.128
Dves4	1330	40.5	NA	NA	42.1	0.81	0.02	18	153.2	760.8	0.123
Dves5	1497	39	NA	NA	49.9	0.87	0.02	21	138.7	726.7	0.122
Dves6	1585	27	NA	NA	NA	0.83	0.05	13	148.6	897.8	0.111

Table 2: Effect of altitude, tree age and tree size on PC1 (Axis 1) and PC2 (Axis 2) scores of each individual

	Ventoux		Issole		Vesubie	
	Axis 1 (60.9%)	Axis 2 (2.35%)	Axis 1 (65.7%)	Axis 2 (2.31%)	Axis 1 (57.8%)	Axis 2 (3.46%)
(Intercept)	9.79e-01 ***	-9.03e-01 ***	9.31e-01 ***	-2.22 ***	1.04 ***	-7.96E-01 ***
altitude	-2.38e-05 NS	6.77e-04 ***	1.79e-05 NS	1.54e-03 ***	-9.09e-05 *	-5.72e-04 ***
age	-2.14e-03 ***	2.05e-03 ***	-1.69e-03 ***	1.87e-03 ***	-1.77e-03 ***	3.45e-04 NS
BA (mm²)	4.07e-07 ***	-6.81e-07 ***	2.17e-07 ·	-2.26e-07 NS	2.76e-07 ***	1.70e-07 NS

Table 3: Effect of rainfalls (P), maximum (Tmax) and minimum (Tmin) temperatures during winter, spring and summer, and of PC1 of previous year score on current PC1 and PC2 scores for each year. Variables from previous year were indicated using *n-1*. The best linear models were chosen by AIC in a stepwise algorithm.

	PC1 scores			PC2 scores		
	Ventoux (R^2=0.51)	Issole (R^2=0.43)	Vésubie (R^2=0.35)	Ventoux (R^2=0.18)	Issole (R^2=0.22)	Vésubie (R^2=0.04)
Intercept	21.56 ^{NS}	5.09 ^{NS}	-16.66 ***	-16.01 ^{NS}	9.45 *	1.73 ^{NS}
PC1 score n-1	-0.19 °	-0.30 *	-0.35 **	-0.06 ^{NS}		
P end sum n-1		0.03 ^{NS}	0.03 *	-0.01 ^{NS}		
Tmax end sum n-1	-2.84 **	-2.43 *		-0.55 ^{NS}		
P winter		0.02 °				-0.01 °
Tmax winter				-1.34 ^{NS}	1.61 **	
P spring		0.06 *	0.02 ^{NS}			
Tmax spring					-1.78 ***	
Tmin spring	3.80 *					
P sum	0.10 ***	0.04 **	0.05 **			
Tmax sum		1.24 ^{NS}		1.41 **		

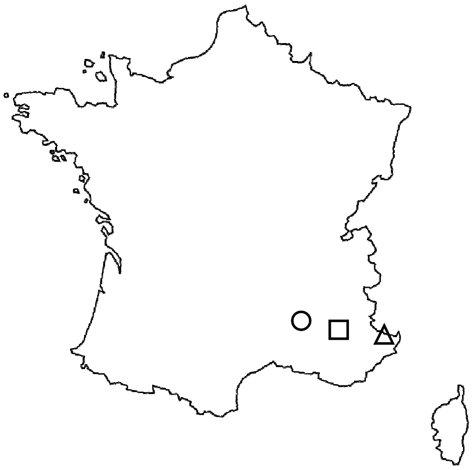

Fig1: Localization of the study sites: Mont Ventoux (circles), Issole (square) and Vésubie (triangle).

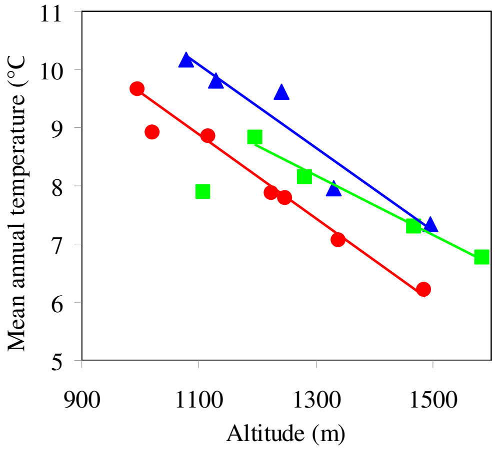

Fig2: Effect of altitude on mean annual temperatures on the North-facing slope of the Mont Ventoux (red), Issole (green) and Vésubie (blue).

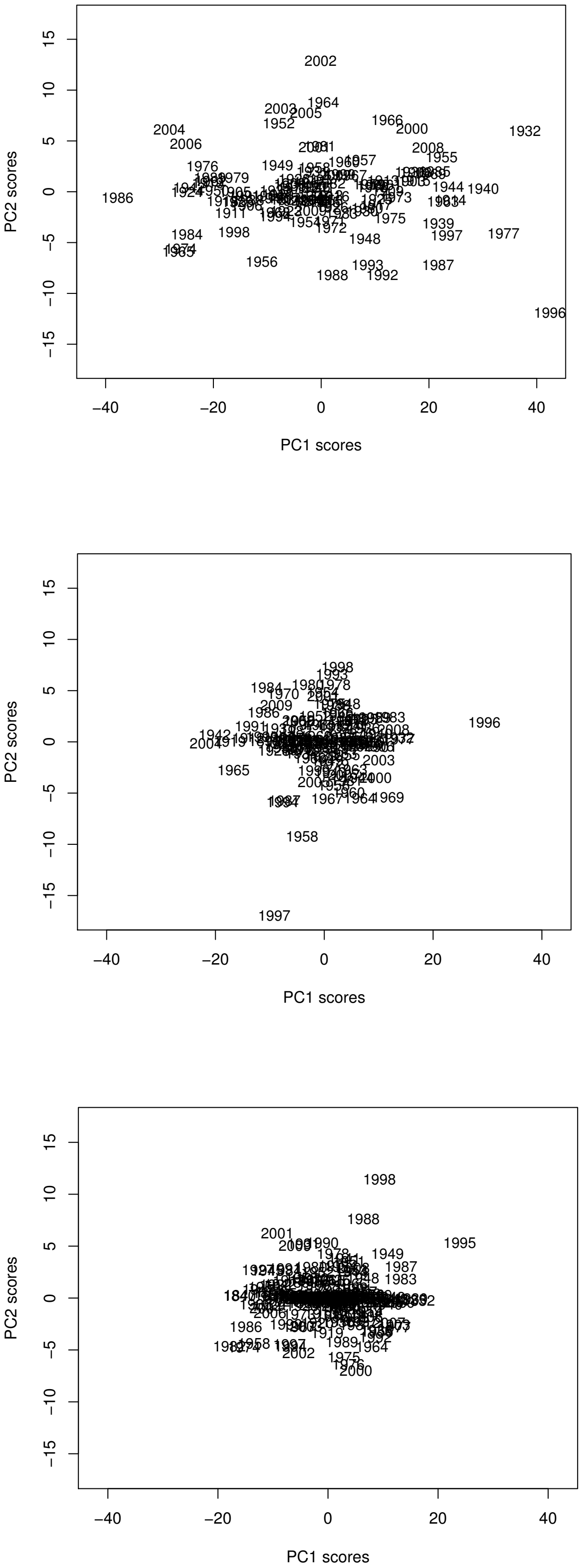

Fig 3: Results of the Principal Components Analysis (PCA) for the interannual variability in growth on Mont Ventoux (up), Issole (middle) and Vésubie (bottom)

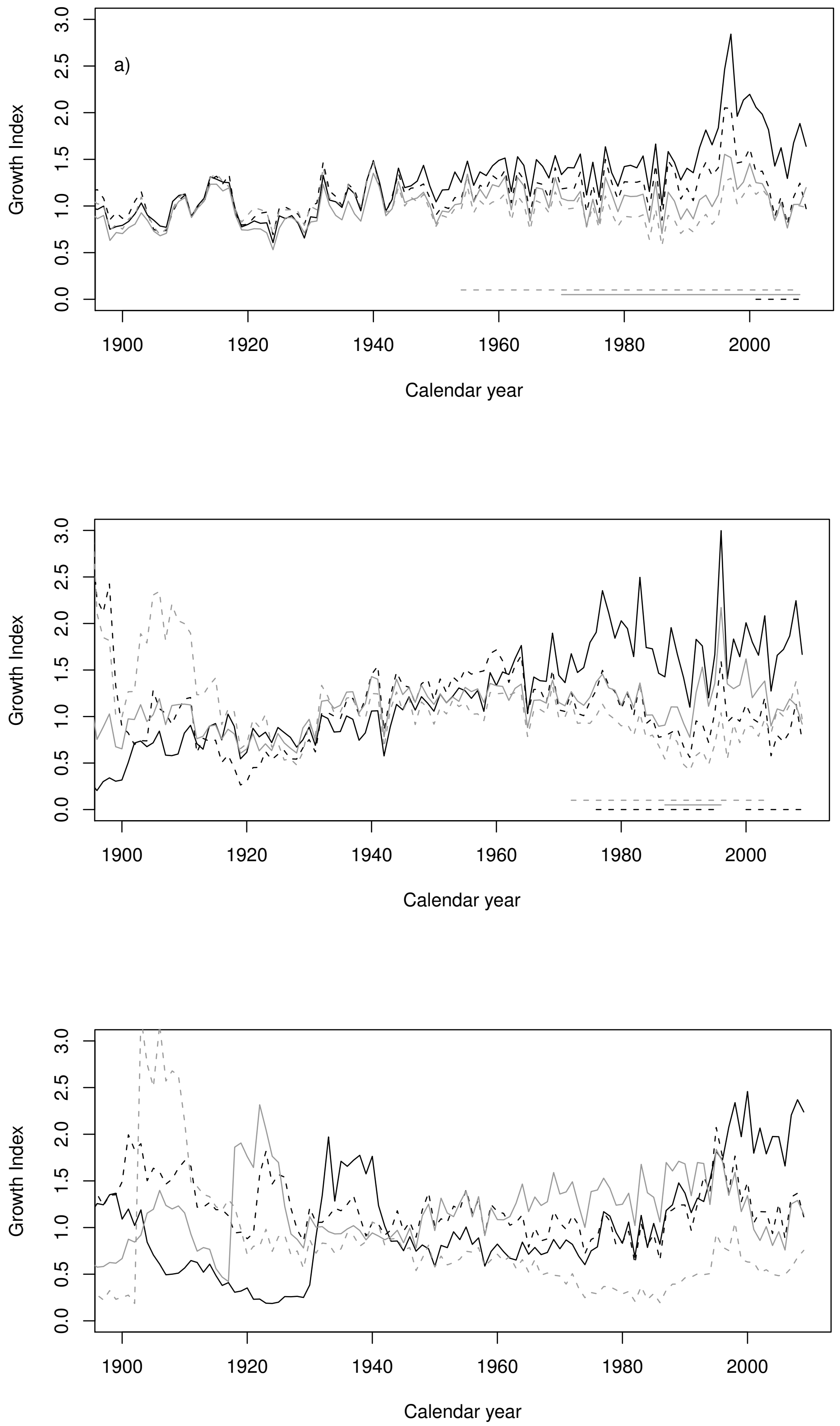

Fig 4: Evolution of growth indices with time of trees with different sapwood area on Mont Ventoux (a), Issole (b) and Vésubie (c). Empty black line: ResSA>1.2; Dotted black line: 1<ResSA<1.2; Grey line: 0.8<ResSA<1; Grey dotted line: ResSA<0.8. Horizontal bars indicates significant differences between each class of crown damage and healthy trees (unpaired t.test; p<0.1)

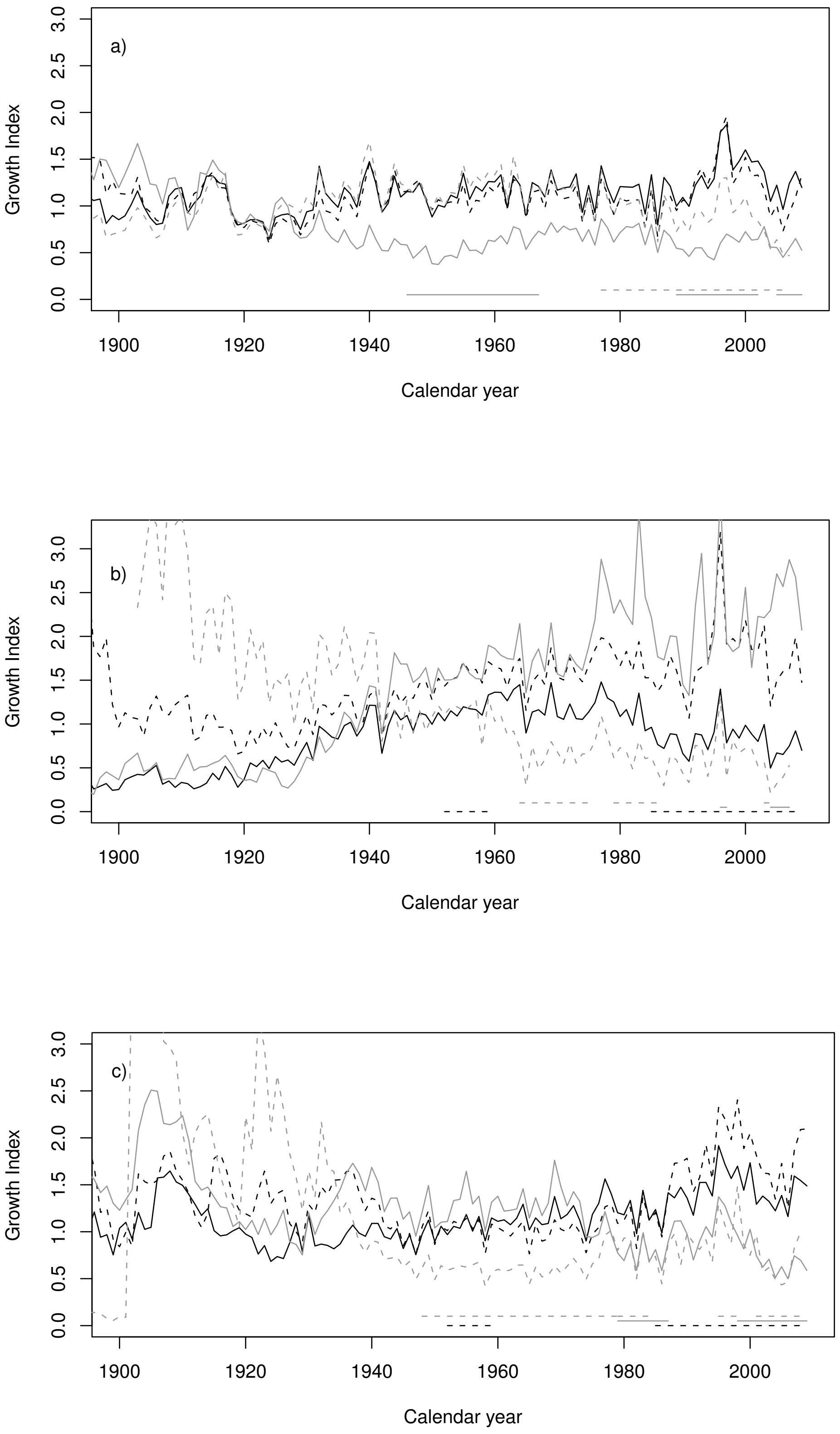

Fig 5: Evolution of growth indices with time of trees with different crown condition on Mont Ventoux (a), Issole (b) and Vésubie (c): Healthy trees (class 0; Empty black line); declining trees (class 1; Dotted black line); severely declining trees (class 2; Grey line) and dead trees (class 3; Grey dotted line). Horizontal bars indicates significant differences between each class of crown damage and healthy trees (unpaired t.test; p<0.1)

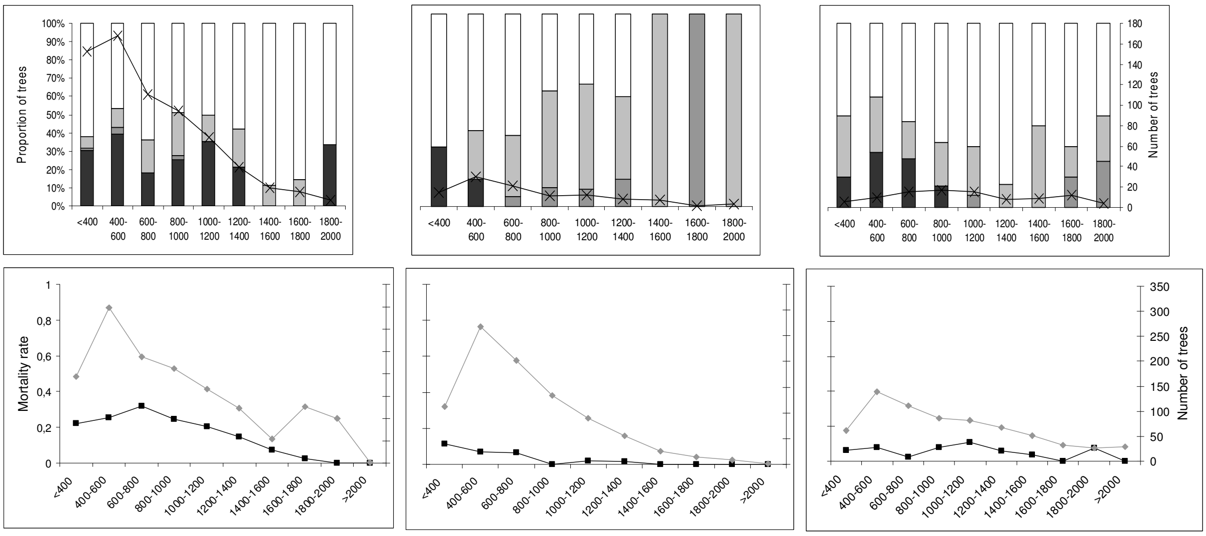

Fig 6a (up): Proportion of dead (black histogram), very declining (dark grey), declining (grey) and healthy (white) trees for each circumference class, and corresponding number of trees cored (black line with crosses) on Mont Ventoux (left), Issole (middle) and Vésubie (right). **Fig 6b (bottom)**: Number of firs mapped and measured during the forest inventory per circumference class (mm; grey), and corresponding proportion of dead firs (black) on Mont Ventoux, Issole and Vésubie

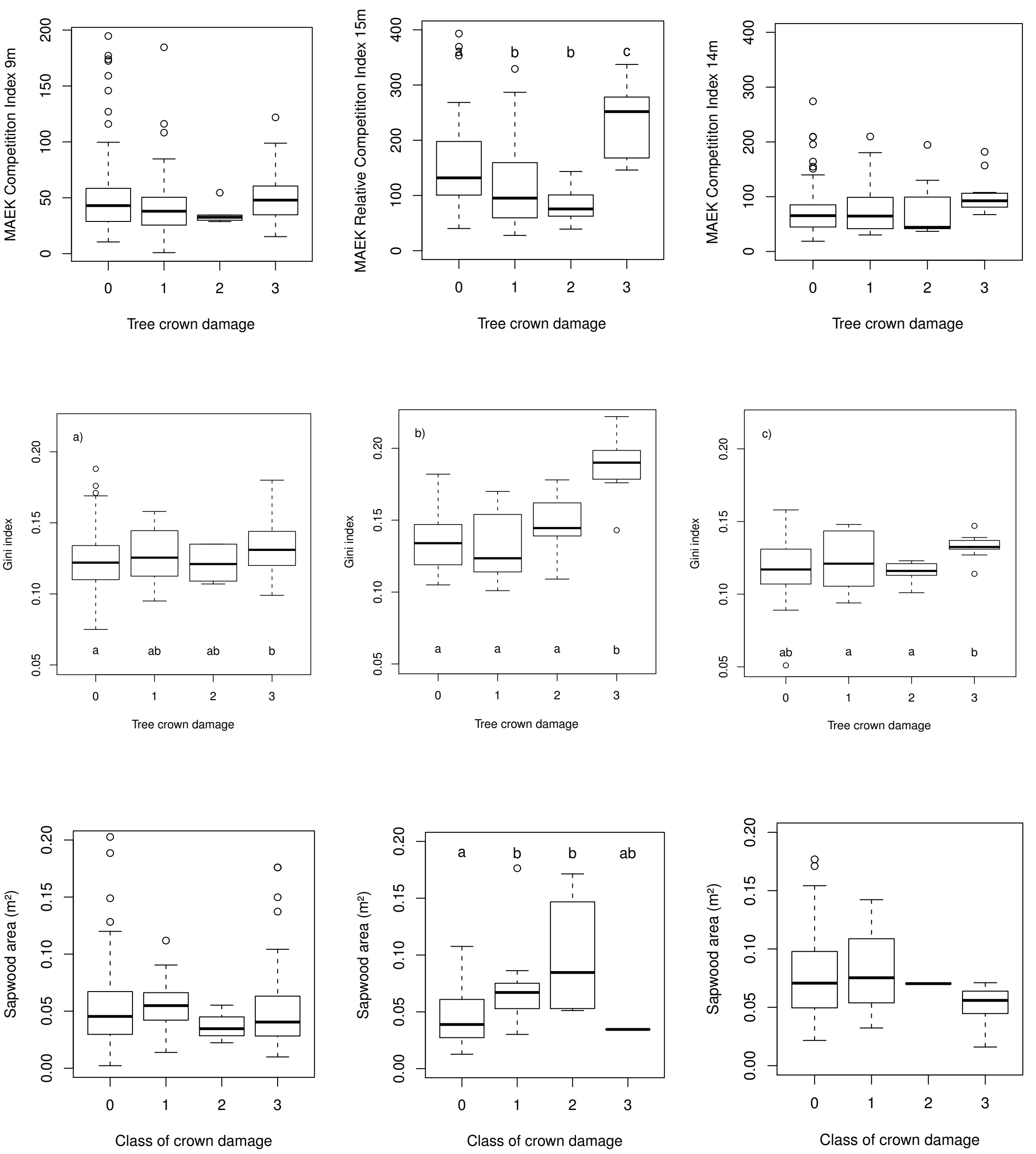

Fig 7a: Relationships between tree crown damage and the relative degree of competition experienced by these trees (RCI_{on_stumps}; MAEK equation) on Mont Ventoux (left), Issole (middle) and Vésubie (right). Different letters indicates significant differences between classes (Tukey HSD, $p<0.05$). **Fig 7b:** Relationships between tree crown damage (0, 1, 2…) and the Gini index on Mont Ventoux (left), Issole (middle) and Vésubie (right). Different letters indicates significant differences between classes (Tukey HSD, $p<0.05$). **Fig 7c**: Relationship between tree crown damage and sapwood area on Mont Ventoux (red), Issole (green) and Vésubie (blue)

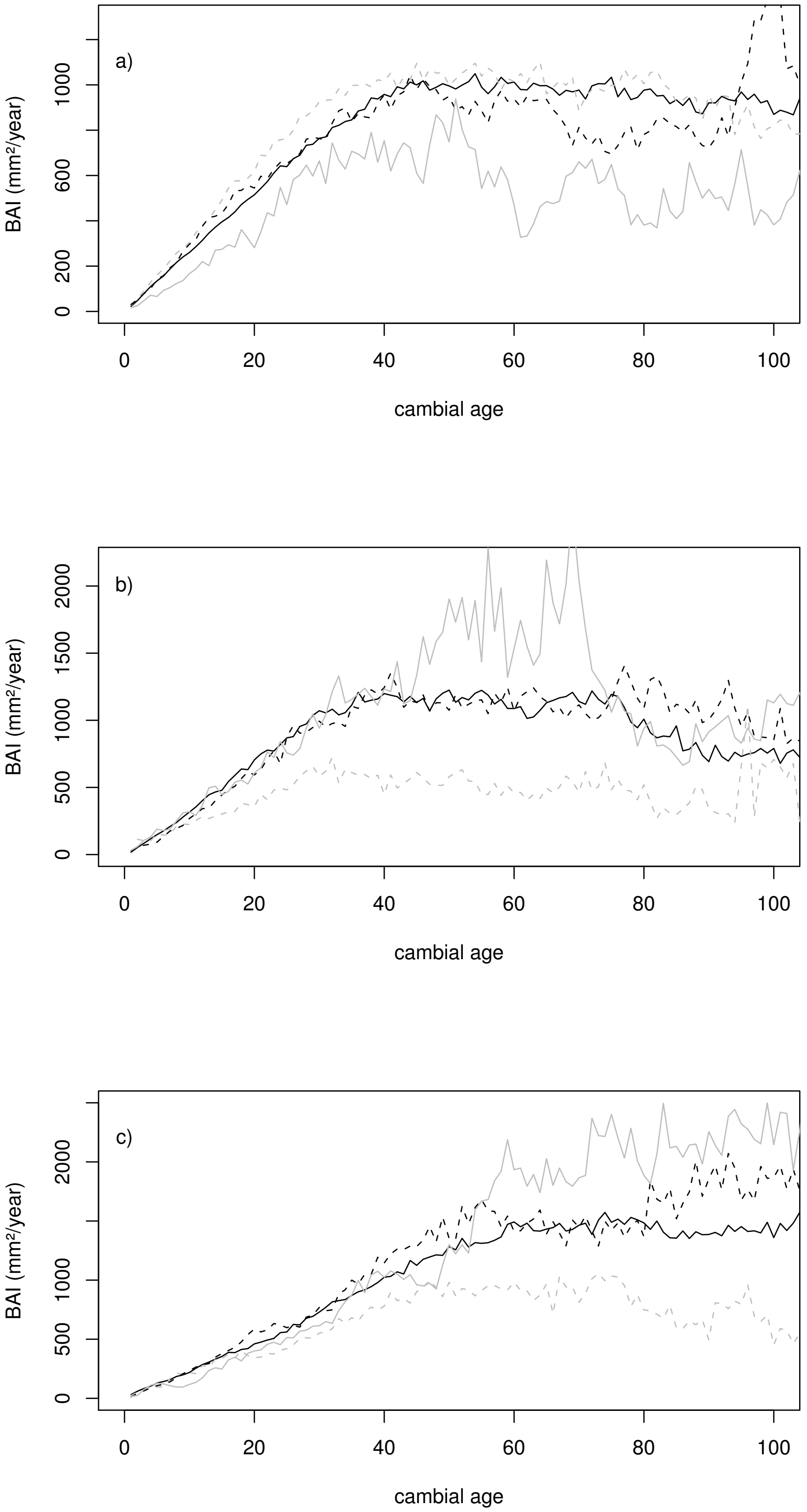

Fig 8: Evolution of tree basal area increment (BAI) with tree cambial age of trees with different crown condition: Healthy trees (class 0; Empty black line); declining trees (class 1; Dotted black line); severely declining trees (class 2; Grey line) and dead trees (class 3; Grey dotted line), on Mont Ventoux (a), Issole (b) and Vésubie (c).

Supplementary material

Tab S1: Coefficients of the best general linear models between sapwood area and diverse tree parameters (Basal Area, cambial age, altitude, Distance/Diameter Ratio competition index) for trees growing on Mont Ventoux, Issole and Vésubie. Models were chosen using a stepwise algorithm minimizing AIC (AIC Ventoux=5698; AIC Issole=1575.8; AIC Vesubie=548.9).

	Ventoux			Issole			Vesubie		
	Estimate	Std Error	p	Estimate	Std Error	p	Estimate	Std Error	p
Intercept	$-1.18.10^{3}$	$5.78.10^{3}$	NS	$1.09.10^{5}$	$6.44.10^{4}$	.	$-1.95.10^{5}$	$9.10.10^{4}$	*
BA	$7.51.10^{-1}$	$7.66.10^{-2}$	***	$2.91.10^{-1}$	$1.19.10^{-1}$	*	$5.39.10^{-1}$	$2.50.10^{-1}$	*
age	$2.94.10^{1}$	$6.29.10^{1}$	NS	$-6.95.10^{2}$	$2.44.10^{2}$	**	$-1.52.10^{3}$	$8.23.10^{2}$	.
alt				$-2.78.10^{1}$	$3.60.10^{1}$	NS	$2.30.10^{2}$	$9.61.10^{1}$	*
CI	$-9.05.10^{-1}$	$6.24.10^{-1}$	NS	$-4.22.10^{1}$	$1.69.10^{1}$	*	$3.94.10^{1}$	$3.64.10^{1}$	NS
BA*age	$-1.51.10^{-3}$	$6.18.10^{-4}$	*	$1.59.10^{-3}$	$1.13.10^{-3}$	NS	$-9.57.10^{-3}$	$1.83.10^{-3}$	***
BA*alt							$9.32.10^{-4}$	$3.39.10^{-4}$	*
age*CI				$-2.36.10^{-1}$	$7.20.10^{-2}$	**	$8.09.10^{-1}$	$3.21.10^{-1}$	*
alt*CI				$1.63.10^{-2}$	$8.94.10^{-3}$	.	$-8.24.10^{-2}$	$3.62.10^{-2}$	*

Annexe 3

Global change induces contradictory age effects on tree-ring growth sensitivity to climate

Cailleret M[1], Bert D[2], Davi H[1]

[1]INRA, URFM, UR 629, Domaine Saint Paul, Site Agroparc, F-84914 Avignon Cedex 9.
[2]INRA, BIOGECO, UMR 1202, F-33612 Cestas, France

En préparation pour *Trees, Structure and Function*

Abstract

Classical dendroclimatic studies generally assume that climate–growth relationships are age independent after removing the biological growth trend. However, as hydraulic conductivity, photosynthetic capacities and carbon allocation change with tree aging, this correction might be inadequate to quantify growth sensitivity to climate. Numerous studies have reported an age effect on sensitivity to climate, but there is no general agreement concerning the direction of this relationship. In some cases the climatic signal was maximized in older trees, while it is the reverse in others. This question is here addressed for *Abies alba* Mill. in two contrasting sites (north and south of France). The evolution with time of mean sensitivity (MS) was analyzed by separating the effects of tree aging and global change by categorizing trees in three age classes <60years (juvenile), 60-120y (adult), >120y (mature). MS increased with tree aging whatever tree age or study site. But the relationship between final MS (calculated from all the rings of the chronology) and tree age differs between sites, depending on how the main growth-limiting factors have evolved with global change. At both sites juvenile trees showed lower MS. When environmental constraints increased (southern site), the increase in MS was higher in adult trees than in mature trees which led to a negative relationship between final MS and tree age. In contrast, a decrease in environmental constraints (northern site) induced a positive relationship. Consequently, our study suggests that comparing final MS of different age-classes' trees is inappropriate for the analysis of the effect of tree aging on sensitivity to climate.

Keywords: Growth; Mean Sensitivity; Age effect; *Abies alba*; Global change; Tree rings.

Introduction

Individual tree growth is mainly dependent on climate, past year's growth, tree age, water availability, soil fertility and on the level of competition. Radial growth is characterized by its average value throughout a tree's life, but also by its inter-annual variability. To estimate this year-to-year variability, most dendrochronological studies have used tree mean sensitivity (MS) calculated either for each individual ring chronology or for the master chronology of a population. MS describes the mean percentage of change between each ring width and the next and is supposed to reflect tree sensitivity to environmental changes, especially inter-annual climatic variation (Fritts 1976). This index reveals the quantitative impact of stressful and also favourable conditions on tree growth. For example, if the main growth-limiting factor is soil water content during summer, a high MS value indicates that the tree is obviously sensitive to summer drought but also to water surplus. In contrast, complacent trees show a low degree of annual growth variation and consequently low MS values (Schweingruber 1989). MS index is also related to climate-growth relationships: the higher the MS value, the better the correlation value (or response function) between ring-widths and climatic variables. Thus, high MS values and uniformity in the biological responses to limiting conditions among individuals are advantageous characteristics for dendroclimatic studies and past climate reconstructions (Esper et al. 2008).

MS differs between species according to their functioning and strategies (Friedrichs et al. 2009). Within a species, site conditions (Szeicz and MacDonald 1994; Levanič et al. 2009), stand density (Gea-Izquierdo et al. 2009), tree suppression (Martín Benito et al. 2008), sex (Rozas et al. 2009) and genetic predisposition (Sánchez-Vargas et al. 2007) can effect tree sensitivity to climate.

Most dendroclimatic and dendroecological analyses have assumed that climate–growth relationships are age/size independent after removing the medium and low frequencies of the tree-ring chronologies (Szeicz and MacDonald 1994). But ecophysiological studies suggest that growth-related environmental signals are likely to evolve with tree age (size), especially due to the increase in hydraulic constraints (Mencuccini et al. 2005).

Studies that have investigated whether climate–growth response changes with tree age show contrasting results, e.g., (i) the climatic signal may be maximized in older trees (Szeicz and MacDonald 1994; Ettl and Peterson 1995; Carrer and Urbinati 2004; Rossi et al. 2008). Yu et al. (2008) have found that Qilian juniper trees (*Sabina przewalskii* Kom.) less than 200 years old were less sensitive than older trees. Wang et al. (2009) showed that for *Larix gmelinii* MS increased with age in the <150 years age class, whereas older trees showed no significant relationship between MS and age. (ii) Conversely, tree-ring widths of young trees may be more sensitive to climate influence (De Luis et al. 2009; Rozas et al. 2009; Vieira et al. 2009). (iii) Finally, there may be no significant change in climatic signal when young and old trees are compared (Fritts 1976; Esper et al. 2008). Esper et al. (2008) explained that these opposing conclusions are likely related to the number of samples analyzed, especially in the young age class.

These divergent responses may also be due to the technique used to determine the age effect on tree sensitivity to climate. It can be analyzed using the relationship between tree age and the final MS value calculated using all the ring chronology, or by comparing climate-growth relationships of different tree ages (synchronic analysis). However these inter-individual analyses do not separate the effects of tree aging and environmental changes, and the interaction between both effects. To our knowledge, few works have studied the evolution of MS with aging (diachronic analysis) and with calendar year, while growth patterns have changed during recent decades due to global change. Increases in radial growth were found during the 20th century (Badeau et al. 1996; Boisvenue and Running 2006; Martinez Vilalta et al. 2008) likely due to increasing temperatures, CO_2 fertilization and nitrogen deposition; while some declines were reported in the Mediterranean region due to reduced precipitation (Sarris et al. 2007; Piovesan et al. 2008). High growth sensitivity to climate was found in water-limited zones (Macias et al. 2006; Andreu et al. 2007), whereas reduced sensitivity was reported for trees growing at high latitudes (Briffa et al. 1998, Linderholm and Linderholm 2004) or high altitude (Buntgen et al. 2008). These recent changes in radial growth sensitivity can also be function of tree age. Young trees are assumed to be more sensitive to changes in climate (Suarez et al. 2004) because they have less access to permanent ground water sources (Caspersen and Kobe 2001). Conversely, older trees have access to permanent ground water sources and may be less impacted by reduced precipitation.

The aims of the present study were to explain the contradictory age effects on tree sensitivity to climate observed in the literature by analyzing the evolution of MS of *Abies alba* (i) with tree aging, (ii) with time, and (iii) by study site. We have re-examined tree-ring data of silver firs from two study sites with different climatic conditions to disentangle all these effects on MS. One group of trees was sampled for a dendroecological study by Bert (1992, 1993) in the Jura Mountains, where the climate is typically semi-continental. The other study site was on Mont Ventoux, a Mediterranean mountain located in the xeric range of silver fir distribution (Cailleret and Davi in revision).

Materials and methods

Study species

Silver fir *(Abies alba* Mill.) is a shade-tolerant conifer distributed through the mountainous regions of France (Pyrénées, Vosges, Jura, Massif-Central, Alps), and currently expanding its range due to pastoral abandonment and forest maturation. This species requires high atmospheric humidity but does not tolerate waterlogged soils. Although silver fir needles persist for seven to nine years, which is usually linked to higher growth inertia and lower climatic sensitivity, MS values generally range between 0.15 and 0.25 (Desplanque et al. 1998; Lebourgeois 2007; Cailleret and Davi in revision). These high MS values indicate that the species is sensitive to resource availability, to variation in environmental conditions, including climate (Battipaglia et al. 2009), and is highly suitable for dendroclimatological analysis.

Study sites.

Analyses were carried out using cores collected for previous dendroecological studies on Mont Ventoux (44°11'N; 5°17'E), a calcareous mountain located in the southwestern Alps, 1909 m above sea level (a.s.l.), and in the Jura mountains on the border between France and Switzerland (Fig 1). The sampling in the Jura consists of 1235 trees from 208 plots located between 550 and 1350m a.s.l (described by Bert 1992; 1993). On Mont Ventoux 300 trees were sampled on the north slope: 73 along an altitudinal transect between 950 and 1500 m (Cailleret and Davi, in revision), and 227 located in 16 plots distributed between 1100 and 1140m. The study sites on Mont Ventoux are under selective forest management, whereas the study sites in the Jura mountains are either even-aged stands or under selective forest management. To remove the effect of current social status, all trees studied were dominant or co-dominant.

Sampling and measurements

Each tree was bored to the pith at breast height (130cm) in 1989 in the Jura Mountains, and between 2006 and 2008 on Mont Ventoux. The cores were planed with a razor blade. Ring-widths were measured at the precision of 0.01 mm using a digitizing table coupled to a computer for the Jura data, and a scanner (1200 dpi) and the software CDendro v5.3 and CooRecorder 5.3 (Cybis Elektronik & Data AB. Sweden) for the Ventoux data. False and missing rings were detected by crossdating using pointer years and correlation values calculated between individual and mean chronologies. When a core did not reach the pith, the number of missing rings and the total missing width were estimated. Cores that were sampled far away from the pith (more than fifty missing rings to the pith) were excluded due to low reliability in estimating age. All estimated ages were cambial age at breast height.

Mean sensitivity calculation

Individual ring-width series were standardized in a two-step proceeding using the ARSTAN software (Holmes 1994). First, a negative exponential curve or a linear regression line was fitted to remove long-term trends. Second, more flexible detrending was undertaken using a cubic smoothing line with a 50% frequency response over 75 years. To obtain residual chronologies, autocorrelation was removed using autoregressive models of specific order for each individual series. For all residual series, Mean Sensitivities (MS) were calculated to characterize relative intensity of year-to-year changes in growth (Fritts 1976), using Visual Basic proceedings.

$$MS = \frac{1}{n-1} \sum_{t=1}^{t=n-1} \left| \frac{2(x_{t+1} - x_{t})}{x_{t+1} + x_{t}} \right|$$

where x_t and x_{t+1} are the ring indices for the years t and t+1, and n is the number of tree-ring series. Two types of measurements were made. Firstly, the value of *final MS* (MSf) was calculated for each individual using all the tree rings of the chronology. Secondly, to estimate temporal evolution with tree aging for each individual, a *current MS* (MSc) was calculated at each cambial age in a cumulative way, using all previous and current ring indices. For example, only the ten first rings were used to determine the MSc value at nine years old. Thus, the real impact of tree aging may be revealed by analyzing the temporal evolution of MSc values calculated for each year. As this calculation is cumulative, the last (final) value of MSc corresponds to the MSf value; and the higher the number of tree rings used for the process, the lower the year-to-year change of MSc. Trees with extreme MS values, generally due to many missing years, were removed from the analysis.

The change in MSc with tree aging was quantified by the slope of the linear regression between MSc and tree age ($S_{MSc\text{-}aging}$). MSc for the five first years was not included in the calculation of $S_{MSc\text{-}aging}$ because the low number of ring-widths used for this five year calculation makes the value unreliable. MSc was considered to evolve with tree aging when $S_{MSc\text{-}aging}$ was statistically significant at the level of 95% (negative or positive).

The method applied to estimate the global change effect on MS was close to the constant age method. This method quantifies changes in the age-specific MS behaviour in a certain calendar year. This analysis was performed for three different age classes: juvenile trees younger than 60 years; adults between 60 and 120 years and mature trees older than 120 years. A tree that germinated in 1850 was successively considered a juvenile until 1910, adult between 1910 and 1970, and mature after 1970. These classes were defined according to physiological changes observed in the Jura Mountains: Basal Area Increment and $\delta^{13}C$ rise up to age 60, and respectively slightly decreased and kept constant afterwards (Bert et al. 1997).

To confirm that the differences in MSf trends between Mont Ventoux and the Jura Mountains were due to differences in site conditions, trees located on dry and wet stations in the Jura were studied separately. Dry stations correspond to Typical and Neutrophileous *Carici-Fagetum*, and wet stations to Mesophileous and Hygrophileous *Abieti-Fagetum* (Bert 1992). All statistical analyses were made using the statistical software R (R for Windows version 2.8.0; R Development Core Team 2008).

Results

Silver firs growing on Mont Ventoux were slightly younger than in those located in the Jura mountains (respectively 88.6 and 92.6 years old; $p=0.086$), but showed equivalent mean sensitivity to environmental changes on average (mean MSf = 0.253 for both; $p>0.1$).

MSc evolution with tree aging

The temporal analysis of the change in MSc (cumulative value calculated at each age) with aging was made for each tree. Young trees showed a stronger trend in MSc change during their life (more negative and more positive $S_{MSc\text{-aging}}$ values) compared to old trees, and higher inter-individual variability (Fig. 2a and 2b). For most trees, MS increased with aging. A significant positive slope was found for 72% and 61% of trees growing on Mont Ventoux and in the Jura Mountains respectively, while it was significantly negative for only 14% and 27%. Comparison of the three age classes indicated that juvenile trees showed a greater increase in MSc during their life than adult and mature trees (Table 1). This trend was apparent for both sites but was stronger on Mont Ventoux where juvenile trees showed a greater increase in MSc with aging than was found in the Jura Mountains ($S_{MSc\text{-aging}} = 10.9.10^{-4}$ vs $5.98.10^{-4}$).

MSc evolution with date

Using an approach close to the constant age method which removes the age effect, MSc was found to decrease on both sites until the 1940s, but has evolved differently afterwards. On Mont Ventoux MSc has increased since the 1960s, especially for adult trees (Fig. 3a). This change in MS was combined with an increase in mean annual temperatures on the order of 0.4°C per decade. This temperature trend was stronger during summer months and was associated with a decrease in summer rainfall since the 1980s (Cailleret and Davi in revision). In contrast, in the Jura Mountains there was no clear change in the MSc values and between 1940 and 1988 (Fig. 3b). In the Jura Mountains the increase in mean annual temperature was only 0.1°C per decade and was more pronounced in autumn and winter (Bert 1992; Lenoir et al. 2008). Moreover, no significant change has been reported for annual summer precipitation.

Age effect on MSf

The relationship between final MS (MSf) and tree age differs between sites. Growth during the juvenile phase (until 60 years old) was characterized by low MSf values on Mont Ventoux and at the dry stations in the Jura Mountains (Fig. 4a; low intercept value in Table 1), however this is not the case when all of the Jura sites were combined or for the wet stations alone (Fig 4b). For the adult and mature phases (after 60 years old) the relationship between tree age and MSf was negative on Mont Ventoux, but positive in the Jura Mountains (Fig. 4a, 4b and Table 1). Evidence of differences between site conditions was supported by the comparison of dry and wet stands in the Jura Mountains. In dry conditions the relationship between MSf and tree age was not significant for trees older than 60 years (slope = $1.14.10^{-4}$; $p>0.1$), while it was positive and significant in the wet stands (slope = $3.72.10^{-4}$; $p<0.001$).

Interaction between Age and Date effects on MSc and MSf

The interaction between age and date effects was observed in particular on Mont Ventoux by changes in the relationship between age and MSc over time (Fig 4a). Before 1960, MSc was observed to increase with tree age. However, as adult trees showed a stronger increase in MS than mature trees between 1960 and 1989 (Fig. 3a), the relationship was negative in 1989 and 2008 (if juvenile trees are excluded). In contrast, the relationship between MSc and age was positive throughout the study period in the Jura Mountains (Fig. 4b). This can be explained by the lack of variation between the age classes in their changes in MSc with time (Fig. 3b).

Discussion

This study provides a detailed analysis of the effect of tree age on the sensitivity of silver fir growth to environmental changes. Two sites with different climatic conditions and evolution were analyzed to separate the effects of tree aging and environmental changes on MS. The methodology used in this study was tested on silver fir because of its high sensitivity to climate and environmental changes but it may be applied to other species.

MS evolution with tree aging

Changes in MS can be caused directly by an increase in climate effects on growth, but may also be due to a higher intrinsec increase in growth variability not correlated with environmental conditions. MS change with tree aging was quantified by the calculation of MS year after year (MSc). This methodology was applied because it more effectively revealed the effect of tree aging than the classical relationship between MSf and tree age. Our results indicate that most individuals showed an increase in their sensitivity to climate with aging

(Table 1 and Fig 1a, 1b). The reason for an age-dependent response of growth sensitivity to climate is likely to be environmental and physiological changes during tree aging. First, for juvenile trees the main growth-limiting factors were not related to climate but to the level of competition for light and soil resources. Their importance changed with tree growth, and the correlation between inter-annual growth variability and climate increased. Aging is also associated with physiological changes (Bert et al. 1997; Mencuccini et al. 2005). Ryan and Yoder (1997) suggested that water transport is the main physiological challenge when trees grow in height. The total resistance of the hydraulic pathway increases as the tree approaches its maximum height due to many factors including gravity and a longer and more complex hydraulic path length through stems and branches. The increase in hydraulic resistance can also lower the supply of water for transpiration and directly induce earlier stomatal closure (Ryan and Yoder 1997), which in turn limits photosynthetic rates (Hubbard et al. 1999). This mechanism is not totally compensated for by a deeper root system, and may be exacerbated by an increase in nutrient limitation with tree age (Martinez Vivalta et al. 2007). Tree growth variability may also increase due to the investment in reproduction in certain years (Mencuccini et al. 2005), and because of the shorter window of the tree-ring production (Rossi et al. 2008).

Global change impact on MS

Global change has been shown to affect tree radial growth on average; and it may also impact its variability; i.e. tree mean sensitivity to environmental conditions. In the Jura Mountains water availability was the primary growth-limiting factor (Bert 1992). Radial growth mainly depended on water supply during early summer of the growing season (May to July) and at the end of the previous summer (August – September; Bert 1992). However, annual ring formation was also negatively influenced by low winter temperatures (January – February).

Consequently the increases in winter temperatures, atmospheric CO_2, and nitrogen deposition observed between 1880 and 1988 in the Jura Mountains have reduced the main growth-limiting factors, particularly because summer rainfalls have not declined. Constant age methods revealed that this has led to an increase in silver fir radial growth (Badeau et al. 1996). Silver fir's sensitivity to enviromental conditions also decreased up to the 1940s and has not significantly changed since then (Fig. 3a). Growth of silver firs located on Mont Ventoux were mainly controlled by the same climatic variables (Cailleret and Davi in revision). However, as in all the Mediterranean region, there has been an increase in summer drought intensity, frequency and duration due to a rise in summer temperatures and decrease in summer rainfalls (Sarris et al. 2007; Piovesan et al. 2008; Cailleret and Davi in revision). This increase in importance of the main-growth limiting factor at the Mont Ventoux site has caused a decrease in tree radial growth (Cailleret and Davi in revision), but also an increase in MSc with date (Fig. 3b).

Interaction between age and date effects

The relationship between MSc and tree age was nearly constant over time in the Jura Mountains, whereas on Mont Ventoux juvenile and mature trees showed a lower increase in MSc than adult trees in the time since the 1960s (Fig. 3a). This result may be explained first because juvenile growth is mostly related to the degree of competition and therefore, changes in climate conditions did not significantly affect it, and changes in MSc should be low on average. The high variability in MSc changes among juvenile trees might be due to changes in available light caused by the harvest or the death of a neighbouring tree (Fig. 2a, 2b). Second, the low increase in MSc for adult trees is likely due to the method of MS calculation which is "cumulative" and thus the higher the number of tree rings used to calculate MSc the lower the year-per-year change (Fig. 2a, 2b).

On Mont Ventoux, MSc increased due to the increase in the main growth limiting factor, summer drought. As MSc of adult trees changed more quickly than for mature trees, the increase in MSc was greater, and led to a negative relationship between MSf and tree age (Table 1; Fig. 5, scenario a). The slightly positive relationship found at the dry stations in the Jura Mountains strengthens this hypothesis (Table 1). In these sites trees did not benefit from temperatures rising because there was also an increase in summer evapotranspiration and drought. In contrast, in the Jura Mountains, especially in the wet stations, the decrease in the main growth limiting factor, low temperatures, led to a decrease in MSc for all tree age classes. Thus, the relationship between MSf and tree age remained positive (Table 1; Fig. 5, scenario b).

Likely causes of the contradictory age effects on MSf

Previous studies focusing on age-dependent tree ring growth response to climate found various conclusions. These differing results can partially be related to the sampling method. According to Esper et al. (2008), climate signal age effects are replication-sensitive and require equal sampling of young and old trees to reach comparable signal strengths, which was not the case in previous studies. Equally, using age-stratified samples does not allow complete separation of the confounding effects of size and age due to environmental factors (De Luis et al. 2009). However, age-dependent responses may also be site-specific (Szeicz and MacDonald 1994; Levanič et al. 2009), and depend on variation in the strength of the main growth limiting factors (Fig. 5). Two possible scenarios emerge from our results:

1. Studies which have shown that younger trees are more sensitive to climate were carried out in the Mediterranean area: on *Pinus pinaster* in Portugal (Vieira et al. 2009) and *Juniperus thurifera* in Spain (Rozas et al. 2009). In these zones the main growth limiting factor is summer water stress. In central Spain, summer drought has

increased since 1961 due to the combination of decreases in summer rainfalls and rising temperatures (DelRio et al. 2005). In Portugal, climate is warming since 1976 and only March rainfalls are declining (Miranda et al. 2002). In these cases, the comparison of MSf values calculated on different age trees revealed a negative relationship between MSf and Age (Fig. 5, scenario a)

2. Studies where the climatic signal was maximized in older trees tended to be undertaken at high altitude or latitude. With rising temperatures and nitrogen deposition the intensity of the main growth limiting factor decreased. For example Carrer and Urbinati (2004) found an increase in MSf with age for *Larix decidua* until 200 years old in a high altitudinal site in Italy. This result was connected with rising temperatures, especially at the end of the 20th century (Brunetti et al. 2004). Equally, results found by Wang et al. (2009), and Yu et al. (2008) at high altitude sites were related to an increase in mean annual temperatures during the last century (Shi et al. 2007; Qian et al. 2001). Thus, the relationship between age and MSf was positive (Fig. 5, scenario b).

Our findings indicate that previous contradictory results on the effect of age on tree sensitivity to climate can be linked to the diverse growth limiting factors at different sites and changes in the strength from these factors. We show that the comparison of MSf calculated for the entire chronology for trees at different ages is an inappropriate method for analyzing the impact of tree aging on its sensitivity to climate. The calculation of MSc year per year seems to be preferable. Further research is needed to test our hypotheses, for example by analyzing a larger tree ring network (more species in contrasting environments) using the same methodology. In addition, studying the change in MS with tree aging in different situations and under diverse climatic scenarios using process-based models can provide a better understanding of the physiological processes linked with tree aging.

Acknowledgements

The authors wish to thank Nicolas Mariotte, William Brunetto and Florence Courdier for their support in the field on Mont Ventoux, and are grateful to Tonya Lander for english correction. Thanks are also due to Michel Becker, Roger Schipfer, François Geremia, and to the International Tree Ring Data Bank for the tree ring data in the Jura Mountains. This study was supported by the French National Research Agency (ANR) in the framework of the DRYADE program.

References

Andreu L, Gutiérrez E, Macias M, Ribas M, Bosch O, Camarero JJ (2007) Climate increases regional tree-growth variability in Iberian pine forests. Glob Change Biol 13:804-815

Badeau V, Becker M, Bert D, Dupouey JL, Lebourgeois F, Picard JF (1996) Long-term growth trends of trees : ten years of dendrochronological studies in France. In Spiecker H, Mielikänen K, Köhl M and Skovsgaard JP (ed) Growth trends in European forests, Springer-Verlag Berlin Heidelberg, European Forest Institute Research Report, pp 167-181

Battipaglia G, Saurer M, Cherubini P, Siegwolf RTW, Cotrufo MF (2009) Tree rings indicate different drought resistance of a native (*Abies alba* Mill.) and a nonnative (*Picea abies* (L.) Karst.) species co-occurring at a dry site in Southern Italy. For Eco Manag 257:820-828. doi:10.1016/j.foreco.2008.10.015

Bert D (1992) Influence du climat, des facteurs stationnels et de la pollution sur la croissance et l'état sanitaire du sapin pectiné (*Abies alba* Mill.) dans le Jura. Etude phytoécologique et dendrochronologique. PhD Thesis. Université de Nancy I Henry Poincaré. France

Bert D (1993) Impact of ecological factors, climatic stresses, and pollution on growth and health of silver fir (*Abies alba* Mill.) in the Jura Mountains: an ecological and dendrochronological study. Acta Oecologica 14:229-246

Bert D, Becker M (1990) Vitalité actuelle et passée du sapin (*Abies alba* Mill.) dans le Jura. Etude dendroécologique. Ann For Sci 47:395-412

Bert D, Leavitt SW, Dupouey JL (1997) Variations of wood $\delta^{13}C$ and water-use efficiency of *Abies alba* during the last century. Ecology 78:1588-1596

Boisvenue C, Running SW (2006) Impacts of climate change on natural forest productivity – evidence since the middle of the 20th century. Glob Change Biol 12:862-882

Briffa KR, Schweingruber FH, Jones PD, Osborn TJ, Shiyatov SG, Vaganov EA (1998) Reduced sensitivity of recent tree-growth to temperature at high northern latitudes. Nature 391:678-682

Brunetti M, Buffoni L, Mangianti F, Maugeri M, Nanni T (2004) Temperature, precipitation and extreme events during the last century in Italy. Glob Planet Change 40:141-149

Büntgen U, Frank D, Wilson R, Carrer M, Urbinati C, Esper J (2008) Testing for tree-ring divergence in the European Alps. Glob Change Biol 14:2443-2453. doi:10.1111/j.1365-2486.2008.01640.x

Cailleret M, Davi H (in revision) How climate impacts the growth of two co-occurring species *Fagus sylvatica* and *Abies alba*: a case study along an altitudinal gradient. Trees

Carrer M, Urbinati C (2004) Age-dependent tree-ring growth responses to climate in *Larix decidua* and *Pinus cembra*. Ecology 85:730-740. doi:10.1890/02-0478

Caspersen JP, Kobe RK (2001) Interspecific variation in sapling mortality in relation to growth and soil moisture. Oikos 92:160–168

Del Río S, Penas A, Fraile R (2005) Analysis of recent climatic variations in Castile and Leon (Spain). Atm Res 73:69-85

De Luis M, Novak K, Čufar K, Raventós J (2009) Size mediated climate-growth relationships in *Pinus halepensis* and *Pinus pinea*. Trees. doi :10.1007/s00468-009-0349-5

Desplanque C, Rolland C, Michalet R (1998) Dendroécologie comparée du sapin blanc (*Abies alba*) et de l'épicéa commun (*Picea abies*) dans une vallée alpine de France. Can J For Res 28:737-748

Esper J, Niederer R, Bebi P, Frank D (2008) Climate signal age effects – Evidence from young and old trees in the Swiss Engaldin. For Eco Manag 255:3783-3789

Ettl GL, Peterson DL (1995) Extreme climate and variation in tree growth: individualistic response in subalpine fir (*Abies lasiocarpa*). Glob Change Biol 1:231–241.

Friedrichs DA, Trouet V, Büntgen U, Frank DC, Esper J, Neuwirth B, Löffler J (2009) Species-specific climate sensitivity of tree growth in Central-West Germany. Trees 23:729-739. doi : 10.1007/s00468-009-0315-2

Fritts HC (1976) Tree Rings and Climate. Academic Press, New York

Gea-Izquierdo G, Martín-Benito D, Cherubini P, Cañellas L (2009) Climate-growth variability in *Quercus ilex* L. west Iberian open woodlands of different stand density. Ann For Sci 66:802. doi: 10.1051/forest/2009080

Hubbard RM, Bond BJ, Ryan MG (1999) Evidence that hydraulic conductance limits photosynthesis in old *Pinus ponderosa* trees. Tree Physiol 19:165–172

Lebourgeois F (2007) Climatic signal in annual growth variation of silver fir (*Abies alba* Mill.) and spruce (*Picea abies* Karst.) from the French Permanent Plot Network (RENECOFOR). Ann For Sci 64:333-343

Lenoir J, Gégout JC, Marquet PA, de Ruffray P, Brisse H (2008) A significant upward shift in plant species optimum elevation during the 20th century. Science 320:1768-1771

Levanič T, Gričar J, Gagen M, Jalkanen R, Loader NJ, McCarroll D, Oven P, Robertson I (2009) The climate sensitivity of Norway spruce [*Picea abies* (L.) Karst.] in the southeastern European Alps. Trees 23:169-180. doi: 10.1007/s00468-008-0265-0

Linderholm HW, Linderholm K (2004) Age-dependent climate sensitivity of *Pinus sylvestris* L. in the central Scandinavian Mountains. Boreal Environ Res 9:307–317

Macias M, Andreu L, Bosch O, Camarero JJ, Gutiérrez E (2006) Increasing aridity is enhancing silver fir (*Abies alba* Mill.) in its south-western distribution limit. Clim Change 79:289-313

Martín-Benito D, Cherubini P, Del Río M, Cañellas I (2008) Growth response to climate and drought in *Pinus nigra* Arn. trees of different crown classes. Trees 22:363-373. doi:10.1007/s00468-007-0191-6

Martínez-Vilalta, J, Vanderklein D, Mencuccini M (2007) Tree height and age-related decline in growth in Scots pine (*Pinus sylvestris* L.). Oecologia 150:529-544. doi:10.1007/s00442-006-0552-7

Martínez-Vilalta J, López BC, Adell N, Badiella L, Ninyerola M (2008) Twentieth century increase of Scots pine radial growth in NE Spain shows strong climate interactions. Glob Change Biol 14:2868-2881. doi: 10.1111/j.1365-2486.2008.01685.x

Mencuccini M, Martinez-Vilalta J, Vanderklein D, Hamid HA, Korakaki E, Lee S, Michiels B (2005) Size mediated ageing reduces vigour in trees. Ecol Lett 8:1183–1190. doi:10.1111/j.1461-0248.2005.00819.x

Miranda PMA, Coelho FES, Tomé AR, Valente MA, Carvalho A, Pires C, Pires HO, Pires VC, Ramalho C (2002) 20th century Portuguese Climate and Climate Scenarios. In Santos FD, Forbes K, Moita R (ed) Climate Change in Portugal: Scenarios, Impacts and Adaptation Measures (SIAM Project), 23-83, Gradiva, 454 pp

Piovesan G, Biondi F, Di Filippo A, Alessandrini A, Maugeri M (2008) Drought-driven growth reduction in old beech (*Fagus sylvatica*) forests of the central Apennines, Italy. Glob Change Biol 14:1265-1281. doi: 10.1111/j.1365-2486.2008.01570.x

Qian W, Zhu Y (2001) Climate change in China form 1880 to 1998 and its impact on the environmental condition. Clim Change 50:419-444

Rossi S, Deslauriers A, Anfodillo T, Carrer M (2008) Age-dependent xylogenesis in timberline conifers. New Phytol 177:199–208. doi: 10.1111/j.1469-8137.2007.02235.x

Rozas V, DeSoto L, Olano JM (2009) Sex-specific, age-dependent sensitivity of tree-ring growth to climate in the dioecious tree *Juniperus thurifera*. New Phytol 182:687-697. doi: 10.1111/j.1469-8137.2009.02770.x

Ryan MG, Yoder BJ (1997) Hydraulic limits to tree height and tree growth. Bioscience 47:235–242. doi: 10.2307/1313077

Sánchez-Vargas NM, Sánchez L, Rozenberg P (2007) Plastic and adaptative response to weather events : a pilot study in a maritime pine tree ring. Can J For Res 37:2090-2095. doi: 10.1139/X07-075

Sarris, D, Christodoulakis, D, Körner, C (2007) Recent decline in precipitation and tree growth in the eastern Mediterranean. Glob Change Biol 13:1187-1200. doi: 10.1111/j.1365-2486.2007.01348.x

Schweingruber FH (1989) Tree Rings – Basics and Applications of Dendrochronology. Kluwer Academic Publishers, Dordrecht, Holland.

Shi Y, Shen Y, Kang E, Li D, Ding Y, Zhang G, Hu (2007) Recent and future climate change in northwest China. Clim Change 80:379-393

Suarez ML, Ghermandi L, Kitzberger T (2004) Factors predisposing episodic drought-induced tree mortality in *Nothofagus* – site, climatic sensitivity and growth trends. J Ecol 92:954-966

Szeicz JM, MacDonald GM (1994) Age-dependent tree-ring growth responses of subarctic white spruce to climate. Can J For Res 24:120-132

Vieira J, Campelo F, Nabais C (2009) Age-dependent responses of tree-ring growth and intra-annual density fluctuations of *Pinus pinaster* to Mediterranean climate. Trees 23:257-265. doi: 10.1007/s00468-008-0273-0

Wang X, Zhang Y, McRae DJ (2009) Spatial and age-dependent tree-ring growth reponses of *Larix gmelinii* to climate in northeastern China. Trees 23:875-885.doi:10.1007/s00468-009-0329-9

Wolf H (2003) EUFORGEN technical guidelines for genetic conservation and use of silver fir (*Abies alba*). International Plant Genetic Resources Institute, Rome, Italy

Yu G, Liu Y, Wang X, Ma K (2008) Age-dependent tree-ring growth responses to climate in Qilian juniper (*Sabina przewalskii* Kom.). Trees 22:197-204. doi: 10.1007/s00468-007-0170-y

Figures

Fig. 1: Geographical location of the study sites : the Jura mountains, eastern France, and Mont Ventoux, South-East France. Silver fir distribution is in grey (from the EUFORGEN network; Wolf 2003)

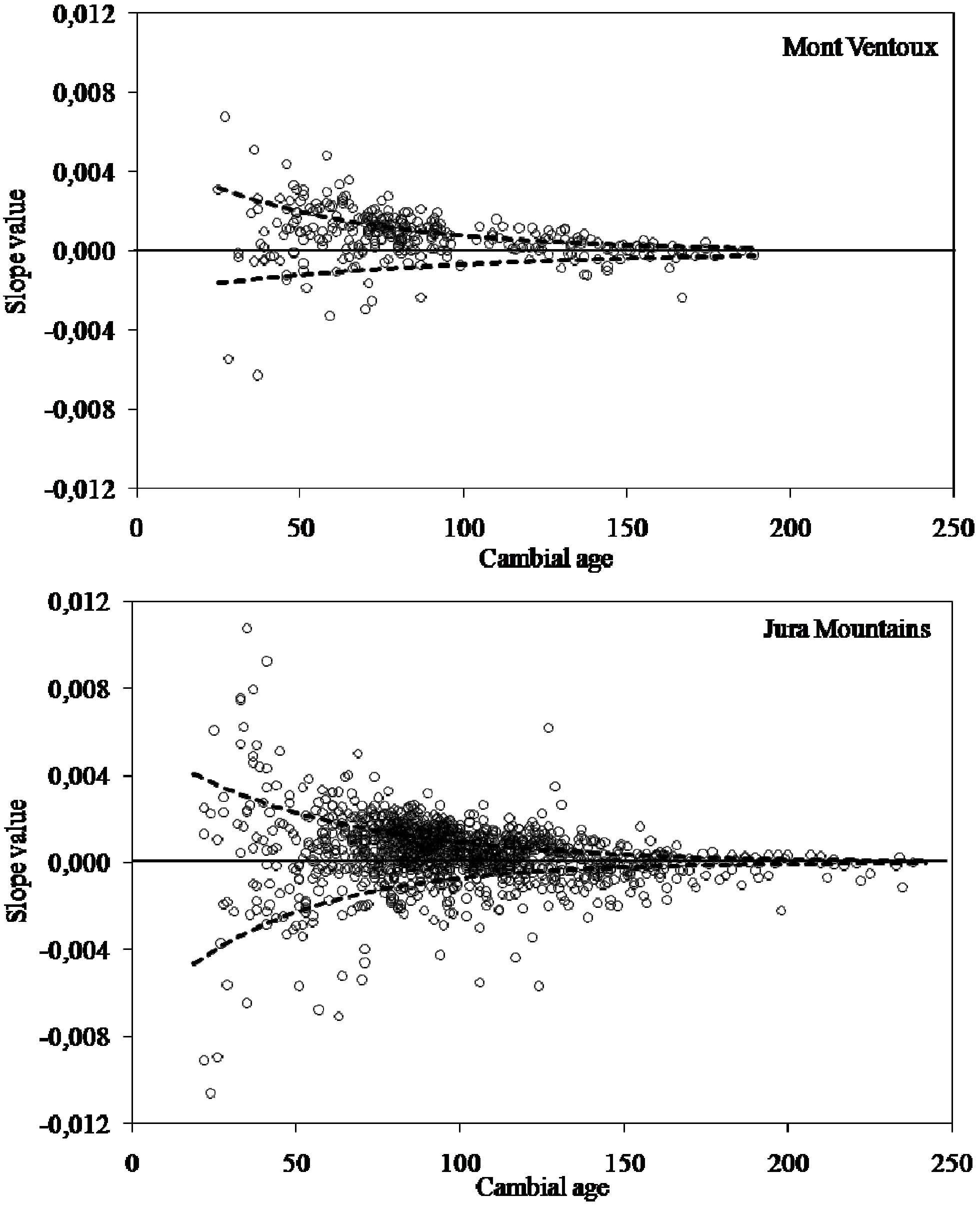

Fig. 2: Effect of tree age on the slope values (calculated on the entire chronology minus the first 5 MSc values) of the linear regression between MSc and tree aging ($S_{MSc\text{-}aging}$) for trees located on Mont Ventoux (2a, above) and in the Jura moutains (2b, below). On both sites, the slope value was significantly positive for 215 and 750 trees respectively, negative for 42 and 336 trees, and non-significant for 43 and 149 trees. Inverse exponential curves were fitted on both negative and positive values to highlight the decrease in the inter-individual variability in slope values with tree age

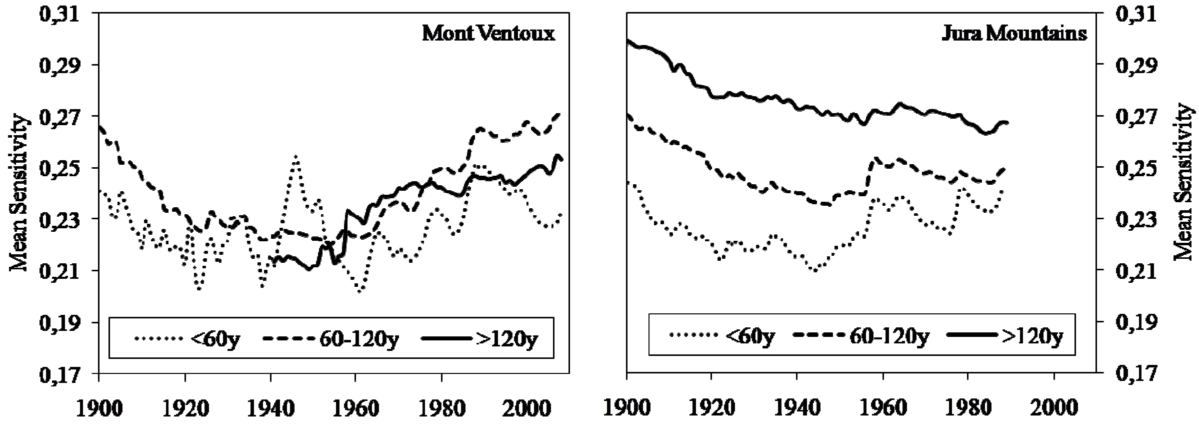

Fig. 3: Change in MSc over time for juvenile (<60y), adult (60-120y) and mature trees (>120y) growing on Mont Ventoux (3a, Left), and on the Jura mountains (3b, Right)

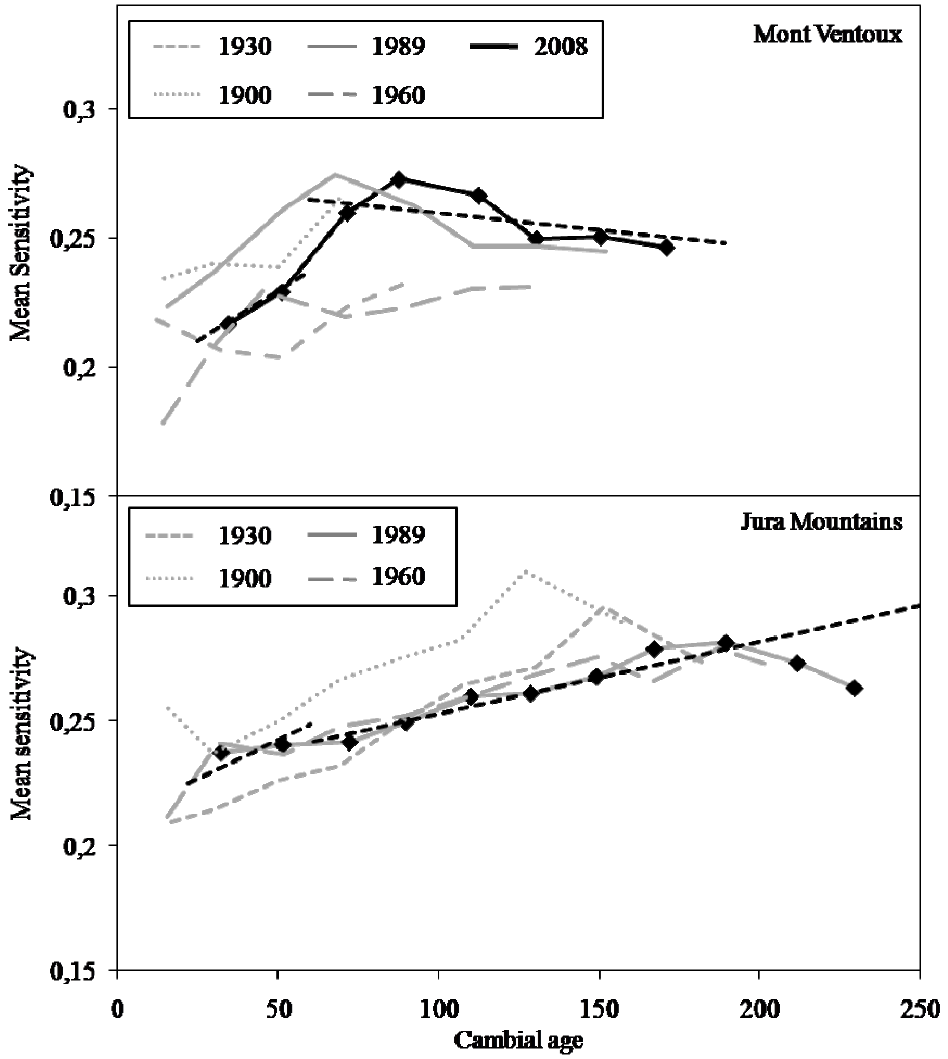

Fig. 4: Evolution of Mean Sensitivity with tree age at different dates for trees located on Mont Ventoux (4a, above) and in the Jura moutains (4b, below). MS were averaged by 20 year-class. Black diamonds are the MSf values. Coefficients of the linear regressions (black dotted lines) between MSf and tree age were calculated for juvenile (<60 years old) and non-juvenile trees and are summarized in Table 1

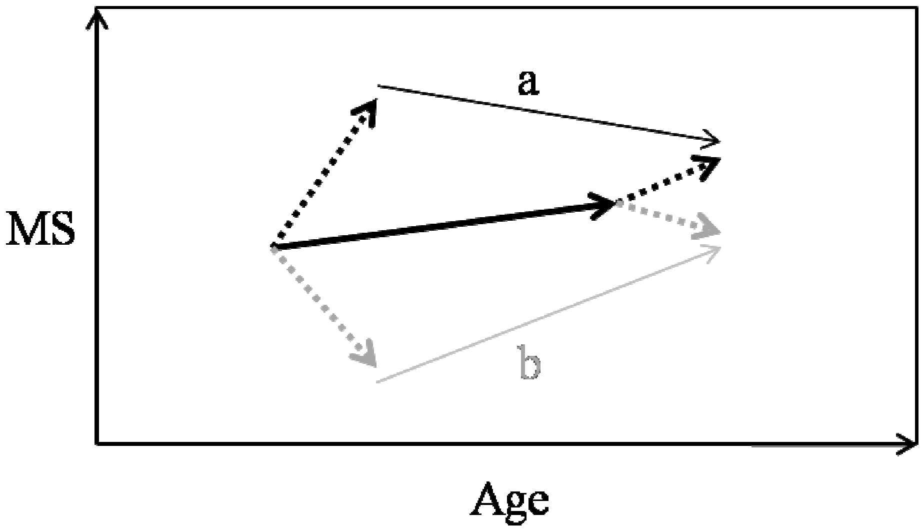

Fig. 5: Summary of the impacts of tree aging (solid black arrow) and changes in the main growth-limiting factors (dotted arrows) on mean sensitivity (MS) to climate, according to tree age. Juvenile trees (younger than 60 years) were not included. The two thin black arrows illustrate the likely relationship found between final MS and tree age. If the strength of the growth-limiting factors increases a negative relationship between final MS and tree age is likely (scenario a, black lines). If it decreases, the relationship should be positive (scenario b, grey lines)

Table 1: Coefficient values of the linear regressions made between final MS (MSf) and tree age, differentiating juvenile (<60) and non-juvenile (≥60) trees, located on Mont Ventoux (Vtx), in the Jura, and in the dry and wet stations in the Jura. Linear regressions were also made between Current MS and tree aging (MSc-aging), averaging juvenile (<60), adult (60-120) and mature (>120) trees.

	N trees	slope (10^{-4})	intercept	p-value
MSf ≤60 - Vtx	67	5.69	0.20	>0.1
MSf >60 - Vtx	233	-1.58	0.28	<0.05
MSf ≤60 - Jura	128	5.63	0.22	>0.1
MSf >60 - Jura	1107	3.21	0.22	<0.001
MSf ≤60 - Jura dry	33	16.9	0.17	<0.05
MSf >60 - Jura dry	110	1.14	0.27	>0.1
MSf ≤60 - Jura wet	71	7.22	0.21	>0.1
MSf >60 - Jura wet	336	3.72	0.22	<0.001
MSc-aging ≤60 - Vtx	67	10.9	0.18	<0.001
MSc-aging 60-120 - Vtx	164	3.72	0.22	<0.001
MSc-aging >120 - Vtx	69	0.67	0.23	<0.001
MSc-aging ≤60 - Jura	128	5.98	0.22	<0.001
MSc-aging 60-120 - Jura	833	4.13	0.21	<0.001
MSc-aging >120 - Jura	272	0.88	0.26	<0.001

Annexe 4

How to predict drought-induced tree mortality from radial growth data?

Cailleret M, Davi H

INRA, URFM, UR 629, Domaine Saint Paul, Site Agroparc, F-84914 Avignon Cedex 9.

En préparation pour *Journal of Ecology*

Abstract

Face to the increasing number of tree mortality reports since last decades, a better knowledge and prediction of the mortality process is required. Experimental studies showed strong interest to determine the functional determinants of the decrease in tree vitality and tree dieback, which can also be done by a process-based modelling approach. These functional models should be the best method to predict tree mortality however they required extensive datasets for parameterization. Consequently, statistical mortality models based on growth data were mainly used to predict mortality that can be explained by changes in tree growth.

A new methodological approach was applied to optimize prediction performance of logistic and stress threshold (ST) models using the area under the curve ROC (Receiving Operator Characteristics) as optimisation and model performance criterion. Their performance and their spatio-temporal stability were also assessed using re-sampling methods. Tree-ring data from dead and living silver fir (*Abies alba* Mill.) trees of Mont Ventoux, south-eastern France were used to calibrate and validate the models.

The performance of both logistic and ST models was improved using relative growth variable as predictor. As dead trees showed higher growth rates during their juvenile phase, current relative growth can be calculating using tree size or mean growth rate during the juvenile phase as reference. Unexpectedly, models without stress memories showed the highest performance. Prediction of ST models with Vitality Index was close to the one of the logistic models, however as their parameterization was more dependant on the proportion of dead trees sampled, their stability strongly evolved according to the equality of the sampling. We conclude that logistic models are more prone to predict tree death all the more since they are more stable in space and time.

Introduction

Forest decline and tree mortality are main processes of forest dynamics and functioning (Franklin *et al.* 1987). It is usually considered as a harmful phenomenon causing a degradation in ecosystem services: tree mortality leads in a decrease of in timber production, carbon sequestration or an increase of fire risks, soil erosion and watershed disturbances (Breshears and Allen 2002; Ford and Vose 2007). But long-term studies showed that it also caused benefits: increasing rate in genetic adaptation by promoting trees more adapted to climate changes (Kuparinen *et al.* 2010) and changes in biodiversity. Mortality occurs at all spatial scales – from the grove to the region of thousand of km² –, and all temporal scales – short or long-term decline – what durably impacts forest services and wood economy of a whole region (Kurz *et al.* 2008). However considerable uncertainty remains in modeling how, where and when can occur die-off events which is a considerable issue in a changing environment. Thus, this phenomenon is not well modeled by process-based models (Davi *et al.* in prep) and must be better integrated in gap models (Keane *et al.* 2001). As the number of decline and mortality reports showed high increase since last decades due to global change (Allen *et al.* 2010), a better understanding of this phenomenon and a better quantitative estimation of the risk of tree mortality is needed to improve these models and to be integrated in future forest management plan.

Tree death, and especially drought-induced mortality, can be modelled in different ways. One of the best approaches is to use process-based models which integrate species-specific knowledge especially on water stress regulation and carbon allocation rules. The mortality process can be well understood as all processes of tree functioning are modeled, but extensive datasets are required for parameterization (Davi *et al.* in prep). Secondly, growth-independent mortality models can be used to assess mortality that cannot be explained by changes in tree growth. These models were performed to predict the impact of disturbances such as bark beetles (e.g. Seidl *et al*. 2007), wild-fires (e.g. Stephens and Finney 2002), and windstorms (e.g. Papaik and Canham 2006) on tree health.

A last method which is commonly used is a statistical modelling using radial growth data, considering that it approximates tree vitality (Dobbertin 2005). Input data can come from forest inventory (Wunder *et al.* 2008b) or tree-ring measurements (e.g. Wunder *et al.* 2006). Even if it does not reflect all the carbon assimilated by a tree over a certain period – e.g. the carbon "lost" for reproduction is omitted –, tree ring series provide high resolution and long-term records of tree growth and are ideal to study temporal processes. This approach reveals which growth variables reflect the more the dieback process.

In mortality models using dendrochronological data, tree death is modelled as a combination of two different sources of mortality: a background and a growth-dependent mortality (Keane *et al.* 2001). Background mortality is usually considered as constant considering a tree can die at any time due to stochastic disturbances. The growth-dependent mortality was modelled using either logistic regression models (LR models) or growth thresholds (usually called stress thresholds [ST] models). Logistic regression models were applied to predict the mortality probability of a tree according to growth level variables and growth trend variables (Bigler and Bugmann 2004). ST models considered that a tree is stressed when growth falls below a given threshold and is subjected to an increased mortality risk (Botkin *et al.* 1972). Gap models mostly used ST models to predict tree mortality as it needs few parameters. Tree can be considered as a system with or without a stress memory (i.e. past growth impact current survival probability or not).

All these mortality models were performed to quantify mortality probabilities likely due to intra- and inter-specific competition (Bigler and Bugmann 2004; Wunder *et al.* 2008a). But, with climate changes, the number of drought- and heat-induced mortality reports has increased over the world since last decades (Allen *et al.* 2010). Chronic increase in temperatures and decrease in rainfalls led to increase in regular mortality (Van Mantgem *et al.* 2009) while the increase in severity and frequency of extreme drought and heat-waves was accompanied with episodic tree mortality (Suarez *et al.* 2004). Moreover, as climatic projections predict an increase in mean temperatures, occurrence and intensity of extreme drought (Meehl and Tebaldi 2004; IPCC 2007), and continuous drying in some regions (Giorgi and Lionello 2008), fragmented or massive die-offs should continue and be amplified. In this context, mortality models focusing on drought-induced tree mortality are needed for a better prediction of climatic impacts on forest health, and for a better knowledge of this dieback process.

Usually LR models showed higher performance than ST models (Bigler and Bugmann 2004; Wunder *et al.* 2006). However no comparative analysis has been made on both optimized models. Therefore our study aimed (i) to create a methodology to optimize the performance of mortality models based on tree-ring data from dead and living silver firs (*Abies alba* Mill.) of Mont Ventoux, southeast France; (ii) to compare performance of improved logistic mortality models and ST models; and (iii) to find what are the growth variables which predict the best drought-induced mortality, which should provide new elements on the understanding of the dieback process.

Materials and Methods

Sample design

Data was collected on Mont Ventoux (44°11’N; 5°17’E), a Mediterranean mountain in south-eastern France. On the north-facing slope, at 1445m a.s.l., mean annual temperature is 6.6°C and mean annual rainfalls are 1300mm which are unequally distributed throughout the year. 39% of the water falls between September and November but only 13% between June and August. An increase in mean annual temperatures, especially during summer, and a decrease in summer rainfalls were observed since last decades (Cailleret and Davi 2011). This increase in intensity, frequency and duration of summer drought has recently led to decrease in tree radial growth and some decline and dieback processes were reported. Declines in tree vitality were especially found for drought-sensitive species such as silver fir (*Abies alba* Mill.). On Mont Ventoux, silver fir is at the xeric range of its distribution range and consequently is predicted to face high risks face to climate change (Ohlemüller *et al.* 2006).

We sampled 69 dead and 158 living dominant silver firs located in 16 plots distributed between 1100 and 1140m. Mortality rate averaged 21% with high variability between plots (0 to 57%) and within plots due to micro-local soil heterogeneity. Substrates are ranged between limestone lithosol to one meter deep colluvium. However, soil water content is probably low considering the percentage of coarse material (between 50 and 80%), high slope (25° on average) and water infiltration into the calcareous bedrock. The study sites are under selective forest management.

Each tree was bored to the pith at breast height (130cm) in 2008. After planning with a razor blade, ring-widths were measured at the precision of 0.01 mm using a scanner (1200 dpi) and the software CDendro v5.3 and CooRecorder 5.3 (Cybis Elektronik & Data AB. Sweden). False and missing rings were detected by cross-dating using pointer years and correlation values calculated between individual and mean chronologies. When a core did not reach the pith, the number of missing rings and the total missing width were estimated. Contrary to previous mortality studies (Bigler and Bugmann 2004; Wunder *et al.* 2006), we used Basal Area Increment (BAI; mm²/year) instead of ring widths, because this variable is closer to biomass increase. BAI were calculated assuming a circular outline of stem cross-sections.

The beginning of the massive decline likely due to drought was noticed in 2002. Thus, models were calibrated on the period 2002-2008 to attempt to focus only on drought-induced mortality. Models were fitted on 1322 measurements from the dead and living trees.

The survival probability of a tree *i* at time *t* ($Psurv_{i,t}$) was predicted using two types of models: logistic and growth threshold models (which are also called STmodels).

Logistic regression models (LR models)

Logistic regression models predict $Psurv_{i,t}$ as

$$Psurv_{i,t} = \frac{\exp(\alpha * X_{i,t})}{1+\exp(\alpha * X_{i,t})}$$

Where the matrix $X_{i,t}$ contains independent variables of a tree *i* at time *t*, and *α* is a vector containing the regression coefficients. A range of growth variables was derived from BAI aimed at optimizing the predictive power of the mortality model. Three types of variables were used: (i) growth level variables, (ii) growth trend variables and (iii) classical dendrochronological parameters.

Growth level variables were defined as the average of growth increments over a certain period of time and should reveal the quantity of resources available for the tree during this period (dependent on site conditions, climate, inter- and intra-specific competition) and tree characteristics. A first set of growth level variables are averages of logarithms of BAI of the last *m* years ($logBAI_m$: absolute value). The second set is composed of relative growth values quantifying the percentage of newly created wood. The first one depends on current basal area ($logrelBAI_{i,t}$) in order to take tree size into account, and has been successfully applied in mortality models (Bigler and Bugmann 2004; Wunder *et al.* 2008a).

$$logrelBAI_{i,t}=\sum_{t=2002}^{t=2007}\log\left(\frac{BAI_{i,t}}{BA_{i,t-1}}\right)$$

As there is a potential relationship between early growth rate and tree longevity (Bigler and Veblen 2009), we introduced mean growth rate during the juvenile phase in the second variable of relative growth. It is based on current BAI and on the mean BAI of the *m* first years of tree life ($logrelBAI^{juv}{}_{i,t,m}$).

$$logrelBAI^{juv}{}_{i,t,m}=\sum_{t=2002}^{t=2007}\log\left(\frac{BAI_{i,t}}{BAI^{juv}{}_{i,m}}\right)$$

Where

$$BAI^{juv}{}_{i,m}=\sum_{m=10}^{m=100}\frac{BAI_{i,1}+...+BAI_{i,m}}{m}$$

Growth trend variables were calculated as the slope of the local linear regressions over the *m* last years of BAI (locreg).

Gini coefficient (G) and First-Order Autocorrelation (A1) were also used in the mortality models to assess if the survival probability evolves according to different tree sensitivity to environmental changes and different growth inertia (Fritts 1976; Biondi and Qeadan 2008). These two parameters were calculated on ring-width chronologies. Logistic regression models were fitted using maximum log-likelihood estimation.

A stepwise algorithm was also the applied to create a model with two variables or more. Six independent variables were included: one absolute and one relative growth level variables, one short-term and one long-term growth trend variables, A1 and G. The model with the best performance was chosen by minimizing AIC (Akaike Information Criterion).

Growth threshold models (ST models)

ST models were also tested considering that stochastic events (e.g. intense drought) can kill a tree at any time. They integrate LR models and are commonly used in succession models (Bugmann 2001) as their calibration is easier. Thirty-four models were tested where $Psurv_{i,t}$ is reduced if BAI falls below a certain threshold of diameter growth (Table 1). Otherwise $Psurv_{i,t}$ is not equal to 1 due to background mortality, and can be expressed as a constant survival probability (Botkin *et al.* 1972):

$$Psurv_{i,t}=q=\sqrt[agemax]{0.02}$$

On silver fir, the maximum age is estimated as 600 years old (Wolf 2003) which results in an annual survival probability (q) of 99.4%.

Based on Botkin *et al.* (1972) and Solomon (1986), three simple ST models were tested. The formulation and the name of the models changed depending on the length of the tree stress memory and on the type of threshold used (Table 1). Models ST1 considered that the tree had no stress memory while we take into account the BAI of two and three consecutive years for models ST2 and ST3. In contrast to previous models, models using Stress Counter ($SC_{i,t}$ for models ST_{SC}) assume that stress tolerance/intolerance of a tree *i* at time *t* depends on the quantity of stress experienced over last years (Bugmann 2001). When $BAI_{i,t}$ falls below a given threshold (Th), the Stress Counter ($SC_{i,t}$) increase depending on the difference between both (Table 1). Stressed trees become healthy ($SC_{i,t}=0$) after experiencing three consecutive years of growth above the threshold. Finally, as tree recovering not only depends on the number of years with growth above the threshold, but also on the positive effect of “good” years, models with Vitality Index ($VI_{i,t}$ for models ST_{VI}) were also tested. $VI_{i,t}$ was calculated every year in order to take into account the positive effect of years with high growth in the calculation of $Psurv_{i,t}$. $VI_{i,t}$ corresponds to the sum of the differences between $BAI_{i,t}$ and Th calculated for *m* years (Table 1). Three stress memories (*m* = 1, 2 and 3 years) were tested. $Psurv_{i,t}$ decreases only when $VI_{i,t}$ is negative.

$Psurv_{i,t}$ is related with $SC_{i,t}$ and $VI_{i,t}$ following a Weibull probability distribution considering that trees with low growth rate (suppressed trees) are also the more shade tolerant and are more capable to survive periods of reduced growth. Initial parameters of the Weibull function were equal to those used by Wunder *et al.* (2006), i.e. a=0.15; b=0.15 and c=2.5, and chaged after the optimization procedure

For each model three different thresholds were used. The first one is an absolute value (Th_{abs} for models ST_{abs}). The second one is a relative threshold (Th_{rel} for ST_{rel}) depending on the site-specific mean growth of the trees at same age *a* ($BAI_{i,a}$ / $BAI_{RC,a}$). $BAI_{RC,a}$ was given by the conventional mean regional age curve (Esper *et al.* 2003) of silver firs growing on Mont Ventoux (Cailleret and Davi 2011). The age-specific maximum growth equation (Moore 1989) was not used here because this equation was obtained for trees growing in specific conditions that are not representative of the biological growth on our study site. Based on the results of logistic models (Fig 1), the third threshold (Th_{relj}) for ST_{relj}) depends on $BAI_{RC,a}$ and on the juvenile growth rate during the 69 first years of tree's life for the studied tree ($BAI^{69}{}_{i}$) and the one given by the regional curve ($BAI^{69}{}_{RC}$).

Estimation of model performance

Predicted values of $Psurv_{i,t}$ given by the models were compared with the individual binary living/death information from the evaluation data set. In the evaluation, the area under the curve (AUC) of a receiver operating characteristic (ROC) plot of each model was calculated. AUC is a graphical method assessing the ability of a model to predict the binary response of an individual, by representing the relationship between the false positive fraction and the true positive fraction of the related confusion matrix of the evaluated model (Fielding and Bell, 1997). Using AUC allows us to assess model performance without defining a threshold of $\mathrm{Psurv}_{i,t}$ (Th_p) which would discriminate trees whose survival is expected (when $\mathrm{Psurv}_{i,t} > \mathrm{Th}_p$) and trees whose death is expected ($\mathrm{Psurv}_{i,t} < \mathrm{Th}_p$). The range of AUC is from 0 to 1 and 0.5 is obtained by a random model. A model providing excellent prediction has an AUC higher than 0.9, a fair model has an AUC between 0.7 and 0.9. Otherwise the model is considered as poor (Swets 1988).

Optimization procedure

As already said, the best parameters of the logistic models were obtained by minimizing Akaike Information Criterion (AIC). Parameters of the ST models were calculated by maximizing AUC: annual survival probability in a stress year (p), growth threshold values (Th), parameters of the relationship between $\mathrm{Psurv}_{i,t}$ and $\mathrm{SC}_{i,t}$ and $\mathrm{VI}_{i,t}$ (a, b, c).

Evaluation of model stability

The goal of this study was to investigate variation of model performance depending on spatial and temporal data sampling. We choose to evaluate only the stability of logistic models and of the best ST model of each group (ST, $\mathrm{ST}_{\mathrm{SV}}$, $\mathrm{ST}_{\mathrm{VI}}$). Model performance of the original model is called *apparent* model performance ($\mathrm{AUC}_{\mathrm{ap}}$).

‘Spatial stability’ of the models was assessed using resampling methods which replace an independent evaluation of the models (Guisan and Zimmermann, 2000). First, bootstrap procedures (Efron and Tibshirani, 1993) were used to estimate the standard error of sensitivity as a measure of model stability (Guisan and Harrell, 2000). This technique estimates the overoptimism in the model performance which occurs when evaluating the model on the same data to which it was fitted. Predictions of the bootstrap models for the original sample led to new values of performance indices whose means resulted in the *bias-corrected* model performance (AUC_{cor}). ‘Spatial stability’ of the models was also assessed by estimating model performance by sampling equal numbers of dead and living trees (AUC_{eq} using 69 trees). 2000 samples of equal size to the dead trees were drawn from the living trees sample without replacement.

Different temporal ranges were used to assess ‘temporal stability’. AUC values were calculated removing each year of data one by one and were averaged to obtain AUC_{temp}. High differences between the expected model performance on these new ranges and those obtained with the original period should reveal if the temporal range studied is too short for a good prediction of tree mortality.

All analyses were performed using R a language and environment for statistical computing. Dendrochronological parameters were calculated using dplR (Bunn 2008). AUC values were obtained using the ROCR package.

Results

LR models

Parameters of the logistic regressions models were chosen with Akaike Information Criterion (AIC) i.e. by maximum likelihood. Theoretically, their performance was optimized using this statistical methodology. The strong negative relationship between AIC and AUC_{ap} of these models strengthen our assumption (Table 2).

The performance of the logistic models was highly dependent on input variables (Table 2). The lowest performance was obtained using first-order ring autocorrelation (A1) and Gini index (G). Psurv decreased with a higher sensitivity to environmental changes and with a higher growth inertia, but the level of good predictions did not exceed 60%. Unexpectedly, growth trends during last years were not good predictors of tree death. AUC_{ap} values of models using locreg as input variables ranged between 0.6 to 0.7 and increased with the length of the temporal scale used (Fig 2; Table 2). The best short-term growth trend variables were obtained using BAI evolution of the last 6 and 10 years. For long-term growth trend variables, the last 25 and 29 years can be used as predictors and give better results than short-term growth variables (Table 2). Higher is the slope of the growth trends (Locreg), higher is the survival probability. In the same way, the level of growth ($logBAI_m$) of the last years was positively related with tree survival probability (Table 2). Predictions of logistic models using these growth variables were better but not suitable, and declined with the increased of the number years averaged for calculating this variable. The absolute growth rate of last year ($logBAI_1$) gave high AUC value (AUC_{ap}=0.719) which increase when this rate is relative ($logrelBAI_1$; AUC_{ap}=0.734). Finally, the model which takes into account juvenile growth rate and growth during the last year ($logrelBAI^{juv}_{69}$) was the more performing of the models using one input variable (Table 2). The effect of the number of years used for calculating the juvenile growth, i.e. the age which differentiate both juvenile and adult phases, was not very significant (Fig 1), but the highest AUC_{ap} was obtained when averaging the 69 first years of tree growth. More than 80% of the predictions were good (AUC_{ap}=0.808) showing that tree vulnerability to dieback is not only dependant on recent growth trends but also on tree conditions during their first years old.

As expected, the highest performance was obtained with the model which integrated more than one growth variables (Table 2). The best model obtained after the stepwise algorithm included all kind of variables except the Gini index. 84% of the predictions were good which is very correct for a mortality model with a dendrochronological basis.

ST models

The performance of mortality models was very variable depending on the type of model, the threshold, and the length of the stress memory used (Table 3 and 4). Concerning the growth threshold which differentiate growth levels of trees which should die and trees which should survive, our simulations showed that using relative threshold slightly increased AUC_{ap} compared with absolute ones (+1 to 3% of good predictions). Such as logistic models, the significant increase in model performance was obtained when the threshold taken juvenile growth rate into account (+5 to 10%). The effect of the type of model used was also significant. Model performance respectively increased from simple STmodels to STmodels with stress counter and STmodels with vitality index. For these models highest AUC_{ap} values were respectively 0.744, 0.77 and 0.812. Finally the level of good predictions was found to decrease with an increase in the length of the stress memory. AUC_{ap} values of ST_{VI} models using Th_{relj} were respectively 0.812, 0.790, 0.768 and 0.745 for 2, 3, 4 and 5 years of tree memory, which corresponds in a decrease in 2.2% of good predictions per year (Table 4). The same trend was obtained on simple STmodels

Model stability

As AUC_{ap} were calculated on an unequal sampling with only seven years of data, re-sampling methods were used to assess model stability. Firstly, using boostrap methods did not decrease the estimation of the model performance ($AUC_{cor} \approx AUC_{ap}$). The comparison of AUC_{ap} and AUC_{eq} also attests that our sampling is only reliable for logistic regression models. With an equal sampling of dead and living trees, the decrease in LR model performance only was only 1% on average. Concerning ST models, AUC_{eq} ranged between 0.53 and 0.66 showing which is very low compared with AUC_{ap} (0.60 – 0.81). Highest AUC_{eq} was not more obtained by ST_{VI} model but by the ST_{SC} model using Threlj. Finally, model performance was not impacted by the temporal range used. Values of AUC_{temp} were very closed to AUC_{ap}.

Discussion

Performance validity and stability of the models

Bootstrapped procedures were used to test the reliability of AUC_{ap} within the study sampling. AUC_{cor} were very closed to AUC_{ap} showing that AUC_{ap} can be used as a good indicator of the performance of the model. LR models built in this study can be considered as stable in space and time. First, differences between model performance assessed using an equal sampling (AUC_{eq}) and AUC_{ap} were minor, showing that the number of dead trees cored for this study is adequate. Secondly, the performance of the model is similar when using different temporal ranges (very small differences between AUC_{app} and AUC_{temp}), which indicates that LR models are reliable in time and not dependant on particular years. Considering previous results we can suppose that LR models are reliable and that growth trends can be used as predictor of tree mortality. The performance of ST models was also not dependant on the temporal range used, but very dependant on the number of trees sampled and should be calibrated using the larger and the more equal sampling as possible.

Therefore, parameters of both models are site- and species-specific as declining processes can differ between sites in the length and intensity of the triggering drought-stress and in the vulnerability of the trees.

Performance comparison of the mortality models.

With the parameters optimization, mortality models provide good prediction of the tree survival probability. High AUC values (>0.8) were obtained using both logistic and ST models. Commonly logistic regression models are considered to obtain the highest performance (Wunder *et al.* 2006). But the difference with ST models was not as important as expected with the optimized one which used vitality index when studying AUC_{ap}. Therefore, in the case of unequal sampling, LR models should be chosen instead of STmodels.

AUC values of LR models using BAI were close to 0.7, indicating that this variable alone should not be used to predict tree mortality. In the same way, the comparison of the performance of ST models indicates that the absolute growth rate (Th_{abs}) is a worst predictor than relative growth rate (Th_{rel}), while the last one is less used (Chao *et al.* 2008). The prediction also increased using Th_{relj}, where we added the variable which assess the potential growth rate during the juvenile ages (69 first years), i.e. the ratio between the mean BAI of the tree and the one calculated with the regional curve. It was confirmed by the comparison of the performance of the logistic models, which only used one input growth variable. The best explanatory variable was $logrelBAI^{juv}_{69}$. While it has been never used in mortality models, it clearly improved their prediction. In the same way classical dendrochronological parameters need to be included. The prediction of the logistic models increased when using Gini coefficient and First-order ring autocorrelation as input variables.

The slope values of the growth trends (locreg) in the last 6 and 25 years increased the performance of the logistic regression model. It reveals that tree decline occurs at different temporal scale. Short and long-term decreases in tree growth were related to a decrease in tree survival probability and can indicate a decline in tree vitality.

The length of the stress memory should also be taken into account as it is negatively related with the performance of the logistic models using BAI alone. This report was also found for simple ST and ST_{VI} models.

The ST models with stress counter (ST_{SC}), which consider a link between stress tolerance and shade tolerance slightly improved AUC values (Table 4). As hypothesised by Keane *et al.* (1996) and Bugmann (2001), this mechanism is physiologically plausible for shade tolerant species such as silver fir but less for pioneer or post-pioneer species such as Norway spruce

(Wunder *et al.* 2006). The best ST models are models with vitality index (ST_{VI}) which also takes into account the positive impact of years with high level of growth. As expected, tree recovering depends on the number of years with growth above the threshold but also on the difference between both. This kind of model should thus be preferred to classical ST models with stress counter (Bugmann 2001).

Biological interpretation

As shown by numerous previous studies, the survival probability of a tree decreases with recent decline in radial growth (Keane *et al.* 2001, Bigler and Bugmann 2004, Das *et al.* 2007, Wunder *et al.* 2008b). This decline was observed at short and long-term (superior to the decade) showing that the dieback process can be launched since many years (e.g. Suarez *et al.* 2004). Our study shows that we need to include both growth trend and growth level analysis to predict tree mortality. But instead of absolute current growth rate values, relative ones should be used to assess tree vigour because it reduces the confounding effect of tree size on growth (Bigler and Bugmann 2004).

As already found by Wunder *et al.* (2006) the performance of both logistic regression and ST models increased with the absence of a short stress memory (2 to 5 years). But this study indicates that tree vulnerability to dieback can depend on the growth rates during the juvenile phase. On the study site, trees with higher growth rates during the young ages were more prone to die. This trade-off between longevity and growth rates was observed between species (Loehle 1988) and recently within a species (Black *et al.* 2008; Bigler and Veblen 2009). Fast growth rates are generally linked to reduced investment in defence (Loehle 1988), resulting in more frequent infestations by pathogens (Bleiker and Uzunovic 2004). They are also associated with high ratios of above- to belowground biomass which results in an increase risk of damage from wind (Loehle 1988), and especially in higher respiration and transpiration rates. It leads in higher water, carbon and nutrient needs which will cause troubles when these supplies fall short (McDowell *et al.* 2008). We usually consider that higher growth rates are linked with lower wood density and increases in xylem vulnerability to cavitation (Enquist *et al.* 1999; Martinez-Vilalta *et al.* 2010; Russo *et al.* 2010), but at the intra-specific level this trade-off is still unclear (Fichot *et al.* 2010). This hypothesis was strengthen by the fact that logistic models using Gini coefficient slightly explains tree survival probability i.e. trees with higher sensitivity to environmental changes and especially to drought periods were more prone to die (Suarez *et al.* 2004). On the study site, dead tree showed a higher First-order ring autocorrelation than living trees. This stronger growth inertia leads to a lower resiliency after an extreme event and a slower recover of vitality after decline. A likely small total leaf area and sapwood area during dry periods can explain this trend.

Statistical mortality models are useful to quantify tree mortality risk for each individual. It also provides new insights on the decline process e.g. by differentiating long and short-term stress memory. But more experimental research is needed for a reliable prediction of drought-induced tree mortality (Allen *et al.* 2010; Sala *et al.* 2010). The physiological mechanisms inducing tree mortality were formalized by Mc Dowell *et al.* (2008) but not yet experimentally proved. Extreme drought can kill a tree through cavitation of water columns within the xylem (Cochard 1991; Breda *et al.* 2006). Water stress also drives carbon assimilation *via* changes in stomatal conductance that lead to carbon starvation and reduced ability to defend against insects or fungi attacks (Desprez-Loustau *et al.* 2006). The carbon starvation hypothesis was recently studied (Mc Dowell *et al.* 2008; Adams *et al.* 2009) but lacks of sufficient evidence for reliable acceptance (Sala *et al.* 2010).

The understanding of the phenomenon can be improved by experimental ecophysiological studies and, in a second step, by integrating species-specific knowledge on regulation of water stress and carbon allocation in process-based models (Martinez-Vilalta *et al*. 2002; Davi *et al.* in prep). This tool should be the most useful to make predictions in a changing environment.

Acknowledgements

The authors wish to thank Nicolas Mariotte, William Brunetto and Florence Courdier for their support in the field on Mont Ventoux and all members of the URFM Unit for discussions that clearly improved the manuscript. We are also grateful to Olivier Chabrol from the UMR 6632 LATP CNRS - University of Provence, for the lending of calculation servers for several weeks. This study was supported by the French National Research Agency (ANR) in the framework of the DRYADE program.

References

Adams HD, Guardiola-Claramonte M, Barron-Gafford GA, Villegas JC, Breshears DD, Zou CB, Troch PA, Huxman TE. (2009) Temperature sensitivity of drought-induced tree mortality portends increased regional die-off under global-change-type drought. *Proceedings of the National Academy of Science*, **106**, 7063–7066.

Allen CD, Macalady A, Chenchouni H, Bachelet D, McDowell N, Vennetier M, Gonzales P, Hogg T, Rigling A, Breshears D et al. 2010. Climate-induced forest mortality: a global overview of emerging risks. *Forest Ecology and Management*, **259**, 660-684.

Bigler C, Bugmann H (2004) Predicting the time of tree death using dendrochronological data. *Ecological Applications*, **14**, 902-914

Bigler C, Veblen TT (2009) Increased early growth rates decrease longevities of conifers in subalpine forests. *Oikos*, **118**, 1130-1138

Biondi F, Qeadan F (2008) Inequality in Paleorecords. *Ecology*, **89**, 1056-1067

Black BA, Colbert JJ, Pederson N (2008) Relationships between radial growth rates and lifespan within North American tree species. *Ecoscience*, **15**, 349-357

Bleiker KP, Uzunovic A (2004) Fast- and slow-growing subalpine fir produce lesions of different sizes in response to inoculation with a blue-stain fungus associated with Dryocoetes confusus (Coleoptera: Scolytidae). *Canadian Journal of Bo*tany, **82**, 735-741.

Breda N, Huc R, Granier A, Dreyer E (2006) Temperate forest trees and stands under severe drought: a review of ecophysiological responses, adaptation processes and long-term consequences. *Annals of Forest Science*, **63**, 625-644

Breshears DD, Allen CD (2002) The importance of rapid, disturbance-induced losses in carbon management and sequestration. *Global Ecology and Biogeography*, **11**, 1–5.

Botkin DB, Janak JF, Wallis JR (1972) Some ecological consequences of a computer model of forest growth. *Journal of Ecology*, **60**, 849-872

Bugmann H (2001) A review of forest gap models. *Climatic Change*, **51**, 259-305

Bunn A (2008) A dendrochronology program library in R (dplR). *Dendrochronologia*, **26**, 115-124.

Cailleret M, Davi H (2011) Effects of climate on diameter growth of co-occuring Faugs sylvatica and Abies alba along an altitudinal gradient. *Trees*, **25**, 265-276

Chao KJ, Phillips OL, Gloor E, Monteagudo A, Torres-Lezama A, Vasquez-Martinez R (2008) Growth and wood density predict tree mortality in Amazon forests. *Journal of Ecology*, **96**, 281-292. doi: 10.1111/j.1365-2745.2007.01343.x

Das, A.J., Battles, J.J., Stephenson, N.L. & van Mantgem, P.J. (2007) The relationship between tree growth patterns and likelihood of mortality: a study of two tree species in the Sierra Nevada. *Canadian Journal of Forest Research*, **37**, 580–597.

Davi H, Simioni G, Marie G, Cailleret M, Delpierre N, Dufrêne E (in prep) Modelling forest functioning under climate change.

Desprez-Loustau ML, Marçais B, Nageleisen LM, Piou D, Vanini A (2006) Interactive effects of drought and pathogens in forest trees. *Annals of Forest Science*, **63**, 596-610

Dobbertin M (2005) Tree growth as indicator of tree vitality and tree reaction to environmental stress: a review. *European Journal of Forest Research*, **124**, 319-333.

Efron & Tibshirani (1993) An introduction to the Bootstrap. Chapman and Hall. New York.

Enquist BJ, West GB, Charnov EL, Brown JH (1999) Allometric scaling of production and life-history variation in vascular plants, *Nature*, **401**, 907–911

Esper J, Cook ER, Krusic PJ, Peters K, Schweingruber FH (2003) Tests of the RCS method for preserving low frequencies variability in long tree-ring chronologies. *Tree-ring Research*, **59**, 81-98

Fichot R, Barigah TS, Chamaillard S, Le Thiec D, Laurans F, Cochard H, Brignolas F (2010) Common trade-offs between xylem resistance to cavitation and other ohysiological traits do not hold among unrelated *Populus deltoids* x *Populus nigra* hybrids. *Plant Cell Env.*, doi: 10.1111/j.1365-3040.2010.02164.x

Fielding AH, Bell JF (1997) A review of methods for the assessment of prediction errors in conservation presence/absence models. *Environmental Conservation*, **24**, 38-49

Ford CR, Vose JM (2007) *Tsuga canadensis* (L.) Carr. mortality will impact hydrologic processes in southern Appalachian forest ecosystems. *Ecological Applications,* **17**, 1156–1167.

Franklin JF, Shugart HH, Harmon ME (1987) Tree death as an ecological process. *Bioscience*, **37**, 550-556.

Giorgi F, Lionello P (2008) Climate change projections for the Mediterranean region. *Global and Planetary Change*, **63**, 90-104. doi:10.1016/j.gloplacha.2007.09.005

Guisan A, Harrell FE (2000) Ordinal response regression model in ecology. *Journal of Vegetation Science*, **11**, 617-626

Guisan A, Zimmermann (2000) Predictive habitat distribution models in ecology. *Ecological Modelling*, **135**, 147-186

IPCC (2007) Climate Change 2007: Impacts, Adaptation and Vulnerability. Contribution of Working Group II to the Fourth Assessment Report of the Intergovernmental Panel on Climate Change. University Press, Cambridge, United Kingdom and New York, NY, USA., Cambridge.

Keane RE, Austin M, Field C, Huth A, Lexer MJ, Peters D, Solomon A, Wyckoff P (2001) Tree mortality in gap models: application to climate change. *Climatic Change*, **51**, 509-540

Kuparinen A, Savolainen O, Schurr FM (2010) Increased mortality can promote evolutionary adaptation of forest trees to climate change. *Forest Ecology and Management*, **259**, 1003-1008.

Kurz WA, Dymond CC, Stinson G, Rampley GJ, Neilson ET, Carroll AL, Ebata T, Safranyik L (2008) Mountain pine beetle and forest carbon feedback to climate change. *Nature*, **452**, 987-990.

Loehle C (1988) Tree life history strategies: the role of defenses, *Canadian Journal of Forest Research*, **18**, 209-222.

Martinez-Vilalta J, Piñol J, Beven K (2002) A hydraulic model to predict drought-induced mortality in woody plants: an application to climate change in the Mediterranean. *Ecological Modelling*, **155**, 127-147.

McDowell NG, Pockman W, Allen C, Breshears D, Cobb N, Kolb T, Plaut J, Sperry J, West A, Williams D et al. (2008). Mechanisms of plant survival and mortality during drought: why do some plants survive while others succumb? *New Phytologist* **178,** 719–739.

Meehl GA, Tebaldi C (2004) More intense, more frequent, and longer lasting heat waves in the 21st century. *Science*, **305**, 994-997

Moore AD (1989) On the maximum growth equation used in forest gap simulation models. *Ecological Modelling,* **45**, 63-67

Ohlemüller R, Gritti ES, Sykes MT, Thomas CD (2006) Quantifying components of risk for European woody species under climate change. *Global Change Biology*, **12**, 1788-1799.

Papaik MJ, Canham CD (2006) Species resistance and community response to wind disturbances regimes in northern temperate forests. *Journal of Ecology*, **94**, 1011-1026.

Russo SE, Jenkins KL, Wiser SK, Uriarte M, Duncan RP, Coomes DA (2010) Interspecific relationships among growth, mortality and xylem traits of woody species form New Zealand. *Functional Ecology*, **24**, 253-262.

Sala A, Piper F, Hoch G. (2010) Physiological mechanisms of drought-induced tree mortality are far from being resolved. *New Phytologist*, **186**, 274–281.

Seidl R, Baier P, Rammer W, Schopf A, Lexer MJ (2007) Modelling tree mortality by bark bettle infestation in Norway spruce forests. *Ecological Modelling*, **206**, 383-399.

Stephens SL, Finney MA (2002) Prescribed fire mortality of Sierra Nevada mixed conifer tree species: effects of crown damage and forest floor combustion. *Forest Ecology and Management,* **162**, 261-271.

Solomon AM (1986) Transient response of forests to CO2-induced climate change: simulation modeling experiments in eastern North America. *Oecologia*, **68**, 567-579

Suarez ML, Ghermandi L, Kitzberger T (2004) Factors predisposing episodic drought-induced tree mortality in Nothofagus – site, climatic sensitivity and growth trends. *Journal of Ecology*, **92**, 954-966.

Swets JA (1988) Peasuring the accuracy of diagnostic systems. *Science*, **240**, 1285-1293

Van Mantgem PJ, Stephenson NL, Byrne JC, Daniels LD, Franklin JF, Fule PZ, Harmon ME, Larson AJ, Smith JM, Taylor AH, Veblen TT (2009) Widepread increase of tree mortality rates in the western United States. *Science*, **323**, 521-524

Wolf H (2003) EUFORGEN technical guidelines for genetic conservation and use of silver fir (*Abies alba*). International Plant Genetic Resources Institute, Rome, Italy

Wunder J, Bigler C, Reineking B, Fahse L, Bugmann H (2006) Optimisation of tree mortality models based on growth patterns. *Ecological Modelling*, **197**, 196-206

Wunder J, Brzeziecki B, Zubura H, Reineking B, Bigler C, Bugmann H (2008a) Growth-mortality relationships as indicators of life-history strategies: a comparison of nine tree species in unmanaged European forests. *Oikos*, **117**, 815-828.

Wunder J, Reineking B, Bigler C, Bugmann H (2008b) Predicting tree mortality from growth data: how virtual ecologists can help real ecologists. *Journal of Ecology*, **96**, 174-187.

Figures

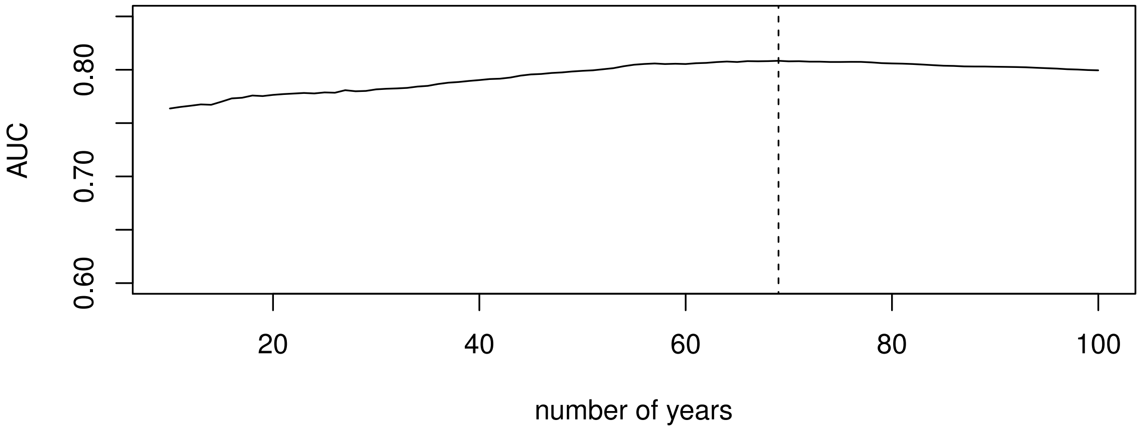

Fig 1: Effect of the number of years used in the calculation of the juvenile growth rate on the performance (AUC) of the logistic model which used this input variable

Fig 2

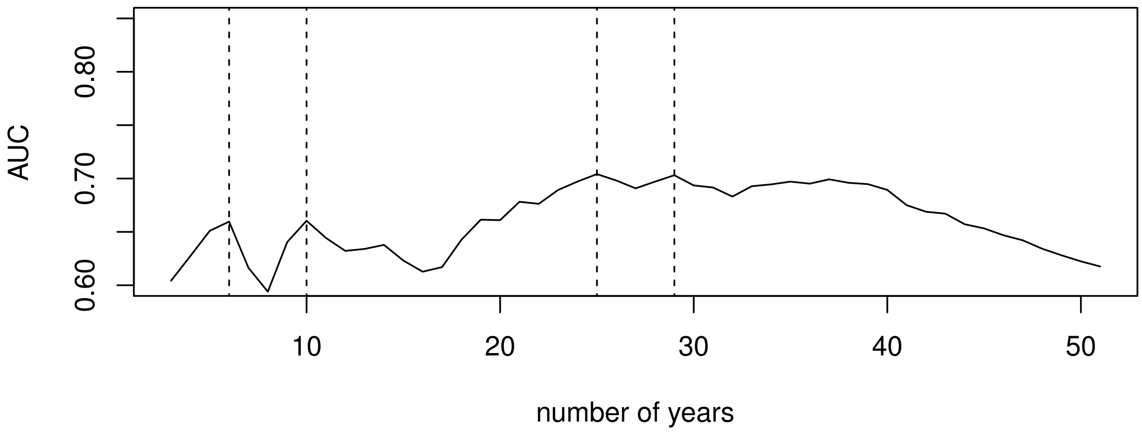

Fig 2: Effect of the number of years used in the calculation of the slope of recent growth trend on the performance (AUC) of the logistic model which used this input variable

Table 1: Formulations of the stress threshold models (ST models)

Model	Equation	Condition
ST1	$Psurv_{i,t} = p$	$BAI_{i,t} < Th$
ST2	$Psurv_{i,t} = p$	$(BAI_{i,t} < Th)$ & $(BAI_{i,t-1} < Th)$
ST3	$Psurv_{i,t} = p$	$(BAI_{i,t} < Th)$ & $(BAI_{i,t-1} < Th)$ & $(BAI_{i,t-2} < Th)$

Model	Equation	Stress Counter	Equations	Condition
$ST_{SV\text{-}W}$	$Psurv_{i,t} = q - a[1 - \exp(-b * SC_{i,t})]^c$	$SC_{i,t} = SC_{i,t-1} + \Delta SC_{i,t}$	$\Delta SC_{i,t} = 10 * [(Th - BAI_{i,t}) / Th$	$BAI_{i,t} < Th$
$ST_{SV\text{-}L}$	$Psurv_{i,t} = q - a * SC_{i,t}$		$\Delta SC_{i,t} = 0$	$BAI_{i,t} > Th$
$ST_{SV\text{-}E}$	$Psurv_{i,t} = q - a * \exp(b * SC_{i,t})$		$SC_{i,t} = 0$	$(BAI_{i,t} > Th)$ & $(BAI_{i,t-1} > Th)$ & $(BAI_{i,t-2} > Th)$

Model	Equation	Condition	Vitality Index
$ST_{VI\text{-}W}$	$Psurv_{i,t} = q - a[1 - \exp(-b * VI_{i,t})]^c$	$VI_{i,t} < 0$	$VI_{i,t} = \sum_{t}^{t-m} (10 * [(Th - BAI_{i,t}) / Th])$
$ST_{VI\text{-}L}$	$Psurv_{i,t} = q - a * VI_{i,t}$		
$ST_{VI\text{-}E}$	$Psurv_{i,t} = q - a * \exp(b * VI_{i,t})$		

With *p*: the survival probability when the tree is stressed; *q*: the survival probability during a non-stressed year (0.994); *a*, *b* and *c* the parameters of the distribution of the relationship between $SC_{i,t}$, $VI_{i,t}$ and $Psurv_{i,t}$.
For each model three thresholds were tested Th_{abs}, Th_{rel}, Th_{relj}.
Three tree stress memories were tested (m=1, 2, 3) for models with Vitality Index.

Table 2: Performance of the best logistic models. AUC$_{ap}$ (*apparent*) was calculated on the initial sampling. To remove the sampling effect, AUC$_{cor}$ (*bias-corrected*) was calculated using bootstrap resampling methods, and AUC$_{eq}$ (*equal sampling*) using an equal number of dead and living trees (average of 2000 samplings). AUC$_{temp}$ was calculated using different temporal ranges.

Growth variables	Effect on Psurv	Model performance				
		AIC	AUC$_{ap}$	AUC$_{cor}$	AUC$_{eq}$	AUC$_{temp}$
logrelBAI$_1$	+	483.5	0.734	0.735	0.720	0.737
logrelBAI$^{juv}_{69}$	+	447.9	0.808	0.808	0.787	0.810
BAI$_1$	+	490.8	0.719	0.719	0.707	0.722
BAI$_2$	+	813.6	0.712	0.712	0.706	0.712
BAI$_3$	+	1080.9	0.689	0.690	0.689	0.688
BAI$_4$	+	1285.3	0.676	0.676	0.675	0.677
BAI$_5$	+	1396.5	0.645	0.644	0.643	0.646
locreg6	+	536.6	0.616	0.618	0.606	0.615
locreg10	+	534.6	0.644	0.645	0.655	0.642
locreg25	+	512.5	0.698	0.697	0.682	0.698
locreg29	+	512.5	0.694	0.693	0.679	0.694
A1	-	1523.1	0.568	0.568	0.561	0.569
G	-	1493.2	0.599	0.599	0.585	0.600
logrelBAI$^{juv}_{69}$, BAI$_2$, locreg6, locreg25, A1		431.3	0.844	0.845	0.825	0.844

Table 3: Optimised parameters value of simple STmodels using three tree stress memories and corresponding AUC$_{ap}$, AUC$_{cor}$, AUC$_{eq}$ and AUC$_{temp}$ values.

Model		Th	p	AUC$_{ap}$	AUC$_{cor}$	AUC$_{eq}$	AUC$_{temp}$
ST1	Thabs	618.0	0.607	0.670	0.670	0.540	0.672
	Threl	0.625	0.462	0.687	0.686	0.549	0.688
	Threlj	0.701	0.574	0.744	0.744	0.570	0.745
ST2	Thabs	709.4	0.621	0.627	0.628	0.534	0.624
	Threl	0.691	0.681	0.650	0.650	0.545	0.647
	Threlj	0.593	0.616	0.734	0.735	0.601	0.732
ST3	Thabs	560.9	0.679	0.602	0.602	0.533	0.601
	Threl	0.685	0.663	0.608	0.609	0.540	0.605
	Threlj	0.762	0.684	0.694	0.694	0.587	0.690

Table 4: Optimised parameters value of STmodels with stress counter (ST_{SC}) and vitality index (ST_{VI}) using different tree stress memories, and corresponding AUC_{ap}, AUC_{cor}, AUC_{eq} and AUC_{temp} values.

Model	Threshold	Mem	Th	a	b	c	AUC_{ap}	AUC_{cor}	AUC_{eq}	AUC_{temp}
ST_{SC}	Thabs		542.2	0.160	0.150	2.000	0.672	0.673	0.572	0.671
	Threl		0.518	0.132	0.106	2.000	0.689	0.688	0.584	0.688
	Threlj		0.550	0.148	0.163	2.000	0.768	0.769	0.661	0.766
ST_{VI}	Thabs	2	982.2	0.100	0.140	1.700	0.710	0.708	0.562	0.707
	Threl	2	0.946	0.145	0.165	2.004	0.723	0.723	0.578	0.721
	Threlj	2	0.873	0.197	0.208	1.850	0.812	0.777	0.610	0.776
	Thabs	3	971.3	0.177	0.190	1.966	0.677	0.677	0.569	0.676
	Threl	3	0.976	0.138	0.185	1.872	0.688	0.687	0.584	0.684
	Threlj	3	0.965	0.161	0.165	1.614	0.790	0.760	0.631	0.756
	Thabs	4	938.4	0.150	0.123	2.013	0.646	0.643	0.563	0.641
	Threl	4	0.916	0.013	0.120	2.088	0.659	0.658	0.578	0.657
	Threlj	4	0.989	0.041	0.048	1.963	0.768	0.733	0.631	0.732
	Thabs	5	688.7	0.144	0.153	2.015	0.616	0.616	0.544	0.614
	Threl	5	0.954	0.006	0.263	1.527	0.638	0.636	0.574	0.633
	Threlj	5	0.970	0.328	0.299	1.713	0.745	0.710	0.628	0.709

Annexe 5

Regulation of silver fir (*Abies alba* Mill.) transpiration during drought in relation to soil characteristics.

Nourtier M[1], Cailleret M[2], Yingge X[1], Huc R[2], Chanzy A[1], Davi H[2]

[1]INRA UMR 114 EMMAH Avignon
[2]INRA UR 629 URFM Avignon

En préparation pour *Annals of Forest Science*

Abstract

- **Context:** Silver fir is declining in the Mediterranean area, at its southern margin where climate is expected to become warmer and drier. At regional scale, its vulnerability seems to be related to temperature and precipitation (altitude, regional climate) while it depends on soil water availability at forest stand scale (soil characteristics, slope).
- **Aim:** In order to understand silver fir vulnerability, the main factors involved in their transpiration regulation and physical adjustments that could explain different death rate according to soil properties are further studied.
- **Methods:** Transpiration and predawn water potential dynamic were measured on trees during several years. Vulnerability curves to embolism of shoots and coarse roots were established. Tree development was assessed using tree growth, sapwood proportion and leaf area. For all studied trees, soil properties were characterised by electric resistivity measurements.
- **Results and conclusion:** Silver fir transpiration was quickly regulated as soil water potential decreased to avoid large embolism. Water stress began faster on soil with higher water availability which can be due to a higher aboveground/belowground development. Severe drought had also consequences on the following year by the delayed decrease of the transpiration level. Transpiration limitation during and after drought influence the carbon balance and would limit carbon reserves. This would explain how vulnerability of trees depends on soil properties.

Introduction

Drought is a main factor driving the tree functioning. A decrease in water availability during the growing period induces highly negative water potential, which can lead into hydraulic failure. To avoid xylem embolism, transpiration can be reduced by stomatal closure but at the expense of photosynthesis, while metabolism has to be maintained through carbon consuming respiratory processes. Consequently, drought induces a reduction in carbon availability for its use (McDowell and Sevanto, 2010) for tree respiration, growth, reproduction and production of defenses against pathogens. Generally, drought-induced tree mortality is considered to be caused by both carbon starvation and/or hydraulic failure (McDowell *et al.*, 2008), but no experimental data has demonstrated one hypothesis or the other (McDowell and Sevanto, 2010; Sala *et al.*, 2010).

In Mediterranean areas climate, water constraint is the main limiting factor for vegetation growth. During last decades, the frequency, duration and intensity of summer drought increased and this trend is predicted to continue in the future according to climatic models (Somot *et al.*, 2008). Even if some studies suggest an increase of forest productivity due to raise in CO_2 concentration and temperatures (Loustau *et al.*, 2005; Davi *et al.*, 2006; Delpierre *et al.*, 2009), in Mediterranean areas the observed trend was a decrease in tree growth (Adams and Kolb, 2005; Sarris *et al.*, 2007; Cailleret and Davi, 2011) and die-off or decline of forests were often mentioned after severe droughts (Peñuelas *et al.*, 2001; Bréda *et al.*, 2006; Lebourgeois *et al.*, 2010). Decline in tree vitality is usually indicated by reduction in total leaf area (defoliation), radial growth (BAI), sapwood area, and quantity of non structural carbon compounds; all these processes being reversible. In the worst cases, when the drought is too long, intense, or occurs too frequently, the process is irreversible and the tree dies. Thus we can expect that massive diebacks would occur more frequently and would affect larger forest areas. This trend being already observed at worldwide scale (Allen *et al.*, 2009; van-Mantgem *et al.*, 2009).

Tree sensibility to drought resides in the stomatal regulation according to soil water availability. However, it also depends on the capacity of trees to exploit these water resources according to the soil conditions and to the root distribution; this last one difficult to access is an essential factor to understand tree vulnerability to drought *(*Sperry *et al.*, 1998; Certini *et al.*, 2000; Martinez-Vilalta *et al.*, 2002; Bréda *et al.*, 2006). Succession of water stress leads to physiological and morphological adjustments of trees to their local environmental conditions (Bréda *et al.*, 2006) such as reduction in leaf area index (Limousin *et al.*, 2009), change in xylem conductivity (Cruiziat *et al.*, 2002), or in the ratios between sapwood, leaf area and root surface. Indeed, trees growing in dry environment seem to adjust their structures to increase availability of water (uptake and storage) and reduce the demand (Becker, 1977; Mencuccini and Grace, 1995; Sperry *et al.*, 1998; Jackson *et al.*, 2000; Bréda *et al.*, 2006). Higher root system development, lower vulnerability to embolism and lower minimum canopy conductance were also found to limit tree vulnerability using a modelling approach by Martinez-Vilalta *et al.* (2002).

Silver fir (*Abies alba* Mill.) was studied because of its high sensitivity to drought and numerous drought-induced declines were reported at its southern and low altitude margin (Aussenac, 2002; Oliva and Colinas, 2007; Peguero-Pina *et al.*, 2007; Battipaglia *et al.*, 2009; Lebourgeois *et al.*, 2010). The study was conducted on the Mont Ventoux, a mountain in the Mediterranean area in the South of France, which presents a high spatial variability in soil water content and where silver fir mortality reach high rates on some plots (Cailleret 2011). We studied the variations in space and time of silver fir regulation of water fluxes according to the local pedological and meteorological conditions. Water fluxes were estimated using sap flux density measurements considering their radial distribution, which also provide information about tree structure (Cermak *et al.*, 2008). Vulnerability of trees to embolism was investigated as a factor explaining vulnerability to drought (Cochard 2006). Effects of transpiration regulation during drought were evaluated on tree growth, tree sapwood and leaf area development.

The aims of this study were to (1) assess the main factors involved in the transpiration regulation of silver fir; (2) study the link between the variability of water stress intensities and soil pedological properties, (3) evaluate some consequences of water stress on tree development and adjustments to local pedological conditions.

Materials and methods

Study sites

This study was conducted on the North facing slope of the Mont Ventoux (South of France, 44°10'28"N, 5°16'44"E), a calcareous and Mediterranean mountain. On the mountain vegetation belt (between 1000 and 1600 m of altitude), silver fir (*Abies alba* Mill.) was recolonizing pioneer pines, which were planted during the nineteenth century. During the last decade silver fir growth currently decline (Cailleret and Davi, 2011). Some trees showing high crown damages and dead trees have already been reported. Mortality rate averaged 21% with high variability between plots (0 to 54%) and within plots due to micro-local soil heterogeneity (Cailleret 2011). The mountain is characterised by a karstic formation and soil width above the substratum is highly variable. At 1200m, annuals rainfalls averaged 1130mm while mean temperature was 7.6°C for the period 1964-2009. However, soil water content is expected to be low due to the high proportion of coarse material (between 50 and 80%), the infiltration of water in the calcareous bedrock, the high slopes (25° on average), and rainfalls seasonality: dry summers and most of the rainfall occurring in autumn which is characteristic of the Mediterranean bioclimate.

Four plots were intensively instrumented at three different altitudes (Tab. 1) to sample different climatic demands. Pedological conditions were also different in terms of soil depth over the bedrock indicating different water availability. Measurements of sap flux density, soil water content and micrometeorological conditions were done during three years (2008-2010) on 2 of these plots (plot 1 and 4) and two years (2009-2010) for the two other plots. Characteristic of each plot and the description of the measurements are presented in Tab. 1.

At 1200 m of altitude, a transect in contour line of 800 m long was also further studied to analyse the soil effects on growth (Cailleret *et al.*, in prep.). Soil properties and tree characteristics (age, height, diameter at breast height, sapwood area and tree health status) situated in the 2 m around this transect were collected. This transect represented a population of 207 trees, in which 49 of them had crown defoliation and discoloration rates higher than 20% (declining trees), 95 were healthy and 63 were dead.

Sapwood and leaf area measurements

All trees were cored at diameter breast height (DBH; 130 cm), perpendicularly to the slope to avoid compression wood. Cores were extracted during the autumn 2006 and 2007 before the experimental period. Sapwood was separated from heartwood by colour testing with perchloric acid (Kutscha and Sachs, 1962). Sapwood length and total length of the core were measured to determine sapwood area. In this study, only sapwood area of healthy tree was considered.

The projected leaf area was measured to have an estimate of the leaf area developed by each tree. The length of the lowest branches of the crown at 4 azimuths (South, East, West and North, the slope being oriented to North) was measured for all sample trees. Leaf area was then calculated from projected area, crown height, the rate of foliar defoliation estimated according DSF protocol and an estimate of average leaf density assessed trough hemispherical photographs. As sapwood and leaf area increased with tree age, age effect was removed to only take into account the soil effect. Relationships between sapwood or leaf area and age were both linear (respectively, $y = 0.05.x - 0.07$, $R^2 = 0.33$; $y = 0.04.x + 6.81$, $R^2 = 0.33$). Therefore, soil influence was study on the residuals of these relationships.

Tree growth rate estimation

On the cores collected, RCS method (Esper *et al.,* 2003) was used to compare radial growth trends between trees. The age effect was removed using annual growth indices calculated using mean age curve of Basal Area (Cailleret, 2011) and growth indices (GI, dimensionless) were studied. A GI superior to 1 indicates that the tree had a better growth than the average at same age. Moreover, as it was illustrated that trees on the transect in contour line which had a higher growth rate during their juvenile phase were more prone to die (Cailleret and Davi, submitted), the mean growth rate over the 35 first years of tree life was calculated for each tree.

Transpiration measurements and calculation

Sap flux density was measured on several trees on each plots (Tab. 1) using the thermal dissipation method (Granier, 1985). A thermal dissipation sap flowmeter is composed of two probes. 2 cm of the probes are inserted radially into the xylem, just below tree bark. One of the two probes is heated at constant energy, while the other remains at the wood temperature. The sap flux density is function of the temperature difference (ΔT) between both probes. To limit the energy cost and the frequency of battery replacement, a cyclic heating was used. Nevertheless, using the heating mode causes some errors because thermal equilibrium is not reached during the measurement. We corrected this error thanks to a method, tested on silver firs on the Mont Ventoux, allowing extrapolating measurements from cyclic heating to ones from continuously heating calculated thanks Granier's calibration (Nourtier *et al.*, 2011). Cycles used in this study have need changed between the beginning and the end of the experiment: from 0.5h-heating/0.5h-cooling during night and daylight (2008) to 1h-heating/1h-cooling during the daylight (2009) and 3h-heating/4h-cooling during the night (2010). Hence different corrections were needed as explained in Nourtier *et al.* (2011).

Because the active length of the probes is 2 cm, the sap flow is only measured in a part of xylem when the sapwood thickness is greater than 2 cm. A scaling-up procedure was applied to estimate the whole-tree transpiration with an approach similar of the one of Delzon *et al.* (2004). On each plot, sap flux density was first measured with 4 sensors on 1 “golden” tree: 3 at western, eastern and northern side of the tree inserted between 0 and 2 cm after the cambium ($J_{0\cdot 2}$ corresponding to the mean of this 3 sap flux densities), and 1 at northern side inserted between 2 and 4 cm ($J_{2\cdot 4}$) to measure radial pattern of sap flow. A correction factor, C, is calculated, at each measurement time, from the sap flux densities calculated at the 2 depths:

$$C = \frac{J_{2\cdot 4}}{J_{0\cdot 2}} \qquad \text{Equation 1}$$

C was applied to the sap flux density (in $L.dm^{-2}.h^{-1}$) at each depth (with a step of 2 cm) of the sapwood thickness measured on the trees. We supposed a linear decrease of the sap flux density with depth in the sapwood:

$$J_{i\cdot(i+2)} = C.J_{(i-2)\cdot i} \qquad \text{Equation 2}$$

On plot 1 and 4, sap flux density was also measured on other trees but only with one sensor inserted between 0 and 2 cm at northern side of the tree. In this case, the correction factor calculated on the “golden” tree of the same plot was applied to the sap flux density measured to calculate deeper ones. This is a strong hypothesis of the experiment because, even if flux between 0 and 2 cm were similar between trees of a same plot, we had no ways to know if it was also the case for sap flux density between 2 and 4 cm. However, some authors found that relationship between radial distribution of sap flux and trees diameters (Delzon *et al.*, 2004; Fiora and Cescatti, 2006) can be homogeneous on a same plot..

Total sap flux, J in L.h^{-1}, is then calculated by adding the sap flux densities and scaling up by the area (in dm²) of each annuli of 2 cm width sapwood (between i and $i+2$).

$$J = \sum_{i=0\cdot 2}^{A_s} J_{i\cdot(i+2)} . A_{i\cdot(i+2)} \qquad \text{Equation 3}$$

Finally, transpiration of each tree, T in mm.h^{-1}, is obtained by divided J by the leaf area of the tree (S, m²).

$$T = \frac{J}{S} \qquad \text{Equation 4}$$

Number of tree for which sap flux density and transpiration are calculated on each plot is presented in Tab. 1.

Soil water content

Soil water content was only assessed using direct and indirect measurements. Firstly, leaf water potential were measured using a Scholander pressure chamber (Scholander *et al.*, 1965) to assess tree water availability. Shoot samples were collected on 17 trees located on the different plots including the 9 trees selected for the measurements of sap flux. Predawn leaf water potential (ψ_{pd}, MPa) was recorded before sunrise between 4:00 a.m. and 5:00 a.m and represents the soil water potential because at the end of night the plant is supposed to be in equilibrium with the soil. Noon leaf water potential (ψ_{min}, MPa) was also measured from the exposed sun crown of the tree (samples collected by climbing the tree), between 12:00 p.m. and 1:30 p.m. Measurements were done on 2 to 4 shoot samples per tree.

Secondly, soil humidity was recorded on plots 1 and 4 using probes sensors inserted into the soil, every 20 cm until 1 m of depth. On both plots, 3 different pits were studied to take into account soil heterogeneity. The pits were installed near the trees where sap flux density was measured. As the relation between the signal of the sensors in Volt and the effective soil water content is not well established, it is expressed in percentage of the maximum value in Volt done over the period, minimum value being set to 0 %.

Characterisation of soil properties using electrical resistivity

The electrical resistivity (ER) can be related to the proportion of coarse material in the soil and allows locating the bedrock (Yingge *et al.*, in prep.). Hence, soil could be characterised by a potential available water capacity. Higher is the ER measured, lower is the potential available water capacity (Yingge *et al.*, in prep.).Thanks to the tomography profile, several classes of resistivity were defined to be representative of potential soil water content. To be realistic about the possible of root vertical distribution in our study area and considering cracks in the bedrock often present in karstic areas, resistivity profiles were considered over a depth of 5 m (Rambal, 1984). 4 classes of resistivity were defined by considering the mean resistivity over the 5 m (for one class mean resistivity over the 1st meter and over the 4 meters below were separated) to highlight the effect of the top layers properties and of soil conditions in depth, and are resumed in Tab. 2.

Trees were spatially located and related to a class of electrical resistivity (ER) using 3D profiles of electrical resistivity (Fig. 5). On plot 3, ER is high (class 4) while ER is low on plot 2 (class 1). On plot 4, ER is medium on the first meter but high on the rest of the soil (class 3). Finally, on plot 1, ER is more variable but in average high and depending on the trees, they are classified either in class 3 or in class 4 (Tab. 2). At a larger scale, trees of the transect in contour line were also classified according to ER, but defined on the 2D profile. This profile clearly highlights the variability of soil resistivity in horizontal but also in depth (Fig. 6).

Micrometeorological measurements

On each intensive plot, a pole was installed on a tree to allow the measurement of micrometeorological variables approximately 1 m above the canopy. Sensors were set up at each extremity of a cross fixed at the top of the pole. Wind speed (u_s), air temperature (Ta), air relative humidity (Rh) and global radiation (Rg - only on plot 1 and 4) were measured every 30 min. Rainfall was also recorded on plot 1 and 4 in a opened area during the year 2009 and 2010, and under the canopy during the year 2008 but only on plot 1.
From these data, a referenced transpiration, T_0, was calculated using the same time resolution than the measured one to represent a potential transpiration of trees only depending of the meteorological conditions and considering no soil drought. The calculation of T_0 is derived from the widely used equation of Penman-Monteith (Monteith, 1973) for the evapotranspiration, but assuming a null contribution from the soil. Value of the stomatal resistance (r_s) required for the calculation of T_0 is obtained using the model CASTANEA (Davi *et al.*, 2005; Dufrêne *et al.*, 2005) parameterised for silver fir considering no water stress under the same meteorological conditions. A transpiration ratio, T^*, is calculated by dividing T by T_0.

$$T_0 = \frac{\Delta.Rn + \rho.c_p.VPD/r_a}{\lambda.(\Delta + \gamma.(1 + r_s/r_a))} \qquad \text{Equation 5}$$

where Rn is the net radiation (W.m^{-2}), VPD is the vapour pressure deficit (MPa), r_a is the aerodynamic resistance (s.m^{-1}), λ is the latent heat of vaporisation (MJ.kg-1), $\gamma$is the psychrométric constant (MPa.°C^{-1}), ρ is the air density (kg.m^{-3}) and Cp is the specific heat of the air (MJ.kg^{-1}.°C^{-1}). Aerodynamical resistance was calculated thanks to the equation established by Brutsaert (1982).

$$r_a = \frac{\ln[(z_m - d)/z_{om}].\ln[(z_h - d)/z_{oh}]}{k^2.u_s} \qquad \text{Equation 6}$$

The fitting parameter z_{om}/z_{oh} (Lhomme *et al.,* 2000), representative of the radiometric thermal roughness length, was set to 1 as it appeared reasonable for forests with $z_{om} = h/10$ (Mölder and Lindroth, 1999; Nakai *et al.,* 2008). h was the tree height and a mean forest height was taken (17 m).

Vulnerability to xylem embolism

Vulnerability to xylem cavitation was assessed on both branches and roots. Only results concerning the roots are presented here as they are more vulnerable to embolism *(Jackson et al.*, 2000). Roots sampled were shallow ones which are supposed to be less sensible to embolism than deeper roots (Jackson *et al.*, 2000). The vulnerability was evaluated using the pressurization method (Cruiziat *et al.*, 2002) on 8 samples from 4 healthy trees taken off during a wet period to avoid already embolized samples. Samples were subjected to pressures from 0 to 7 MPa with a step of 1 MPa. The percent loss of conductivity (*PLC*) was calculated from the maximum of conductivity at 0 MPa. The vulnerability curve was then fitted to the exponential sigmoid equation from Pammenter and Willigen (1997).

$$PLC = 100.\left(1 + e^{a.(\psi - b)}\right) \qquad \text{Equation 7}$$

where ψ is the water potential, corresponding to the pressure applied and a and b are constants, b corresponding to the potential at 50 % of *PLC* (PLC_{50}).

Results

Regulation of transpiration by meteorological conditions and soil water content

T_0 was found to only slightly decrease with the altitude (Fig. 1). Maximum values were respectively 0.65 mm.h^{-1} for plot 1, 0.61 mm.h^{-1} for plot 2 and plot 3 and 0.58 mm.h^{-1} for plot 4. During summer, T_0 was high and rainfall was low for both years 2009 and 2010 revealing two years with intense droughts (Fig. 1). On plots 1 and 4, rainfall deficit, calculated as the cumulated difference between precipitation (*P* in mm.j^{-1}) and T_0 (in mm.j^{-1}), was estimated for the summer 2009 from the day of the year 100. This deficit always negative during all the summer reached a value of -385 mm on plot 1 revealing an intense drought (Fig. 2). The deficit was less negative for the plot 4 located higher in altitude (plot 4; Fig. 2) due to a slightly lower climatic demand (T_0). Hence, it is a reason why the water stress recorded was also slightly lower for trees on this plot (Fig. 1 and Tab. 3).

Levels of transpiration of all the studied trees were always low: under 0.25 $mm.h^{-1}$ and the ratio T/T_0 never exceeded 0.4. This indicates that there was a permanent regulation of the transpiration by the stomata conductance. Comparing the measured transpiration to the potential one, confirms the high level of water stress experienced by the trees during these years. Therefore, on all plots transpiration has felled to very low level during both summers 2009 and 2010 (Fig. 1 and Tab. 3).

On plot 1, soil water content recorded on the first meter of soil decreased faster and the water stress was more intense (transpiration almost null) and longer (Fig. 1). Transpiration is well correlated with soil water content (R^2 of the linear regressions were 0.52 for plot 1 and 0.26 for plot 4) especially when it was limiting for transpiration (below 15 % for plot 1 in Fig. 3). In other words, there was an important control of the transpiration according to soil water content. When the soil water level was sufficient, e.g. the plot 4, VPD was the second factor of regulation. Indeed, correlation coefficients of the linear relations between VPD and T^* for a soil water content higher than 15 %, were respectively for plots 1 and 4, 0.59 and 0.57. And transpiration rate became almost null, when VPD was exceeding 2 MPa (Fig. 3), which corresponds to the minimum leaf water potential.

To avoid embolism, stomata were quickly closed as soil water potential decreased. At the minimum water potential measured (-2 MPa), the loss of conductivity was low: 16.1 % (Fig. 9). The 50 % loss of conductivity (PLC_{50}) corresponded to a water potential of -3.8 MPa. According to the minimal water potential and to the observed regulation of the transpiration, at -3.8 MPa, stomata were totally closed but embolism occurred before in root tissues.

Lack of transpiration recovery after water stress

In 2010, snow amount at the end of the winter and spring rainfalls were abundant as during the 2 previous winters. Soil water content was high and levels of T_0 were similar than the ones in 2008 and 2009 (Fig. 1). However transpiration rates were clearly lower (see plots 1 and 4 on Fig. 1 and Tab. 3), than the ones measured in 2008 and 2009 before summer. This is mainly due to the loss of sap flux density in the inner sapwood as shown in Fig. 4. The sap flux density recorded on the sensor between 2 and 4 cm depth in the sapwood fell down under 0.05 $L.dm^{-2}.h^{-1}$ during the summer drought in 2009, and stayed at a low level (under 0.1 $L.dm^{-}$

^{2}.h^{-1} on the 4 sensors) in autumn while soil water content increased. This phenomenon was observed on all the trees with a monitoring of the sap flux radial distribution. Moreover, there was also a decrease in sap flux density between 0 and 2 cm depth.

After the 2010 drought, sap flux density in the inner sensor had stayed low. Therefore, the sap was only conducted on a 2 cm width of the sapwood after the 2009 drought. An increase of the sap flux density of the inner sapwood during 2010 spring was only observed for tree 5 on plot 3. It represented about 50 % of the external sap flux density before summer 2010 but it decreased again to a low level after the drought of 2010 (Fig. 4).

The total transpiration rate observed after 2010 drought was very low. As an example, maximum T of tree 2 decreased until 0.03 mm.h^{-1} after 2010 summer, while it was 0.08 mm.h^{-1} in 2008 and 0.05 mm.h^{-1} in 2009 after summer (Fig. 1). In contrast with post effect of 2009, the decrease of transpiration after 2010 summer was, this time, mainly due to a decrease of sap flux density in the outer sapwood (between 0 and 2 cm depth; Fig. 4).

Impacts of soil characteristics on tree functioning

At large scale, we found that tree death depends on soil properties (Fig. 6 and Fig. 7). Unexpectedly, there were more dead trees on classes 1 and 2 corresponded to soils with potentially more available water capacity. On classes 3 and 4, with potentially less available water capacity, there were more healthy trees and less dead ones but also, more declining ones (Fig. 7).

To explain this pattern we related soil classes determinated by ER and mean radial growth. As found by Cailleret et al. (in prep), mean radial growth index over the 35 first years of tree life can be used as an indicator of tree vulnerability to dieback. This variable was studied according to the combination of the health status and the classes of ER on the trees of the transect in contour line. Class 2 was removed from this analysis because of the low number of trees in each category. The differences between categories were only significant for dead tree of class 1 ($p < 0.05$, Tukey test). In classes 3 and 4, dead trees seemed to have a higher juvenile growth rate than declining and healthy trees (Fig. 10). Declining trees seemed to have also higher growth rates than healthy ones. In class 1, juvenile growth rates were similar for all health status (*Dead*, *Declining* or *Healthy*). Healthy trees of class 1 were higher than the one of healthy trees of classes 3 and 4, suggesting they had higher aboveground development.

When studying only growth index according to soil ER classes without consideration for the health status, growth at the beginning of the year 1900 was lower for class 3 (Fig. 11). Above all, from the year 1976, year with an exceptional intense drought, growth index of trees on the class 1 differentiated from the others. Until now, it has been lower since this date revealing the low vigour of trees on this type of soil after an intense drought.

Trees 1 and 3 on plot 1 had higher rates of transpiration because they had larger sapwood (Tab. 3) and the factor C applied to the transpiration calculation of these trees was high due to the radial distribution of sap flux density for tree 2 in Fig. 4). Therefore, comparison of transpiration rates between these trees is not relevant. Our interest will more be focused on the dynamic comparison.

At local scale, after the 2009 drought, all trees had approximately the same rate of transpiration (Fig. 1), sap flux being predominantly localized in the outer xylem except for tree 5 which had, consequently, a higher transpiration rate (Fig. 4 and 1). The influence of soil on minimal ψ_{pd} was statistically significant (ANOVA, *p-value* < 0.01) and in each soil class, altitude was not a first order factor influencing ψ_{pd} (ANOVA, *p-value* > 0.5). Trees of plot 4 had the lowest decrease of transpiration level (Fig. 1) due to the soil structure (class 3) but also to the lower climatic demand at this higher altitude (Fig. 2). Trees of the class 3 of soil resistivity (with intermediate potential soil available water) showed the highest transpiration at high T_0 level during the 2009 drought (Tab. 3). Moreover, their transpiration rate decreased slower at the beginning of the drought and they were the ones experienced the lowest level of water stress (trees 2 and 3 on Fig. 1 and Tab. 3). Besides, minimum predawn water potentials were less negative for this class during the drought (Tab. 3 and Fig. 8), confirming the observations done on transpiration. When drought started, ψ_{pd} decreased faster for trees on soil of classes 4 and 1 (Fig. 8). At the end of the drought in 2009, ψ_{pd} measured for class 1 reached the minimum leaf potential, ψ_{min} (-2 MPa; Fig. 8), while ψ_{pd} was about at the same level for all trees in 2008 and in 2009 before the drought (data not shown). In addition, the decrease in transpiration was the most rapid for the tree of class 1 (Fig. 1).

The mean value of the residuals from the ratio sapwood / leaf area (for trees on transect in contour line) was relatively constant according to the classes of resistivity except for the class 3. Distribution of these variables according to the resistivity classes was not significantly different (ANOVA, *p-value* > 0.1).

Discussion

Transpiration regulation of silver fir

Silver fir is sensitive both to atmospheric and soil drought. Compared to other species, its minimum leaf water potential is not very negative in comparison with the threshold of its vulnerability to cavitation (root PLC_{50} = -3.8 MPa). Indeed, our results show that silver fir regulates very quickly its transpiration as already mentioned by previous studies (Aussenac, 2002; Peguero-Pina *et al.*, 2007). As soon as the soil water potential started to decrease, stomatal conductivity was reduced and, as a consequence, embolism and hydraulic failure would be limited. Hence, at the minimum water potential we measured, a 16 % loss of conductivity of the roots was estimated, which is low comparing to other species (Bréda *et al.*, 2006). This leads to a decrease of the transpiration when conditions are too dry during summer and so, to a decrease of the photosynthesis (carbon uptake) while metabolism respiration is maintain (carbon consumption). The transpiration stayed to a reduced level (< 0.02 $mm.h^{-1}$) during more than 1.5 month in 2009. During intense and/or long drought, the carbon demand declined due to reduction in growth respiration (Granier *et al.*, 2007) but maintenance respiration had to be maintained thanks to the use of non-structural carbohydrates reserves. Hence, during these drought periods, tree can act as a carbon source (Granier *et al.*, 2007) and it can lead to death if stress is too long.

Transpiration loss and roots' dynamic: long term consequences of drought on water uptake

Suffering from a high water stress had consequences on tree functioning for the following years. It led to a loss of water amount conducted in the inner sapwood and so, a loss of transpiration rate. A high differentiation of radial sap flow distribution dynamics was observed within the sapwood. After an intense water stress, sap was only transported in the outer xylem part. The water transported in the inner sapwood would correspond to the water uptake by the roots located in the deeper soil layers (Nadezhdina *et al.,* 2007; Cermak *et al.*, 2008; Nadezhdina *et al.*, 2008; Nadezhdina, 2010). Therefore, this loss of sap flux density in the inner xylem would be due to a cessation of the water uptake by deeper fine roots while shallower ones were preserved. This can be explained by a stronger vulnerability to embolism of deep roots (Jackson *et al.*, 2000; McElrone *et al.*, 2004) or to a lower water stocks in deeper soil during drought. Another hypothesis is that, during drought, there was a redistribution of the flow from deep soil layers to the outer xylem (Nadezhdina, 2010).

There was probably an increase in root embolism and/or mortality often observed during the water stress (Bréda *et al.*, 2006; Sala *et al.*, 2010). But, transpiration is also directly influenced by total leaf area (Eq. 4). Therefore, transpiration reduction could be due to the loss of needles that was actually observed on Mont Ventoux during the droughts of 2009 and 2010 (data not shown) like in other sites (Bréda *et al.*, 2006; Limousin *et al.*, 2009). This loss of needles could be located on the lower branches of the trees also related to the inner xylem (Fiora and Cescatti, 2008), because these needles were less essential for the photosynthesis.

Our results also showed that transpiration during the year following the severe drought was still limited, and in 2010 water was only conducted in the outer xylem except for one tree. For this tree, the new start of the sap flux in the inner xylem indicates that the part of the sapwood where the flow has been stopped during drought can be refilled after it. This counter example seems to indicate that the post effects of severe drought are not due to sapwood embolism. Therefore, only a part of the root system would continue to uptake water after the drought and even the following year. This water uptake could be localised in all soil layer and redistributed in the outer xylem or only top roots would stay active. Indeed, this long-term impacts of drought could be related to the fine root turnover which depends on their depth. Mainiero and Kazda (2006) showed that fine roots could be replaced in the top soil layers in spite of a severe drying of this layer. Hence, a lack of root turnover in deeper soil would explain the decrease of water uptake that we observed. Another possibility is the death of the coarse roots that were exploring deep soil layers.

To summary, before drought, when soil water content was high, water uptake would occur in all soil layers as sap fluxes were measured in the outer and inner parts of the xylem. At the beginning of the drought, a progressive decrease in the proportion of water uptake in top soil layers in favour to the deep layers would occur as it was observed in several studies (Warren *et al.*, 2005; Schiller *et al.*, 2010) and would be associated to a redistribution of the water from deep layers to the outer xylem.

Effect of soil properties on tree sensitivity to drought

The spatial distribution of dead trees is very heterogeneous and especially depends on soil properties (Fig. 7; Cailleret *et al.* in prep). They were mostly located on classes 1 and 2 of ER. The contrary was expected because of the higher *a priori* water content on this type of soil (Yingge et al., in prep.). Dendrochronological study confirmed that trees with a higher growth rate during their juvenile phase were more prone to die (Cailleret *et al.* submitted). These differences are probably due to physiological adjustments of trees to their local conditions. Trees with a higher juvenile growth rate would have had a higher above ground development and then, a higher ratio between aboveground and belowground biomass compared to the others, which led in a higher water demand.

On the class 1 of ER, showing a higher proportion of dead trees, growth rates seemed to be more homogeneous and was superior to the one of living trees of classes 3 and 4 arguing for higher aboveground development. The little differences between growth rates of dead, declining and healthy trees for this class of soil indicates a similar vulnerability for all trees and maybe little delay between the beginning of decline and the death on this class of ER. This hypothesis seems to be confirmed by the new reports of dead trees on the transect in contour line: over the 9 dead trees in 2009 and 2010, 8 were on class 1. Hence, trees located on soils with high water availability (classes 1 and 2 of ER) were more vulnerable to drought. By comparison to their allocation to growth and to aboveground development, these trees probably allocated less carbon to their roots during their juvenile phase because of higher water availability on this type of soil explaining their higher vulnerability during the mature period in case of repeated and intense droughts. Indeed, this is shown by the predawn water potential measurements. It fell down its lowest value during drought on class 1 of ER while trees on other types of soil showed a slightly higher potential, probably because of higher root area and maybe deeper (Otieno *et al.*, 2006) and then, a better exploration of the soil. Finally, difference of trees vulnerability would depend on the differential juvenile development of the aboveground and belowground part and the root vertical distribution of the trees according to soil properties. Soil properties influenced this juvenile development and hence, the vulnerability during the mature phase by the potential water content.

Considering trees of classes 3 and 4 of ER, dead ones had a higher juvenile growth rate. This high growth rate was not expected on these dryer soils. Low competition during their juvenile phase could explain this. It could also be due to different properties of the soil on the third space direction, which was not assessed by the 2D profile. This bias can be particularly important for trees which directly grew on high resistivity soils (class 4), but which can reach soil pockets with higher water content and would explain the high variability of tree responses to drought stress within these ER classes. These trees with access to areas with higher water content would have had a higher growth rate with a favoured aboveground development compared to the belowground one. Trees located on the driest soils (classes 3 and 4), seemed to be less vulnerable to drought probably due to a preferential carbon allocation to roots during the juvenile phase inducing a higher root development compared to their leaf one and maybe deeper (Otieno *et al.*, 2006). This would allow compensating the lack of water in the soil, by increasing water uptake and decreasing water losses. On class 4, the water available is very limited inducing quick decrease in transpiration rate during drought. There is slightly more water available for trees located on soil class 3, which can explain why they less suffered from water stress. As their carbon assimilation is expected to be longer, they would be the less vulnerable trees to drought which was confirmed by the low rate of dead trees.

The adjustment of the leaf/root area ratio is an important factor to limit water stress and a decrease was observed on dry soils at the intraspecific scale (Sperry *et al.*, 1998; Hacke *et al.*, 2000). This was also detected on young silver firs growing in control environment: the ones growing in drier soils had a lower leaf to root ratio (Becker, 1977). In the same way, this ratio is the lowest for the species more adapted to drought (Martinez-Vilalta *et al.*, 2002; Bréda *et al.*, 2006; West *et al.*, 2008). On drier soils, roots also explore deeper layers (Sperry *et al.*, 1998; Jackson *et al.*, 2000). Thus, trees with high leaf/root area ratio and shallower root system would be more vulnerable to water stress because their exploitation of water resources would not be sufficient for their leaf development in case of drought.

Consequences of drought on silver fir vulnerability to death

During last years, several hypotheses of drought-induced tree death were presented and debated (McDowell and Sevanto, 2010; Sala *et al.*, 2010) but actually no experimental data clearly proved one of those. Following our results, we can affirm that silver fir death is probably not due to large hydraulic failure because of its quick stomatal closure but mainly to carbon starvation. The quantity of available carbon decreased due to the reduction of photosynthesis, and become only dependent on non-structural carbohydrates reserves after a given threshold. When the level of available carbon is not sufficient to support cell metabolism, the tree dies. This decrease of carbon availability could also be caused by disturbances in the carbon transport in the phloem or the carbon mobilization from reserves (Sala *et al.*, 2010).

At long term, in the case of repeated droughts, carbon uptake and stock decrease every year inducing a decline in tree vitality (Niinemets, 2010). Therefore, a hypothesis would be that the stock of fine roots and needles lost during summer drought could not be completely replaced, which would induce reduction in water absorption and carbon assimilation for the following year. That is why, water balance of the previous year is often mentioned as an important factor limiting silver fir development, especially tree growth (Granier *et al.*, 2007; Battipaglia *et al.*, 2009; Lebourgeois *et al.*, 2010) and why repeated droughts would lead to the decline of silver fir forests. However, the decline of fine root and needle biomass caused by drought will also diminish the respiration costs and, finally, may improve carbon balance of the plant (Sala *et al.*, 2010). Moreover, the decrease of carbon stock limits tree defence against pathogens and may increase their vulnerability during the following years (Mattson and Haack, 1987; Bréda *et al.*, 2006). Indeed, bark beetles are present on the Mt Ventoux and significantly aggravate the decline in vitality for trees already weakened, leading to quick death (Gillmann, 2010).

Conclusion

This study showed some physiological responses of silver fir trees on the Mt Ventoux to drought. It illustrated direct effects of the water stress during the current and lag-effects on the following years. We focused on how these effects could explain decline and mortality of trees after drought. The present study led to formulate hypothesis about tree adjustments to their local environment, particularly concerning the ratio between root and aboveground systems. These adjustments would have consequences on the water stress intensities and would then explain differences in trees vulnerability and in carbon amount that can be mobilized. The "patchy" distribution of tree mortality on the study site would therefore be correlated to soil properties heterogeneity in term of potential water content; this potential water content being related to the depth and the stone content of the soil.

To confirm or not our hypotheses, measurements on roots biomass, distribution and dynamic would be necessary. Information on the belowground system are often lacking because of its difficulty to access. Modelling the mechanisms implied in tree responses to drought by taking into account water and carbon balance according to different root densities and distributions and, to soil types would also allow testing these hypotheses. A focus on the consequences on carbon availability for allocation, especially to fine roots, should be done.

Acknowledgements

The research was funded by the project ANR-06-VULN-004 (Agence Nationale de Recherche) and by the ONF (Office National des Forêts). We thank B. Bes and A. Chapelet for their important help for all the measurements in the field as well as N. Mariotte, F. Courdier, W. Brunetto, D. Gounelle and G. Sappe. We also thank A. Jouineau for its help in the root collection for measurements of the vulnerability to embolism. A special thanks to A. Granier for the several discussions helping for the understanding of the results.

The research was funded by the project ANR-06-VULN-004 (Agence Nationale de Recherche) and by the ONF (Office National des Forêts) through a PhD grant.

References

Adams H.D. and Kolb T.E., 2005. Tree growth response to drought and temperature in a mountain landscape in northern Arizona, USA. J. Biogeog. 32: 1629-1640.

Allen C.D., Macalady A.K., Chenchouni H., Bachelet D., McDowell N., Vennetier M., Kitzberger T., Rigling A., Breshears D.D., Hogg E.H., Gonzalez P., Fensham R., Zhang Z., Castro J., Demidova N., Lim J.-H., Allard G., Running S.W., Semerci A. and Cobb N., 2010. A global overview of drought and heat-induced tree mortality reveals emerging climate change risks for forests. For. Ecol. Manage., 259, 660-684

Aussenac G., 2002. Ecology and ecophysiology of circum-Mediterranean firs in the context of climate change. Ann. For. Sci. 59: 823-832.

Battipaglia G., Saurer M., Cherubini P., Siegwolf R.T.W. and Cotrufo M.F., 2009. Tree rings indicate different drought resistance of a native (*Abies alba* Mill.) and nonnative (*Picea abies* (L.) Karst.) species co-occuring at a dry site in Southern Italy. For. Ecol. Manage. 257: 820-828.

Becker M., 1977. Contribution à l'étude de la transpiration et de l'adaptation à la sécheresse des jeunes plants résineux. exemple de 3 sapins du pourtour méditerranéen (*Abies alba*, *A. Nordmanniana*, *A. numidica*). Ann. For. Sci. 34(2): 137-158.

Bréda N., Huc R., Granier A. and Dreyer E., 2006. Temperate forest trees and stands under severe drought: a review of ecophysiological responses, adaptation processes and long-term consequences. Ann. For. Sci. 63: 625-644.

Brutsaert W., 1982. Evaporation into the atmosphere. Theory, history, and applications, Kluwer Academic Publishers, 305 p.

Cailleret M., 2011. Causes fonctionnelles du dépérissement et de la mortalité du sapin pectiné en Provence. PhD Thesis Université de Aix Marseille 3.

Cailleret M., in prep. Comparison of drought-induced decline and mortality processes on silver fir among three sites in Provence, south-east France. Ann. For. Sci.

Cailleret M. and Davi H., 2011. Effects of climate on diameter growth of co-occuring *Fagus sylvatica* and *Abies alba* along an altitudinal gradient. Trees 25(2): 265-276.

Cailleret M. and Davi H., submitted. How to predict drought-induced tree mortality from radial growth data ? J. Ecol.

Cermak J., Nadezhina N., Meiresonne L. and Ceulemans R., 2008. Scots pine root distribution derived from radial sap flow patterns in stems of large leaning trees. Plant Soil 305: 61-75.

Certini V.G., Corti G. and Ugolini F.C., 2000. Influence of soil properties on the mortality of silver fir in Tuscany, Italy. Forstw. Cbl. 119: 323-331.

Cochard H (2006) Cavitation in trees. Comptes Rendus de Physique, 7: 1018-1026.

Cruiziat P., Cochard H. and Améglio T., 2002. Hydraulic architecture of trees: main concepts and results. Ann. For. Sci. 59: 723-752.

Davi H., Dufrêne E., Francois C., Maire G.L., Loustau D., Bosc A., Rambal S., Granier A. and Moors E., 2006. Sensitivity of water and carbon fluxes to climate changes from 1960 to 2100 in European forest ecosystems. Agric. For. Meteorol. 141: 35-56.

Davi H., Dufrêne E., Granier A., Dantec V.L., Barbaroux C., François C. and Bréda N., 2005. Modelling carbon and water cycles in a beech forest. Part II: Validation of the main processes from organ to stand scale. Ecol. Modell. 185: 387-405.

Delpierre N., Soudani K., François C., Köstner B., Pontallier J.Y., Nikinmaa E., Misson L., Aubinet M., Bernhofer C., Granier A., Grünwalds T., Heinesch B., Longdoz B., Ourcival J.M., Rambal S., Vesala T. and Dufrêne E., 2009. Exceptional carbon uptake in European forests during the warm spring of 2007: a data-model analysis. Global Change Biol. 15: 1455-1474.

Delzon S., Sartore M., Granier A. and Loustau D., 2004. Radial profiles of sap flow with increasing tree size in maritime pine. Tree Physiol. 24: 1285-1293.

Dufrêne E., Davi H., François C., Maire G.L., Dantec V.L. and Granier A., 2005. Modelling carbon and water cycles in a beech forest. Part I: Model description and uncertainty analysis on modelled NEE. Ecol. Modell. 185: 407-436.

Fiora A. and Cescatti A., 2006. Diurnal and seasonal variability in radial distribution of sap flux density: implications for estimating stand transpiration. Tree Physiol. 26: 1217-1225.

Fiora A. and Cescatti A., 2008. Vertical foliage distribution determines the radial pattern of sap flux density in *Picea abies*. Tree Physiol. 28: 1317-1323.

Gillmann M., 2010. Influence et rôle de deux facteurs biotiques (*Viscum album* L. et *Scolytidae*) impliqués dans le processus de dépérissement et de mortalité du Sapin pectiné (*Abies alba* Mill.), INRA Avignon, URFM - Université de Rennes 1, pp. 42.

Granier A., 1985. A new method of sap flow measurement in tree stems. Ann. For. Sci. 42: 193-200.

Granier A., Reichstein M., Bréda N., Janssens I.A., Falge E., Ciais P., Grünwald T., Aubinet M., Berbigier P., Bernhofer C., Buchmann N., Facini O., Grassi G., Heinesch B., Ilvesniemi H., Keronen P., Knohl A., Köstner B., Lagergren F., Lindroth A., Longdoz B., Loustau D., Mateus J., Montagnani L., Nys C., Moors E., Papale D., Peiffer M., Pilegaard K., Pita G., Pumpanen J., Rambal S., Rebmann C., Rodrigues A., Seufert G., Tenhumen J., Vesala T. and Wang Q., 2007. Evidence of soil water control on carbon and water dynamics in European forests during the extremely dry year: 2003. Agric. For. Meteorol. 143: 123-145.

Hacke U.G., Sperry J.S., Ewers B.E., Ellsworth D.S., Shäfer K.V.R. and Oren R., 2000. Influence of soil porosity on water use in *Pinus taeda*. Oecologia 124: 495-505.

Jackson R.B., Sperry J.S. and Dawson T.E., 2000. Root water uptake and transport: using physiological processes in global prediction. Trends in plant science 5(11): 482-488.

Kutscha N.P. and Sachs I.B., 1962. Color tests for differentiating heartwood and sapwood in certain softwood tree species. Report 2246, Forest Products Laboratory, Madison, WI, pp. 16.

Lebourgeois F., Rathgeber C.B.K. and Ulrich E., 2010. Sensitivity of French temperate coniferous forests to climate variability and extreme events (*Abies alba*, *Picea abies* and *Pinus sylvestris*). J. Vegeta. Sci. 21: 364-376.

Lhomme J.P., Chehbouni A. and Monteny B., 2000. Sensible heat flux-radiometric surface temperature relationship over sparse vegetation: parameterizing B^{-1}. Boundary Layer Meteorol. 97: 431-457.

Limousin J.M., Rambal S., Ourcival J.M., Rocheteau A., Joffre R. and Rodriguez-Cortina R., 2009. Long-term transpiration change with rainfall decline in a Mediterranean *Quercus ilex* forest. Global Change Biol. DOI: 10.1111/j.1365-2486.2009.01852.x.

Loustau D., Bosc A., Colin A., Ogée J., Davi H., François C., Dufrêne E., Déqué M., Cloppet E., Arrouays D., Bas C.L., Saby N., Pignard G., Hamza N., Granier A., Bréda N., Ciais P., Viovy N. and Delage F., 2005. Modeling climate change effects on the potential production of French plains forests at the sub-regional level. Tree Physiol. 25: 813-823.

Mainiero R. and Kazda M., 2006. Depth-related fine root dynamics of *Fagus sylvatica* during exceptional drought. For. Ecol. and Manag. 237: 135-142.

Martinez-Vilalta J., Piñol J. and Beven K., 2002. A hydraulic model to predict drought-induced mortality in woody plants: an application to climate change in the Mediterranean. Ecol. Model. 155: 127-147.

Mattson W. and Haack R., 1987. Role of drought in outbreaks of plant-eating insects. Biosci. 37(2): 110-118.

McDowell N., Pockman W.P., Allen C.D., Breshears D.D., Cobb N., Kolb T., Plaut J., Sperry J., West A., Williams D.G. and Yepez E.A., 2008. Mechanisms of plant survival and mortality during drought: why do some plants survive while others succumb to drought? New Physiol. 178: 719-739.

McDowell N. and Sevanto S., 2010. The mechanisms of carbon starvation: how, when, or does it even occur at all? New Phytol. 186: 264-266.

McElrone A.J., Pockman W.T., Martinez-Vilalta J. and Jackson R.B., 2004. Variation in xylem structure and function in stems and roots of trees to 20 m depth. New Phytol. 163: 507-517.

Mencuccini M. and Grace J., 1995. Climate influences the leaf area/sapwood area ratio in Scots pine. Tree Physiol. 15: 1-10.

Mölder M. and Lindroth A., 1999. Thermal roughness length of a boreal forest. Agric. For. Meteorol. 98-99: 659-670.

Monteith J.L., 1973. Principles of Environmental Physics, Edward Arnold, London.

Nadezhdina N., 2010. Integration of water transport pathways in a maple tree: responses of sap flow to branch severing. Ann. For. Sci. 67(107).

Nadezhdina N., Cermak J., Meiresonne L. and Ceulemans R., 2007. Transpiration of Scots pine in Flanders growing on soil with irregular substratum. For. Ecol. Manage. 243: 1-9.

Nadezhdina N., Ferreira M.I., Silva R. and Pacheco C.A., 2008. Seasonal variation of water uptake of a *Quercus suber* tree in Central Portugal. Plant Soil 305: 105-119.

Nakai T., Sumida A., Daikoku K., Matsumoto K., Molen M.K.v.d., Kodama Y., Kononov A.V., Maximov T.C., Dolman A.J., Yakubi H., Hara T. and Ohta T., 2008. Parametrisation of aerodynamic roughness over boreal, cool- and warm-temperate forests. Agric. For. Meteorol. 148: 1916-1925.

Nourtier M., Chanzy A., Granier A. and Huc R., 2011. Sap flow measurements by thermal dissipation method using cyclic heating: a processing method accounting for the non-stationary regime. Ann. For. Sci. DOI: 10.1007/s13595-011-0065-3.

Oliva J. and Colinas C., 2007. Decline of silver fir (*Abies alba* Mill.) stands in the Spanish Pyrenees: Role of management, historic dynamics and pathogens. For. Ecol. Manage. 252: 84-97.

Otieno D.O., Kurz-Besson C., Liu J., Schmidt M.W.T., Vale-Lobo R., David T.S., Siegwolf R., Pereira J.S. and Tenhunen J.D., 2006. Seasonal variations in soil and plant water status in a *Quercus suber* L. stand: roots as determinants of tree productivity and survival in the Mediterranean-type ecosystem. Plant Soil 283: 119-135.

Pammenter N.W. and Willigen C.V., 1997. A mathematical and statistical analysis of the curves illustrating vulnerability of xylem to cavitation. Tree physiol. 18: 589-593.

Peguero-Pina J.J., Camarero J.J., Abadia A., Martin E., Gonzalez-Cascon R., Morales F. and Gil-Pelegrin E., 2007. Physiological performanace of silver-fir (*Abies alba* Mill.) populations under contrasting climates near the south-western distribution limit of the species. Flora 202: 226-236.

Peñuelas J., Lloret F. and Montana R., 2001. Severe droughts effects on mediterranean woody flora in Spain. For. Sci. 47: 214-218.

Rambal S., 1984. Water balance and pattern of root water uptake by *Quercus coccifera* L. evergreen scrub. Oecologia 62: 18-25.

Sala A., Piper F. and Hoch G., 2010. Physiological mechanisms of drought-induced tree mortality are far from being resolved. New Phytol. 186: 274-281.

Sarris D., Christodoulakis D. and Körner C., 2007. Recent decline in precipitation and tree growth in the eastern Mediterranean. Global Change Biol. 13: 1187-1200.

Schiller G., Ungar E.D., Cohen S. and Herr N., 2010. Water use by Tabor and Kermes oaks growing in their respective habitats in the Lower Galilee region of Israel. For. Ecol. Manage. 259: 1018-1024.

Scholander P.F., Hammel H.T., Bradstreet E.D. and Hemmingsen E.A., 1965. Sap pressure in vascular plants. Negative hydrostatic pressure can be measured in plants. Science 148: 339-346.

Somot S., Sevault F., Déqué M. and Crépon M., 2008. 21st century climate change scenario for the Mediterranean using a coupled atmosphere-ocean regional climate model. Global Planet. Change 63: 112-126.

Sperry J.S., Adler F.R., Campbell G.S. and Comstock J.P., 1998. Limitation of plant water use by rhizosphere and xylem conductance: results from a model. Plant, Cell and Envir. 21: 347-359.

van-Mantgem P.J., Stephenson N.L., Byrne J.C., Daniels L.D., Franklin J.F., Fulé P.Z., Harmon M.E., Larson A.J., Smith J.M., Taylor A.H. and Veblen T.T., 2009. Widespread increase of tree mortality rates in the Western United States. Science 323(DOI: 10.1126/science.1165000).

Warren J.M., Meinzer F.C., Brooks J.R. and Domec J.C., 2005. Vertical stratification of soil water storage and release dynamics in Pacific Northwest coniferous forest. Agric. For. Meteorol. 130: 39-58.

West A.G., Hultine K.R., Sperry J.S., Bush S.E. and Ehleringer J.R., 2008. Transpiration and hydraulic strategies in a Piñon-Juniper woodland. Ecol. Appl. 18(4): 991-927.

Yingge X., Chanzy A. and Nourtier M., in prep. Evaluation of electrical tomography to estimate soil water storage capacity of rocky soils.

Tables

Table 1: Characterisation soil, trees and location of each intensive plot and description of the experimental design

Plot n°	Altitude (m)	Slope	Number of trees with		Soil humidity measurement	Mean of trees'			Class of soil depth
			sap flux sensors	ψ_{pd} and ψ_{min} measurement		age (y)	height (m)	DBH (cm)	
1	1020	36°	3	7	Yes	63	16	28	Low and medium
2	1100	47°	1	2	No	81	12	25	High
3	1100	44°	1	4	No	105	15	31	Low
4	1360	27°	4	4	Yes	156	15	36	Medium

Table 2: Description of the classes of resistivity

Class n°	Interval of resistivity (Ohm.m)	Trees of the plot located on this class	Number of trees of the transect located on this class
1	0 - 500	4	51
2	0 – 500 over the 2 first meters and, > 1000 below 2 m depth		5
3	500 - 1000	3 – 6 – 7 – 8 – 9	22
4	> 1000	1 – 2 – 5	22

Table 3: Comparison of the tree maximum and minimum transpiration level, predawn water potential and development of sapwood and leaf areas according to soil classes of resistivity

Class of resistivity	Tree n°	Max T before 2009 drought ($mm.h^{-1}$)	Min T during 2009 drought ($mm.h^{-1}$)	Max T during 2010 spring ($mm.h^{-1}$)	Min ψ_{pd} during 2009 (MPa)	Sapwood area (dm²)	Leaf area (m²)
1	4	-	0.004	0.049	-1.99	3.63	18.3
3	3	0.23	0.007	0.054	-0.93	10.56	24.4
	6	0.081	0.01	-	-1.14	6.30	16.0
	7	0.089	0.005	0.06	-1.02	1.51	17.2
	8	0.059	0.006	0.060	-1.17	1.68	9.9
	9	0.06	0.01	0.056	-0.99	2.11	15.9
4	1	0.11	0.005	0.062	-1.27	4.71	14.6
	2	0.14	0.002	0.047	-1.37	6.58	27.6
	5	-	0.004	0.081	-1.62	2.30	11.0

Figures

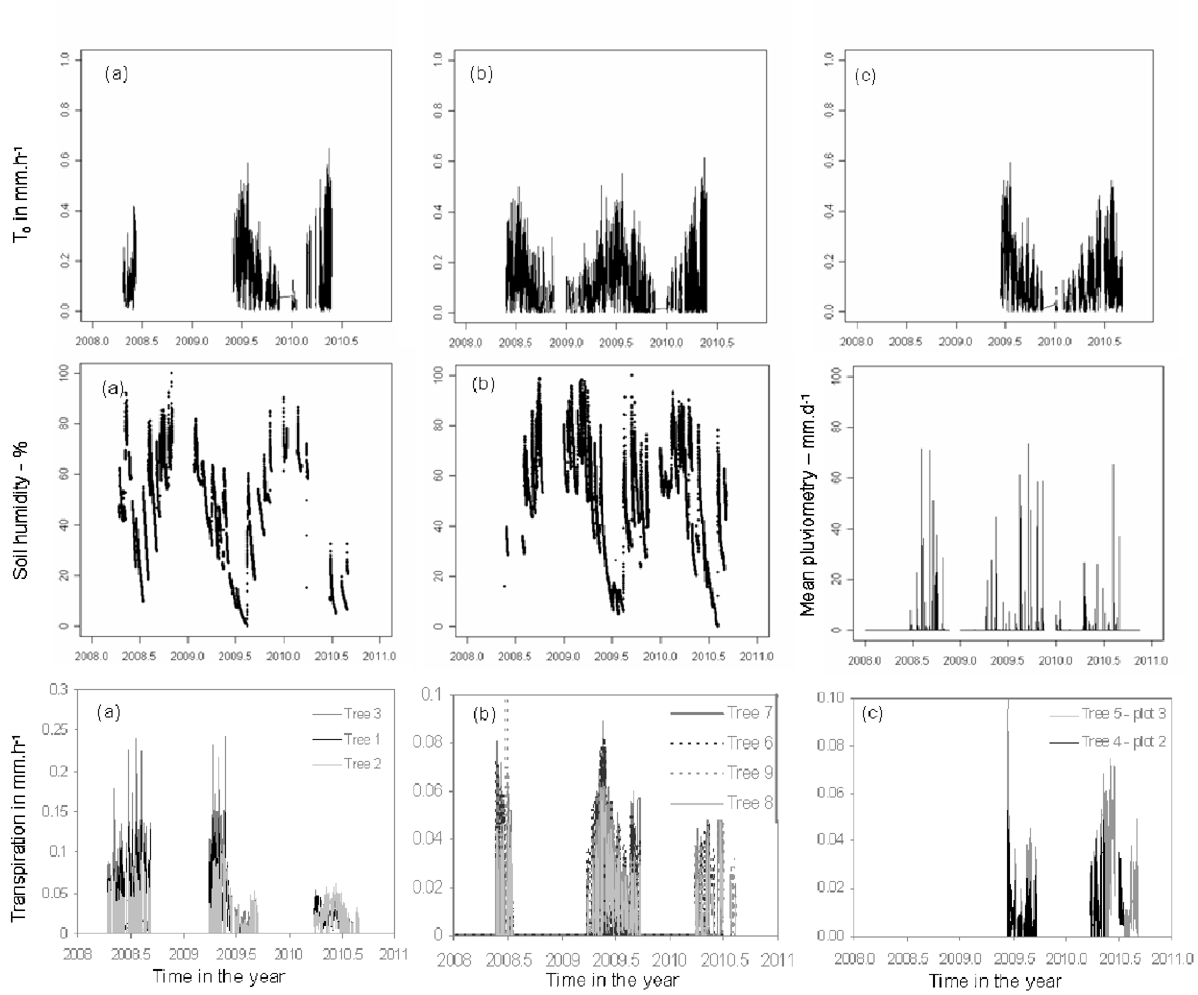

Figure 1: Evolution in time, over the 3 years, of T_0 on each plot, soil humidity on plots 1 and 4 and transpiration for all the trees. Rainfall was measured on plot 4. Figures with (a) correspond to plot 1, (b) to plots 4 and (c) to plot 2 and 3.

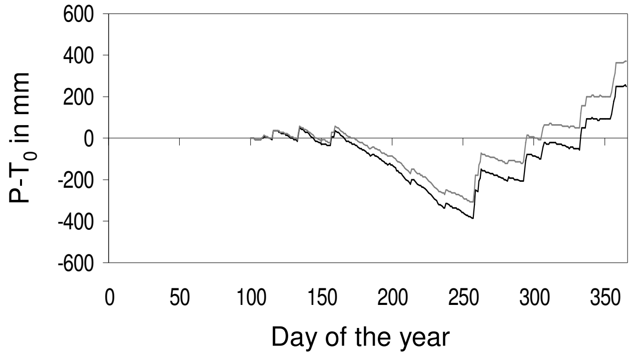

Figure 2: Cumulated difference between precipitation (*P* in mm.j^{-1}) and T_0 (in mm.j^{-1}) calculated from the day 100 during the year 2009 for the plots 1 (in black) and 4 (in grey).

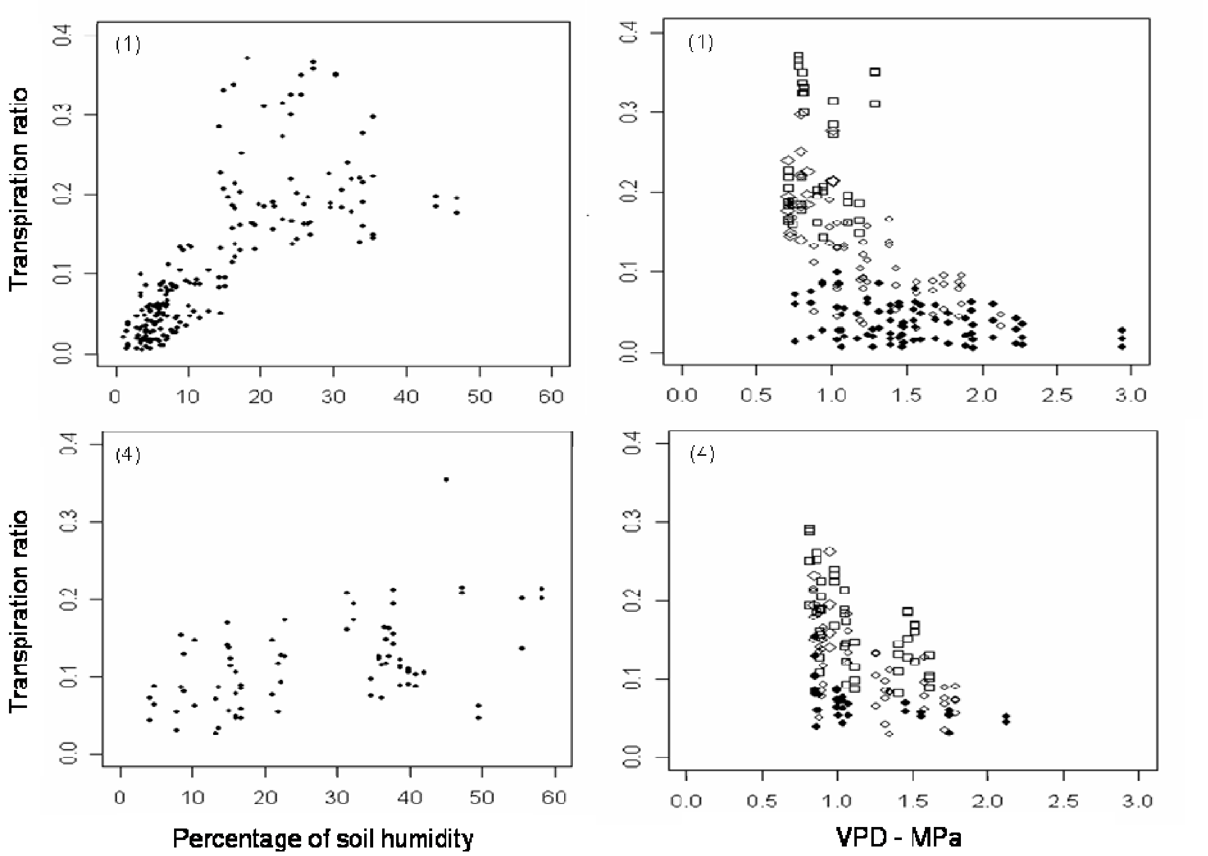

Figure 3: Regulation of the transpiration with the decrease of the percentage of soil humidity and with the increase of the *VPD* (different shapes of symbols correspond to level of humidity – diamond-shaped: >40%, squares: 20%<-<40%, unfilled round: 10%<-<20%, filled rounds: <10%) for plot 1 at the top and for plot 4 at the bottom. Only data corresponded to T_0>0.15 mm.h^{-1} and *Rn*>400 W.m^{-2} at 12:00 are represented.

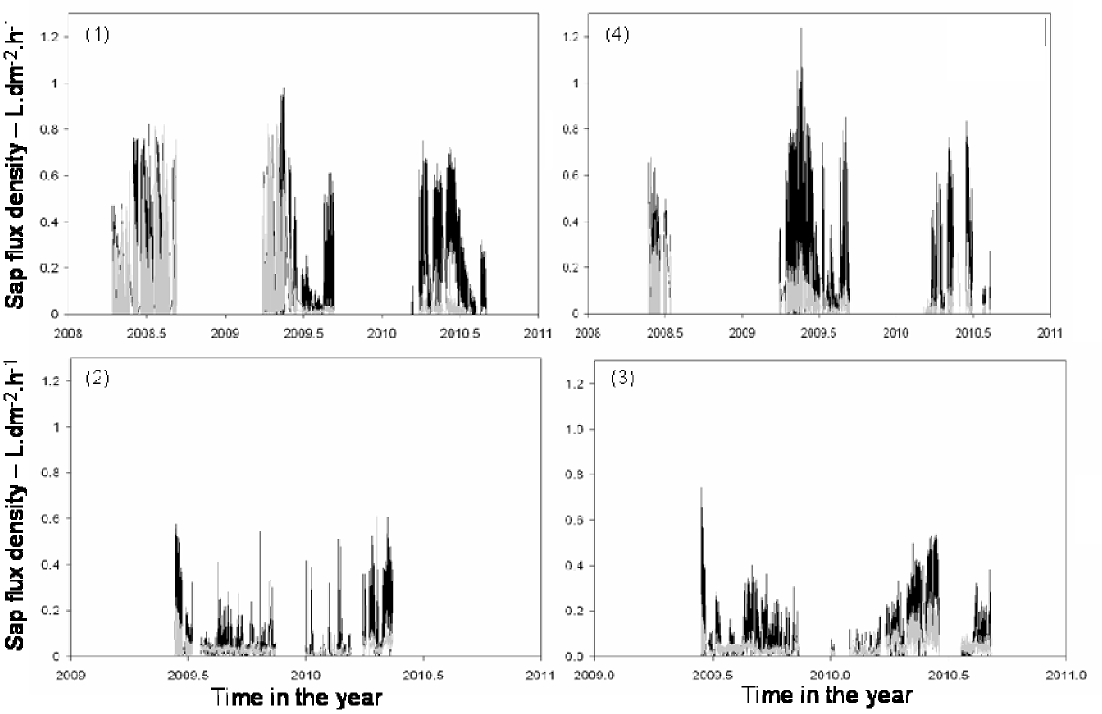

Figure 4: Radial distribution of the sap flux density for the trees with an inner sap flowmeter on each plot. Black and dark grey lines correspond to the sensors between 0-2 cm into the trunk and clear grey lines to the sensors between 2-4 cm. Numbers in bracket correspond to the plots.

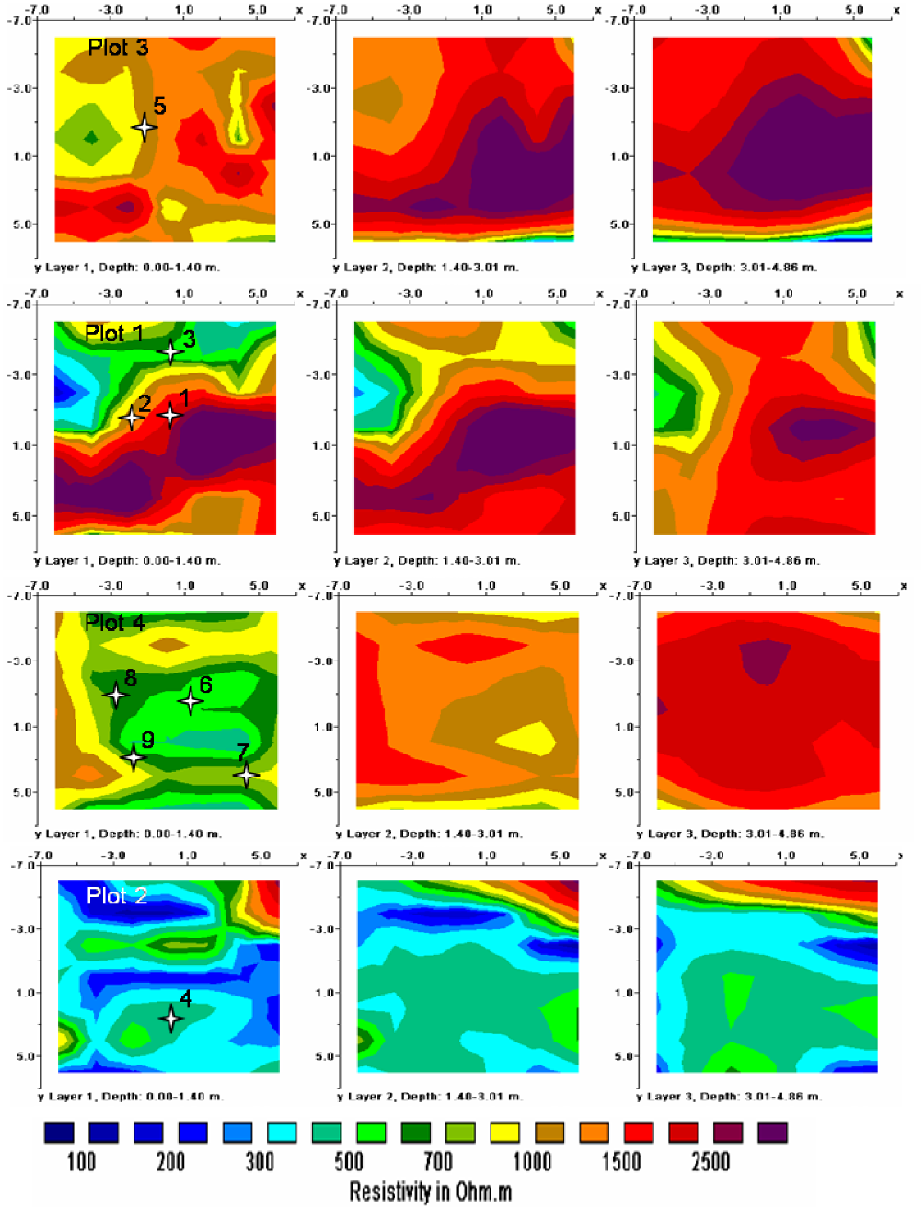

Figure 5: Profile of 3D resistivity (in Ohm.m) on the 4 plots with the location of the tree (star with number). Profiles are decomposed in 3 layers per site (from left to right): from 0 to 1.4 m depth, from 1.4 to 3 m depth and from 3 to 4.8 m depth.

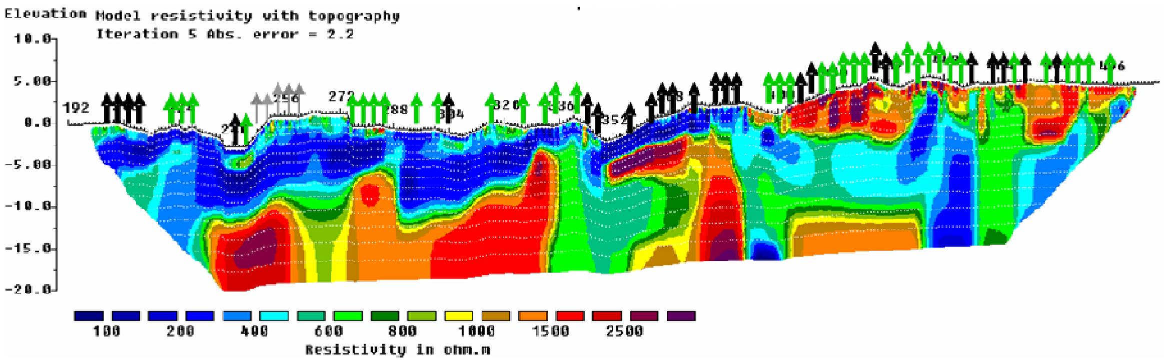

Figure 6: Extract of 300 m long of the profile of 2D electrical resistivity (in Ohm.m) over a depth of 20 m. Health status of trees located close to the transect is figured: dark trees were dead ones, grey ones were declining and the green were the healthy ones.

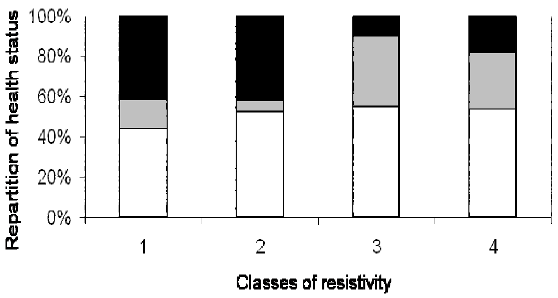

Figure 7: Proportion that represented the health status on each class of resistivity (total number of trees: 100). Black areas correspond to dead trees, grey areas to declining trees and white areas to healthy trees.

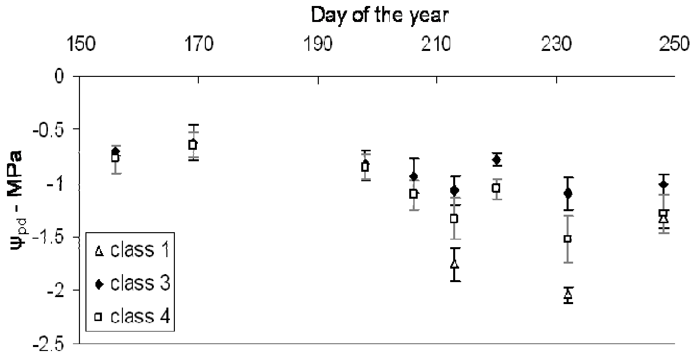

Figure 8: Evolution during the year 2009 of the mean of predawn water potentials according to classes of soil resistivity.

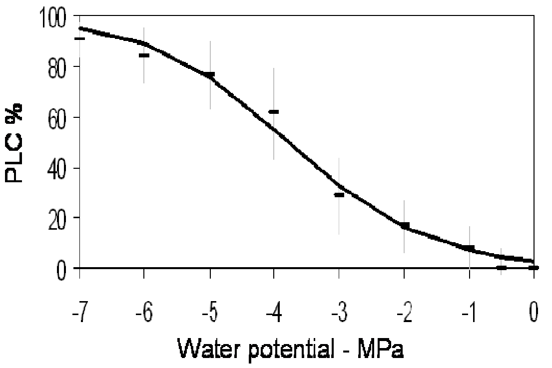

Figure 9: Vulnerability curve of xylem to embolism illustrated as the percentage loss of conductivity according to the water potential. Black line corresponds to the fitted exponential sigmoid and black points show the mean of the measurements. Coefficients of the Eq. 6 were a = 0.93 and b = -3.78 MPa.

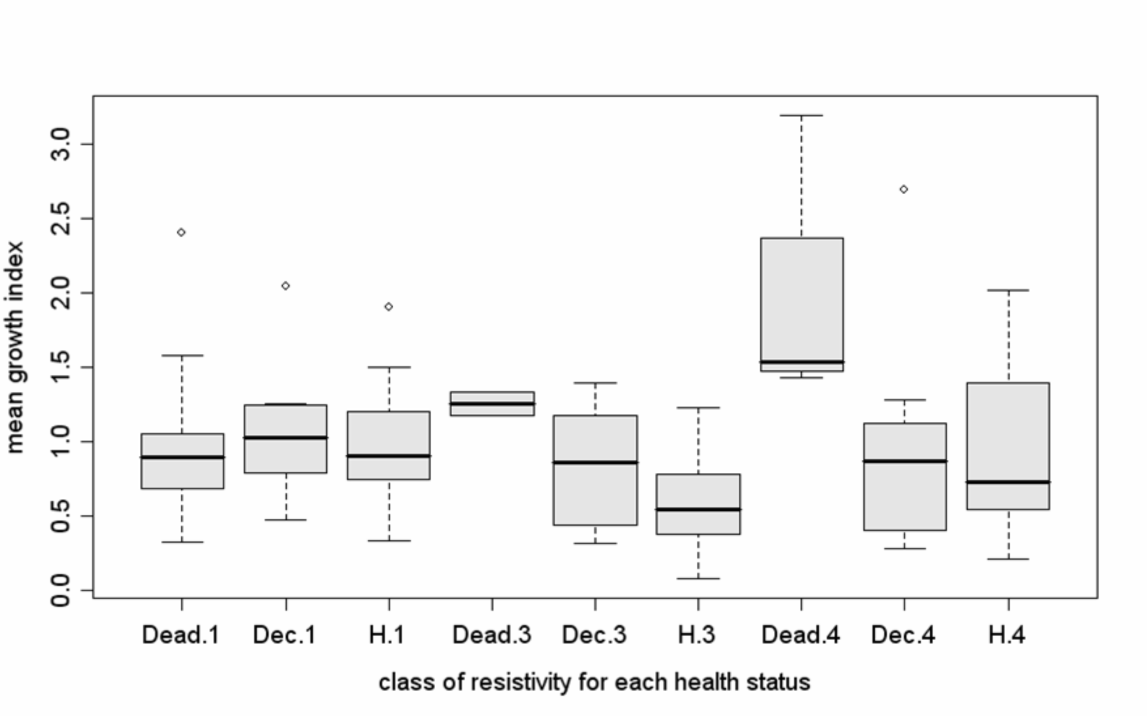

Figure 10: Boxplots of the mean rate over the 35 first years of growth according to classes of ER and to the health status for the trees situated on the transect in contour line. Numbers correspond to ER classes. *H* corresponds to healthy trees, *Dec* to declining ones and *Dead* to dead ones.

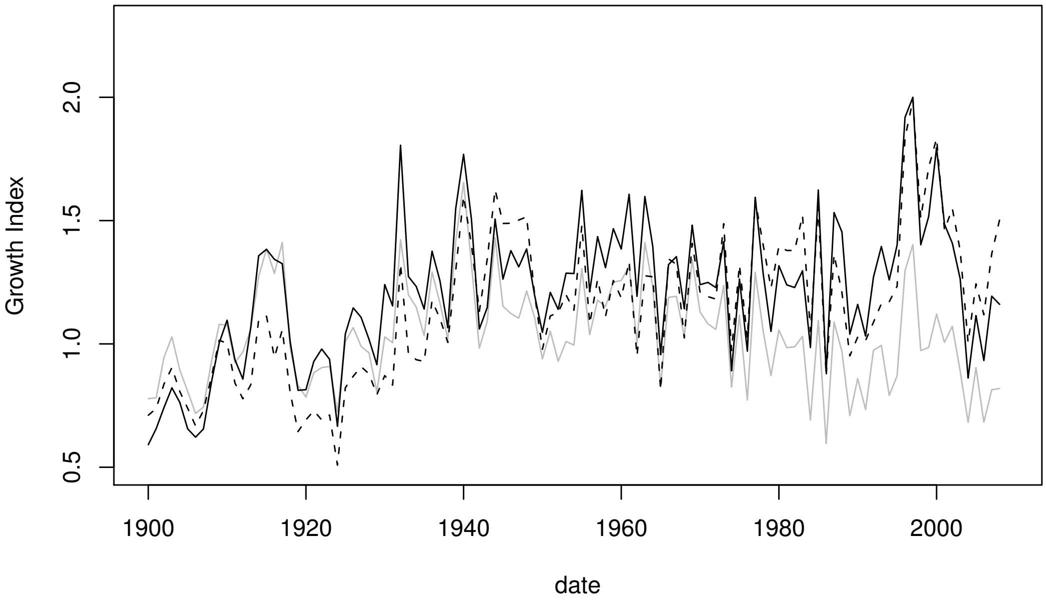

Figure 11: Radial growth trends during 20th and 21st century according to ER classes. Black solid line corresponds to class 4, black dashed line to class 3 and grey line to class 1.

Annexe 6

Partitioning of silver fir Leaf Mass Area (LMA) and Leaf Area (LA) variations, from organs to populations

Taugourdeau O[1], Cailleret M[2], Barthélémy D[3], Caraglio Y[4], Courdier F[2], Sabatier S[4], Davi H[2]

[1]Université Montpellier 2, UMR AMAP Montpellier, 34000 France
[2]INRA UR 629 URFM, 84914 Avignon
[3]INRA, UMR AMAP Montpellier, 34000 France
[4]CIRAD, UMR AMAP Montpellier, 34000 France

En préparation pour *Functional Ecology*

Abstract

Context. Functional traits are now widely used to assess plants responses to environment and offer a powerful framework to address ecological questions. Leaf traits are ones of the most used functional traits, due to the ease of sampling and the numerous functions of leaves. Leaf Area (LA) and LMA (Leaf Mass/LA) are known to be sensitive to environmental gradients at inter-individual and intra-individual scale but the endogenous sources of phenotypic variations and their interactions remain mainly unknown.

Methods. To compare different scales of LMA and LA variations in silver firs (*Abies alba* Mill.), one diachronic and two synchronic protocols were performed along a Mediterranean altitudinal gradient. These protocols took into account the following sources of variations: needle year, needle age (up to 15y), horizontal and vertical crown position, axis properties, tree development (from sapling to reproductive tree), light environment and altitude.

Main Results. A strong positive relationship, with an asymptotic shape, was found between needle age and LMA. The effect of needle aging on LA was positive but low. LMA and LA increase with tree development, decreasing axis ramification order (only for LMA) and decrease when axes are in inter-whorl position. Light only explains respectively for LA and LMA, between 0 and 14% of traits variations when endogenous sources of variations explain between 13 and 71%. It clearly highlights the importance of organ aging, sapling development and structure on leaf traits variations. Causes and consequences of theses variations are discussed.

Future studies recommendations. (i) methodological: indications about individual development and the axis that hold the leaf may provide useful information to minimize leaf traits sampling bias and effort. (ii) ecological: A quantification of architectural variations (plant development and structure) is needed prior to quantifying the consequences of leaf traits variation. (iii) modeling: canopy models may be highly improved with taking into account some endogenous source of variations, in particular organ ageing for evergreen species.

Keywords: leaf traits, phenotypic plasticity, light environment, intra-crown variations, elevation, *Abies alba* Mill., plant architecture

Introduction

An increasing number of studies showed strong interest in functional traits, i.e. traits that reflect adaptation to, and performance in, different environments (Violle et al. 2007). These traits are an efficient and accessible way to understand the factors that determine fitness and its components (survival, growth, reproductive effort). Fitness is related both to environmental conditions and to phenotypic attributes that determine the performance of an individual in a specific environment (Ackerly & Monson 2003). As functional traits can indicate how an individual responds to its environment, their study offers a powerful approach to address ecological questions (Mcgill et al. 2006). Adaptation was assessed by comparing strategies of different species while local adaptation and plasticity were determined at the intra-specific scale. They can provide informative insights into community composition and ecosystem functioning, to critical aspects of the consequences of global change (Mcgill et al. 2006; Westoby & Wright 2006). In this context, essential requirements in how tree functioning vary within and across species and environments to predict future ecosystems responses, and their evolutivity (Thuiller et al. 2008). As the analysis of the variability of all processes of tree functioning can not be taking into account, focus must be on key variables with important physiological significance. Leaf traits are ones of the most used functional traits, due to the ease of sampling and the numerous functions of leaves. If the main aim of leaves is to assimilate carbon via photosynthesis, their physiological and morphological characteristics revealed the type and the intensity of the environmental constraints. Indeed, light conditions, soil water availability, temperatures and soil nitrogen concentrations strongly impact their traits such as their area, their mass and the ratio between both (Niinemets 2001; Ordoñez et al. 2009).

Leaf area (LA) influences plant performance by several mechanisms. Firstly, species with small leaves such as conifers tend to have large boundary layer conductance (Monteith & Unsworth 1990). As a result, small differences between air temperature and leaf temperature were observed because heat is easily convected from the leaf to the surrounding air (Martin et al. 1999), leading to lower respiration and transpiration costs. In another part, leaf size may also decline due to overall carbon limitation in stressful environments, making construction of large leaves with extensive vascular and cell-wall fractions overtly expensive (Niinemets et al. 2007). Variations in LA are also associated with changes in within-leaf support investments (e.g. proportion of lamina) and in leaf chemical (e.g. fraction of nitrogen, carbon-rich chemicals such as lignin) and structural characteristics (Niinemets et al. 2007). LA may provide insights on the plant strategy in the trade-off between LA and leaf number (“Durian theory”, (Corner 1949)]; “leafing intensity premium”, (Kleiman & Aarssen 2007)]).

Leaf Mass per Area (LMA) is defined as the ratio between leaf mass (LM) and leaf area (LA) and is mainly linked with leaf thickness and density (Poorter et al. 2009). As it strongly impacts leaf photosynthesis, water use efficiency and carbon uptake by plant canopies, LMA is considered as a key functional trait (Poorter et al. 2009). Plants with high LMA tend to have high N percentage and carbon assimilation rates per unit of leaf area. It also provides information on plant strategy in terms of leaf lifespan (Wright et al. 2004) and shade tolerance (Lusk & Warton 2007). Due to the number of process they resume, both LMA and LA traits are well related to more integrated variables such as tree height (Rijkers, Pons, & Bongers 2000; Martínez-Vilalta et al. 2010), and are key parameters of process-based models simulating plant growth (Davi et al. 2006).

Identifying the sources of variations of LA and LMA responds to two main goals: in one hand, identifying potentials sources of variations of plant strategy, leaf functions and structures and, in the other hand, improving sampling methods to reduce unwanted sources of variations (Garnier et al. 2001). Inter-specific variations of LA and LMA are generally associated with three main sources: environment (Poorter et al. 2009), succession strategy (Henry & Aarssen 2001) and phylogeny (Antunez, Retamosa, & Villar 2001). Intra-specific sources of variations can be divided into a genetic part which is closely related with inter-specific sources of variations, and a phenotypic part. The phenotypical variations can be decomposed into exogenous (i.e. phenotypical plasticity) and endogenous sources: plant structure, plant ontogeny and organ ageing (Poorter et al. 2009). Many studies on phenotypic plasticity highlighted the sensitivity of LA and LMA to environmental gradients at inter-individual (Poorter et al. 2009) or intra-individual scale (Davi et al. 2008; Hulshof & Swenson 2010) but only few studies highlight the endogenous sources of phenotypic variations (Coste et al. 2009) and the interaction between both. The integration of endogenous sources of variations may highlight some adaptation poorly investigated but may also provide relevant constraints for optimal trait values. For example, light availability decreases with leaf ageing on evergreen species due to shading by younger needles. LMA should decrease to be optimized face with this new environmental condition, but the reverse trend was found (Poorter et al. 2009).

Material and methods

Sites and species characteristics

The study was conducted on Mont Ventoux (44°11'N; 5°17'E), a calcareous mountain located in the southwestern Alps, 1,909 m above sea level (a.s.l.). Originally forested, Mont Ventoux suffered massive deforestation from the 12th century onwards as the wood from the trees was used to serve the demands for shipbuilding, firewood and charcoal and because of grazing. In 1850, it was almost entirely deforested and silver firs (*Abies alba* Mill.) was reduced to small forest islands. Silver fir gradually recolonized its original distribution area in the 20th due to a decrease in grazing combined with reforestation efforts. Substrates range between limestone lithosol to one meter deep colluvium, however, soil water content is probably low (Cailleret & Davi 2010). On the north-facing slope of Mont Ventoux (weather station of Mont Serein, 1,445 m a.s.l., 1993–2006), mean annual temperature has been 6.8°C. The distribution of rainfall (1,300 mm on average) is characteristic of a Mediterranean climate: the driest season is summer and rainfall occurs mostly in autumn. The north aspect of Mont Ventoux, as other Mediterranean mountains, present increasing rainfall and decreasing mean annual temperature with increasing elevation (Cailleret & Davi 2010).

Biological Dataset

Data Set 1: leaf traits variations with aging

The accurate impact of needle aging on LMA and LA was assessed by sampling needles generated the same year on the same trees at two different dates. Needles produced in 2007 were sampled from two twigs at the top of the canopy in 2007 and 2009 on the same 20 adult trees. As the number of needles per cm of shoot did not change significantly, we assume that needles were sampled on the same ramification order (**Table 1**). On the 2007 twigs, LMA and LA of the 2003, 2004, 2005 and 2006 needles were also measured. Needles were removed from the shoots and their projected area estimated with a high-resolution scanner equipped with WinDIAS software (Delta-T, Cambridge UK). Needle dry mass was recorded (after desiccation at 60 °C for 2 days), and leaf mass per area (leaf dry mass / projected leaf area) was calculated.

Data Set 2: Intra-crown variations of leaf traits variations with age

Eight adult trees (which reached the canopy) at different altitudes (3 at 1150m, 2 at 1250m and 3 at 1350m) were identified, measured and cut in autumn 2009. Their height and DBH (Diameter at Brest Height: at 1.3m) respectively averaged 11.6m (±1.7) and 20.6cm (±3.5). Each crown was vertically divided in 5 equals' parts and one branch per part was measured (branch height, diameter and length) and three twigs per branch located at different distance from the trunk were sampled. To assess light conditions at the twig level, the distance to the top of the crown (D_{top}) and to the peripheral part of the crow (D_{ext}) were calculated. On each twig, needles with different ages, based on annual shoot dating, were separated and measured using the same procedure than in Data Set 1.

Data Set 3: Ontogeny and architecture

In summer 2009, after shoot and leaf extension, 60 juvenile trees were sampled in various understory conditions and site elevation (17 at 1150m, 24 at 1250 and 19 at 1350m). Sampled tree height ranged from 3cm to 3m and base diameter from 0.14 to 7cm. Their light environment was estimated by canopy openness based on a hemispherical photography taken above the top of each tree (Frazer, Canham, & Lertzman 1999). Canopy openness range from 7.0 to 53.5% of incident light and was independent of tree heights ($P>0.05$ for a rank-sum Spearman correlation test).

For each tree, the highest two-year old branch was collected. For smallest trees, branches presented only 2 annual shoots without any twigs (Figure 1). In the other hand, branch of highest trees present up to 4 one-year old vigorous lateral twigs, called pseudo-whorl (PW) due to their apparent whorl relative position, and up to 11 one-year old less vigorous lateral twig, called inter-whorl (IW) due to their relative position to PW (Figure 1).

For every sampled annual shoot, the following information were measured: date of extension, ramification order, axis position (PW or IW, Figure 1), total fresh needle surface (see below) and total dry needle biomass (after desiccation at 60 °C for 2 days). Theses two measures were used to perform the annual shoot average LMA (in g m^{-2}).

The total needle surface of each annual shoot was estimated by putting all annual shoot needles on the glass of a bi-tube scanner (EPSON V700). Bi-tube acquisitions limit shadow artifact. All images were analyzed with ImageJ (Abràmoff, Magalhaes, & Ram 2004), automatic threshold and particles detection, to get the total needle surface of the annual shoot.

Statistical analyses

Modeling needle aging

Firstly, the existence of a progressive change during aging of both LMA and LA needle traits was assessed by focusing on First-Order autocorrelation of temporal series.

LMA increased with needle aging following an asymptotic equation.

$$LMA_{sim} = a - [(a-b) * \exp(-c * age)]$$

With *a* the maximum LMA obtained after aging, *b* the LMA of the needles of current year, *c* the value of the slope of LMA increase. For each twig, observed LMA (LMA_{obs}) were fitted against the asymptotic equation, and the resulting LMA_{sim} were studied when they did not integrate bias due to deficient measurements or small needle sampling. The quality of the fit was dependent on the number of different age classes. A fit was considered as reliable when the linear regression between LMA_{sim} and LMA_{obs} was significant ($p<0.05$), and only if *a* and *b* ranged between 160 and 520 ($g.cm^{-2}$) which respectively are the minimum and maximum values of LMA_{obs}. At the end of the procedure, 54 twigs (on 144) were considered as reliable with age of the older needles averaging 8.6 ± 3.3 years, which corresponds to 390 needle samples.

Linear regression models showed the best significance to represent changes in LA. The effect of the calendar year on the slope of relationship between LA and needle age was assessed by modeling these linear regression for different temporal range for each twig (from 4 years of needles to 15) and using a jackknife procedure. Finally, inter-annual variations in the residuals of the linear models and the asymptotic equations (observed / predicted values) were analyzed to estimate the date effect on LA and LMA.

To make the link between adult and juvenile data sets, needles of the years 2008 and 2009 were also analysed separately from the others needles age.

Partitioning source of variation

Linear models with random effects were used to identify the effects of covariables, as fixed effects, on LMA or LA. Due to the number of measurements made on each tree, an individual random effect was included in the model. Monte-Carlo resamplings were used to assess the confident interval of the fixed effects (Bates & Maechler 2010).

Variance partitioning was made by a variance analysis (Anova type II) on the parameters of classical linear regression models (fixed effects) and the consistency between fixed effects models and mixed effects models was checked for every model.

All data analyses were made on R 2.11 (R Development Core Team 2010) with the library lme4 (Bates & Maechler 2010) for linear models with mixed effects and the library car (Weisberg & Fox 2010) for the variance partitioning.

Results

Needles aging vs. date effect (Data Set 1)

In 2007, LMA of current year needles averaged 288g.m^{-2} (SD=35 g.m^{-2}). The diachronic analysis carried out on the 2007 needles showed that the increase in LMA during the two firsts years of needle lifespan was very high in the order of + 30g.m^{-2}.year^{-1} which correspond to an increase of 20% of initial LMA (Figure 2a; Table 1). This increase in LMA was due to a higher increase in Leaf Mass (LM +66.6% in two years) than in LA (+35.5%). R² of the models fitted using asymptotic equation averaged 0.86, indicating their reliability for studying impact of needle aging on LMA. Younger was the needle; stronger was the increase in LMA with aging. This hypothesis was also reinforced by the amplitude of LMA changes observed during the first year of leaf lifespan. LMA of 2008 needles was 35.1g.m^{-2} higher than 2009 needles for adult trees. First-order autocorrelation of individual series averaged 0.43 (Confidence Interval: [0.37 – 0.49]; one sample t.test) showing that LMA of the year previous needle formation (*n-1)* was positively correlated with the LMA of the year *n*, and thus, indicating only a slight effect of calendar year on LMA. We can then consider that changes in LMA with needle age correctly reflect the impact of aging. The analysis of the residuals of the asymptotic models revealed that needles in 2009 seemed to have lower LMA values than expected (Figure 3a). However, it can also be due to bias due to deficient fit at the ordinate.

LA of the needles of the 2007 year averaged 0.21cm² and increased in the order of 40.10^{-3} cm².year^{-1} between 2007 and 2009 (Figure 2b; Table 1). This increase is lower than the difference in LA between 2008 and 2009 needles (+65.4.10^{-3} cm².year^{-1}) observed in adult trees, indicating a slower increase in LA during the second year or a strong impact of the date of needle leaf-out. The slopes of the linear relationships between LA and needle age calculated using the jackknife procedure were mostly not significant (60.5%) or positive (36.5%) and averaged + $5.8.10^{-3}$ $cm^2.year^{-1}$. As shown by Figure S1a, the slope values were generally positive when needles formed before 2003 were used. When the older needle of the twig was formed in 2006, slopes could be negative. This pattern was highlighted when 2009 needles were not taken into account for the slope calculation (Figure S1a). It was explained by the strong effect of the calendar year on needle LA. Indeed, low R² values of linear models (mean=0.27) indicate that most of the temporal variability was not explained by age. In the same way, first-order autocorrelation only averaged 0.14 [0.05 – 0.23] indicating a weak positive relationship between LA of needles previous year with LA of current year needles. Residuals of the linear models fitted on LA data showed strong inter-annual variability with higher values in 2007 and 2008 than in 2006 (and 2005) (Figure 3b)

To summarize, even it was not always significant, relationship between LA and age was mostly positive whatever the temporal range studied (Figure S1b). Due to strong date effect, and as each twig had not the same number of needles years, different relationships between trees or within the crown can not be interpreted as different strategies.

Effect of crown position and environment on all needles (Data Set 2)

Mixed effects linear models were used to calculate the proportion of deviance explained by each variable and show that more than 53% of the variance in LMA was explained by needle age when considering all needles (Table 2). Light conditions seemed to have lower importance because Dtop and Dext only explained 17% and 0.1% of the variance. Negative relationships indicate that needles of the inner part of the crown had lower LMA than the others. These differences were due to different trends in LMA increases with aging according to needle position within the crown. Indeed, higher is the distance between the studied needle and tree top; lower is the LMA of current year needle (*b* value; Table 3). In the same way, needles in the inner part of the crown showed low slope values of LMA increase with leaf aging (*c* value; Table 3). As indicated by the significance of the coefficients of the asymptotic equations, elevation seemed to be positively related with LMA of current year needle and did not impact needle aging (*c* value; Table 3). However, when grouping together all needle ages, neither the effect of elevation nor the tree diameter effect was significant on LMA (Table 2) that may be explain by the use of a linear relationship between LMA and needle age.

Concerning LA, the integration of environmental variables did not improve the predictability of linear mixed effect models. Most of the variance (above 86%) was neither explained by needle ontogeny nor by its position within the crown (Table 2). Factors which explains part of LA variability were needle aging (8.4%), site elevation (3.6%) with positive relationships with LA. Higher is the distance between needle position and tree top and crown limit, lower is needle LA, but these effects only explained 1.3% of LA variations. Such as for LMA, no effect of tree DBH and elevation was observed on LA.

Results from 2008 and 2009 needles were close to those obtained with all needles' years (Table 4). LMA significantly decrease with the increasing distance of the needle to the upper and extern part of the crown. Needle aging strongly impacted LMA but explained only 18.8% of the variance which is low compared with the 53.1% observed with all needles. LA was positively related with needle age and elevation, and negatively with the distance to the top of the crown. However the measured variables only explained 44% of the variance.

Effect of architecture and environment on Dataset3 needles

Needle aging explained 31.5% of LMA variations (+ 34.7g.m^{-2}.year^{-1}, Table 5). At axis scale, together ramification order and axis type variables explained 4.7% of LMA variations. LMA decreased when the ramification order increase and when the axis is in IW position. Tree base diameter explained a large part of LMA variations, 15.7%, with a positive effect on LMA. Tree height only explained 1.7% of LMA variations with a negative effect. Due to the high correlation (R^2=0.95) found between tree base diameter and tree height, the negative effect of tree height correspond to a small shift of the linear relation between base diameter and LMA for high trees (data not shown). No significant effect of tree age was found. At inter-individual scale: 9.6% of LMA variations were explained by the positive effect of light environment and 2.7% by the negative effect of elevation. In conclusion, the main effects on LMA (up to 5% of variations explanation) were, in decreasing importance order, needle aging (31.5%), tree base diameter (15.7%) and light environment (9.6%) and more than 65% of the LMA variations were explain by this simple model (*i.e.* no interactions between variables).

For LA (Table 5), needle aging only explained 5.6% of variations and followed a positive relationship. Axis scale explained 10.6% of LA variations, with a negative effect of being an IW axis: 10.0% of LA variations. At individual scale, only the tree base diameter had an effect (6.4% of LA variations). Neither light environment nor elevation had any effect of LA variation. In conclusion, the main effects on LA were, in decreasing importance order, axis type (10.0%), tree base diameter (6.4%) and needle aging (5.6%), and less than 23% of the LA variations were explained by this model.

Discussion

Aging vs. date effect

Our measurements show needle retention of up to 15 years in silver fir. During these 15 years, both LMA and LA increase. The diachronic analysis made on 2007 needles confirms that changes in LMA were due to a true aging effect. This increase in LMA with needle aging was due to higher increase in LM than in LA. If (Bernier et al. 2001) used linear models to assess the positive relationships between needle age and LMA; an asymptotic equation should be preferred. It indicates that older is the needle, lower is the increase in LMA. If a slight effect of the date of needle formation exists, it is most probably covered by aging effect, which was confirmed by low inter-annual variability of the residuals of the asymptotic models. 2007 needles seemed to have higher LMA values which partly explain high LMA values of the needles analyzed using the diachronic approach. This also could be due to a sampling at the upper part of the crown in 2007 than in 2009 (in the first meter of the top crown).

As the effect of needle aging on LA was linear and very slight, the shape of LMA curve was determined by changes in LM. A gradual increase in LM after an initial exponential expansion phase was expected, which is a common trend on evergreen species (Mediavilla & Escudero 2003). This increase in LM is mainly caused by an increase in the amount of cell wall components per leaf, in mineral contents in older needles (Porté & Loustau 1998), or possibly to other deposits of structures (lignin content…).

On the contrary, a strong impact of the date of needle formation was observed on the residuals of linear models for LA estimates. The decrease in LA between 2003 and 2006 was related with the accumulation of summer drought during this period (Cailleret & Davi 2010). Decreases in LA during drought years may be due to decrease in the turgor pressure, which limits cell expansion and reduces the carbon sink of growth (Woodruff, Bond, & Meinzer 2004). It can also be due to lag-effects of previous droughts. Indeed leaf size was reduced in stress environments to minimize transpiration and leaf heating. It may also decline due to overall carbon limitation making construction of large leaves overtly expensive (Niinemets et al. 2007). This hypothesis was confirmed by the decrease in radial growth observed on Mont Ventoux between 2003 and 2006 (Cailleret & Davi 2010).

Plant architecture and needle traits

LMA and LA increase with sapling base diameter, an indicator of sapling development. In the same time, LMA and LA decrease when axes are in inter-whorl position and with axis ramification order (only for LMA). These effects clearly correspond to endogenous source of variations because sampled tree size were independent of light environment and elevation and sampled annual shoots were close and share virtually the same local environment. On adult trees, no effect of tree development, assessed by DBH, was found on LMA or LA. It indicates that theses relationships may be non linear. If the link between LMA and plant development was generally found on saplings (Coste et al. 2009; Taugourdeau et al. 2011), (Thomas 2010) showed on *Acer saccharum* and *Tilia americana* that LA increased until a species-specific threshold of DBH where the trend began to reverse. The covariations between LMA and LA are probably linked to the greater investment in structural support when leaf area increases (Niinemets et al. 2007).

Progressive LA and LMA variations with sapling development may highlight an underlying link with some physiological process rather than a hypothetical continuous change of genetic expression. Moreover, this underlying process may also be the cause of variations between ramification order and axes types. A good candidate will be water conduction. It may constraint vacuole turgor and LA and LMA, but unlike on coast redwood (Koch et al. 2004), conduction constraints may not be a direct effect of height rather than an effect of sapwood area and efficiency. In fact, tree diameter is a proxy of sapwood area in non-stressed environment (Cailleret 2011) and shoot diameter is also linked with shoot sapwood area (Cochard et al. 2005) and is highly linked with axes properties in the direction as LMA and LA (result not shown). Further studies are needed to confirm the underlying causes of theses architectural variations and their exact effects on leaf functions and structures.

These strong phenotypic correlations can express both developmental constraints and adaptation. (Wagner, Pavlicev, & Cheverud 2007) tackle that variational modules may be adaptative in a changing environment: for example, in a forest understory, light availability will increase with plant development, thus increasing LMA and LA with development can be an adaptation to understory development for shade tolerant species.

Inter-axis leaf traits variations in the same tree may be the result of axis specialization. The separation of long shoots with an exploration function and short shoots with an exploitation function was a concept commonly used (Barthélémy & Caraglio 2007). Following this hypothesis, short axes are expected to have a high ratio between shoot C assimilation and shoot C cost (*i.e.* low LMA and high leaf mass fraction). Silver fir do not present clear short shoots such as *Pinus* genus (i.e. dwarf shoot) or *Fagus sylvatica* (Nicolini & Chanson 1999), but the current results highlight a gradient between exploration functions to exploitation functions with axis order increase and contrasted axis type. Decreasing leaf mass fraction and increasing annual shoot lengths with increasing LMA (data not shown) are consistent with this hypothesis. In the same perspective, during sapling development, successive ramification orders 2 PW present also a shift from exploitation to exploration function. This loss of exploitation properties is offset by the apparition of PW3 and IW3 (Figure 1) with greater exploitation abilities (high Leaf Mass fraction and lower LMA). This shift of function between axes ramification orders during development is close to the concept of intercalation (Barthélémy & Caraglio 2007).

Environmental effect (direct impact and interaction with needle aging)

The strong variability in the parameters of the asymptotic models indicated that changes in needle traits with aging were not constant between trees and within a tree. The increase in LMA with aging is lower when the needle is located in the inner part of the crown. These changes can be caused by local light environment (plasticity) and/or allocation strategy, and are clearly adaptative. As shade-leaves were less useful for whole tree carbon assimilation than sun-leaves (Evans & Poorter 2001), the quantity of carbon and nutrients allocated during aging may be reduced. However, they combined the function of carbon and nutrient storage organ, which was very useful in a stressed environment. Inter-sapling variations of LMA are also linked with light availability like found in many cases (Poorter et al. 2009).

Hierarchization of endogenous and exogenous source of LA and LMA variations

Environmental sources are minor relative to endogenous sources of variations. The length of the studied environmental range is maybe to small to highlight any strong effect of elevation. Indeed extreme parts of silver fir distribution range on Mont Ventoux were not sampled. Studied trees were located between 1200m and 1400m a.s.l. while the distribution area is between 1000m and 1600m a.s.l.. Light environment, both at intra and inter-individual scale, had a significant effect on LA and LMA but this effect remain minor in comparison to endogenous source of variations which did not match with previous studies carried out deciduous or evergreen species where LMA was mainly controlled by light conditions (*e.g.* Davi *et al.* 2008).

The existence of strong endogenous sources of trait variations may be adaptative but also a constraint for optimizing traits in response to environmental variations (both for plasticity and local adaptation). The current study clearly highlights the importance of sapling development, organ aging and sapling structure on leaf traits. Thus quantifying the consequences of leaf traits variations needs a quantification of the architectural variation of the structure that hold theses leaves (Barthélémy & Caraglio 2007). Futures work on the phenotypic link and genetic expression that underlie the different traits gradients found in plants may provide meaningful tools for understanding the consequences of variational modules in plants in term of reaching optimal trait values (Wagner et al. 2007).

Methodological and modelling implications

Organ ages is already integrated in sampling protocol, but the current study highlight how much critical is this point. Some indications about the axis that hold the leaf and individual development may also provide useful information to minimize sampling bias and effort.

As needle aging explains more than 50% of LMA variations and 8% of LA variations for adult trees, a complete canopy model of evergreen conifers should account for all of these needle characteristics (Ogée *et al.* 2002). This model should take into account the interaction between both spatial and temporal changes because needle aging differs within the crown. This should be the case especially for trees with high needle lifespan (> 5 years) such as silver fir. Photosynthesis models working at the whole-canopy scale should also take into account horizontal variations of light conditions within the crown. Thus, canopy should not be divided into vertical layers (m) but into layers which contain the same amount of leaf area (m^2/m^2; Davi *et al.* 2006).

Acknowledgements

The authors wish to thank Pierre Cretin-Maitenaz, William Brunetto, Nicolas Mariotte, and Mehdi Pringarbe of the Experimental Unit of Mediterranean Forestry for help during leaf sampling and measurements. AMAP (Botany and Computational Plant Architecture) is a joint research unit that associates CIRAD (UMR51), CNRS (UMR5120), INRA (UMR931), IRD (R123) and Montpellier 2 University (UM27) France; http://amap.cirad.fr/.

References

Abràmoff, M.D., Magalhaes, P.J. & Ram, S.J. (2004) Image processing with ImageJ. *Biophotonics international*, **11**, 36–43.

Ackerly, D.D. & Monson, R.K. (2003) Waking the sleeping giant: the evolutionary foundations of plant function. *International journal of plant sciences*, **164**, 1–6.

Antunez, I., Retamosa, E.C. & Villar, R. (2001) Relative growth rate in phylogenetically related deciduous and evergreen woody species. *Oecologia*, **128**, 172-180.

Barthélémy, D. & Caraglio, Y. (2007) Plant architecture: A dynamic, multilevel and comprehensive approach to plant form, structure and ontogeny. *Annals of Botany*, **99**, 375-407.

Bates, D. & Maechler, M. (2010) *lme4: Linear mixed-effects models using S4 classes. R package*.

Bernier, P., Raulier, F., Stenberg, P. & Ung, C. (2001) Importance of needle age and shoot structure on canopy net photosynthesis of balsam fir (Abies balsamea): a spatially inexplicit modeling analysis. *TREE PHYSIOLOGY*, **21**, 815-830.

Cailleret, M. (2011) Dépréssiement du sapin au Mont Ventoux.

Cailleret, M. & Davi, H. (2010) Effects of climate on diameter growth of co-occurring Fagus sylvatica and Abies alba along an altitudinal gradient. *Trees*, **25**, 265-276.

Cochard, H., Coste, S., Chanson, B., Guehl, J.-M. & Nicolini, E. (2005) Hydraulic architecture correlates with bud organogenesis and primary shoot growth in beech (Fagus sylvatica). *Tree Physiology*, **25**, 1545-1552.

Corner, E.J.H. (1949) The durian theory or the origin of the modern tree. *Annals of Botany*, **13**, 367.

Coste, S., Roggy, J., Garraud, L., Heuret, P., Nicolini, E. & Dreyer, E. (2009) Does ontogeny modulate irradiance-elicited plasticity of leaf traits in saplings of rain-forest tree species? A test with Dicorynia guianensis and Tachigali melinonii (Fabaceae, Caesalpinioideae). *Annals of Forest Science,* **66**.

Davi, H., Barbaroux, C., Dufrene, E., Francois, C., Montpied, P., Brea, N. & Badeck, F. (2008) Modelling leaf mass per area in forest canopy as affected by prevailing radiation conditions. *Ecological Modelling*, **211**, 339-349.

Davi, H., Bouriaud, O., Dufrene, E., Soudani, K., Pontailler, J., Le Maire, G., Francois, C., Breda, N., Granier, A. & Le Dantec, V. (2006) Effect of aggregating spatial parameters on modelling forest carbon and water fluxes. *Agricultural and Forest Meteorology*, **139**, 269-287.

Evans, J.R. & Poorter, H. (2001) Photosynthetic acclimation of plants to growth irradiance: the relative importance of specific leaf area and nitrogen partitioning in maximizing carbon gain. *Plant, Cell & Environment*, **24**, 755-767.

Frazer, G.W., Canham, C.D. & Lertzman, K.P. (1999) *Gap Light Analyzer (GLA), Version 2.0: Imaging software to extract canopy structure and gap light transmission indices from true-colour fisheye photographs, users manual and program documentation*. New York.

Garnier, E., Shipley, B., Roumet, C. & Laurent, G. (2001) A standardized protocol for the determination of specific leaf area and leaf dry matter content. *Functional Ecology*, **15**, 688–695.

Henry, H.A.. & Aarssen, L.W. (2001) Inter-and intraspecific relationships between shade tolerance and shade avoidance in temperate trees. *Oikos*, **93**, 477–487.

Hulshof, C.M. & Swenson, N.G. (2010) Variation in leaf functional trait values within and across individuals and species: an example from a Costa Rican dry forest. *Functional Ecology*, **24**, 217-223.

Kleiman, D. & Aarssen, L.W. (2007) The leaf size/number trade-off in trees. *Journal of Ecology*, **95**, 376–382.

Koch, G.W., Sillett, S.C., Jennings, G.M. & Davis, S.D. (2004) The limits to tree height. *Nature*, **428**, 851–854.

Lusk, C.H. & Warton, D.I. (2007) Global meta-analysis shows that relationships of leaf mass per area with species shade tolerance depend on leaf habit and ontogeny. *New Phytologist*, **176**, 764–774.

Martin, T.A., Hinckley, T.M., Meinzer, F.C. & Sprugel, D.G. (1999) Boundary layer conductance, leaf temperature and transpiration of Abies amabilis branches. *Tree Physiology*, **19**, 435.

Martínez-Vilalta, J., Mencuccini, M., Vayreda, J. & Retana, J. (2010) Interspecific variation in functional traits, not climatic differences among species ranges, determines demographic rates across 44 temperate and Mediterranean tree species. *Journal of Ecology*.

Mcgill, B., Enquist, B., Weiher, E. & Westoby, M. (2006) Rebuilding community ecology from functional traits. *Trends in Ecology & Evolution*, **21**, 178-185.

Mediavilla, S. & Escudero, A. (2003) Leaf life span differs from retention time of biomass and nutrients in the crowns of evergreen species. *Functional Ecology*, **17**, 541-548.

Monteith, J.L. & Unsworth, M.H. (1990) Principles of environmental physics, 291 pp. *Edward Arnold, London*.

Nicolini, E. & Chanson, B. (1999) The short shoot, an indicator of beech maturation (Fagus sylvatica L.). *Canadian Journal of Botany*, **77**, 1539-1550.

Niinemets, Ü. (2001) Global-scale climatic controls of leaf dry mass per area, density, and thickness in trees and shrubs. *Ecology*, **82**, 453-469.

Niinemets, \Ü, Portsmuth, A., Tena, D., Tobias, M., Matesanz, S. & Valladares, F. (2007) Do we underestimate the importance of leaf size in plant economics? Disproportional scaling of support costs within the spectrum of leaf physiognomy. *Annals of Botany*, **100**, 283.

Ordoñez, J.C., Van Bodegom, P.M., Witte, J.M., Wright, I.J., Reich, P.B. & Aerts, R. (2009) A global study of relationships between leaf traits, climate and soil measures of nutrient fertility. *Global Ecology and Biogeography*, **18**, 137-149.

Poorter, H., Niinemets, U., Poorter, L., Wright, I.J. & Villar, R. (2009) Causes and consequences of variation in leaf mass per area (LMA): a meta-analysis. *New Phytol New Phytol*, **182**, 565-588.

Porté, A. & Loustau, D. (1998) Variability of the photosynthetic characteristics of mature needles within the crown of a 25-year-old Pinus pinaster. *Tree physiology*, **18**, 223.

R Development Core Team. (2010) *R: A language and environment for statistical computing, version 2.11. 1*. R Foundation for Statistical Computing Vienna.

Rijkers, T., Pons, T.L. & Bongers, F. (2000) The effect of tree height and light availability on photosynthetic leaf traits of four neotropical species differing in shade tolerance. *Functional Ecology*, **14**, 77-86.

Taugourdeau, O., Chaubert-Pereira, F., Sabatier, S. & Guédon, Y. (2011) Deciphering the developmental plasticity of walnut saplings in relation to climatic factors and light environment. *Journal of Experimental Botany*; doi: 10.1093/jxb/err115

Thomas, S.C. (2010) Photosynthetic capacity peaks at intermediate size in temperate deciduous trees. *Tree physiology*, **30**, 555.

Thuiller, W., Albert, C., Araújo, M.B., Berry, P.M., Cabeza, M., Guisan, A., Hickler, T., Midgley, G.F., Paterson, J., Schurr, F.M., Sykes, M.T. & Zimmermann, N.E. (2008) Predicting global change impacts on plant species' distributions: Future challenges. *Perspectives in Plant Ecology, Evolution and Systematics*, **9**, 137-152.

Violle, C., Navas, M., Vile, D., Kazakou, E., Fortunel, C., Hummel, I. & Garnier, E. (2007) Let the concept of trait be functional! *Oikos*, **116**, 882-892.

Wagner, G.P., Pavlicev, M. & Cheverud, J.M. (2007) The road to modularity. *Nature Reviews Genetics*, **8**, 921–931.

Weisberg, S. & Fox, J. (2010) *An R Companion to Applied Regression*. Sage Publications, Inc.

Westoby, M. & Wright, I.J. (2006) Land-plant ecology on the basis of functional traits. *Trends in Ecology & Evolution*, **21**, 261-268.

Woodruff, D.R., Bond, B.J. & Meinzer, F.C. (2004) Does turgor limit growth in tall trees? *Plant, Cell & Environment*, **27**, 229–236.

Wright, I.J., Reich, P.B., Westoby, M., Ackerly, D.D., Baruch, Z., Bongers, F., Cavender-Bares, J., Chapin, T., Cornelissen, J.H.., Diemer, M. & others. (2004) The worldwide leaf economics spectrum. *Nature*, **428**, 821–827.

Figures

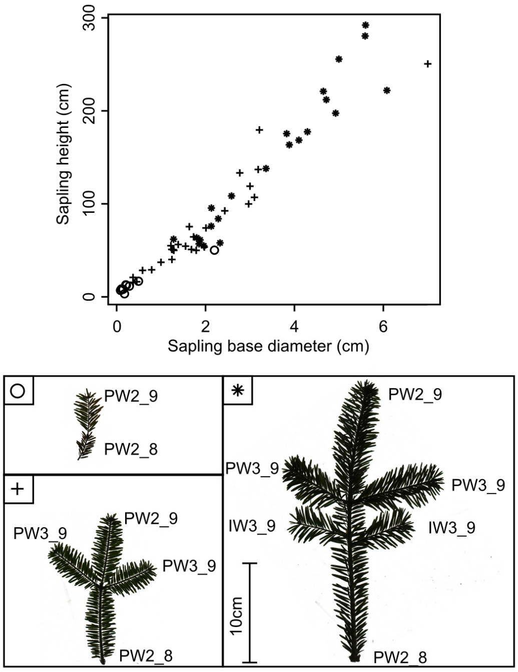

Figure 1. Axes and saplings characteristics (Dataset 3). Point forms correspond to sampled axis complexity: empty circles: no lateral twigs; crosses: pseudo-whorl (PW) twigs; stars: PW and inter-whorl (IW) twigs. One representative sampled axis per axes complexity are represented with the same scale. Every annual shoot are labeled: **PW2_8**: PW axis, ramification order: 2, extended year: 2008; **PW2_9**: PW axis, ramification order: 2, extended year: 2009; **PW3_9**: PW axis, ramification order: 3, extended year: 2009 and **IW3_9**: IW axis, ramification order: 3, extended year: 2009.

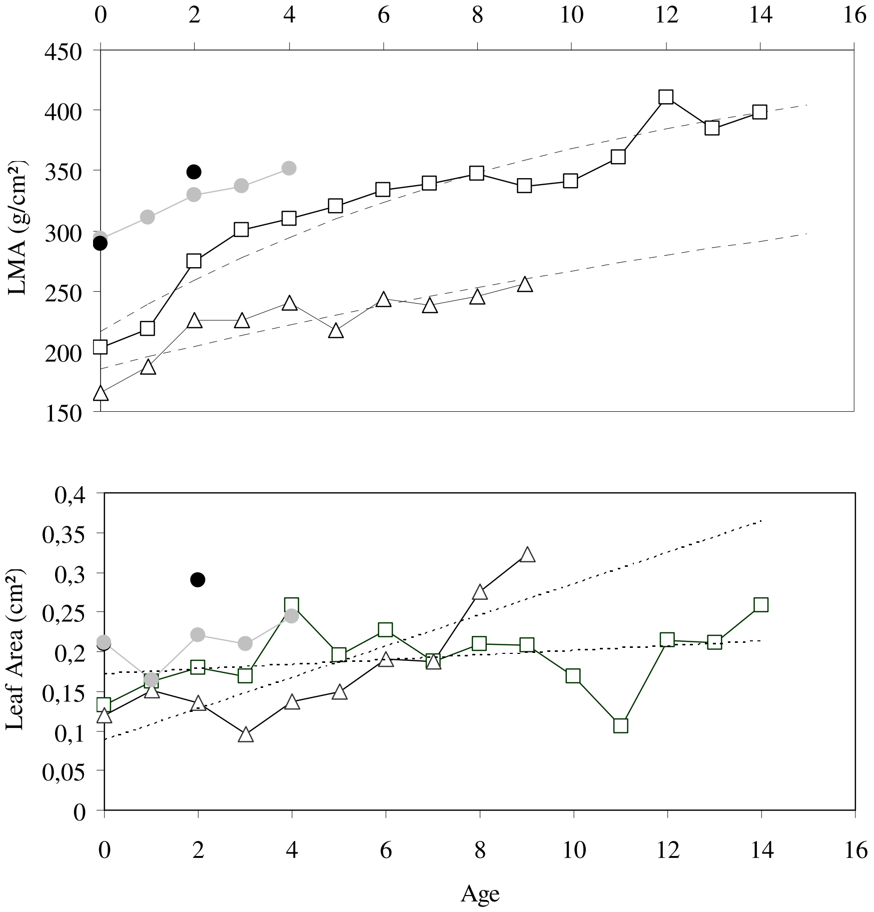

Figure 2: Evolution of LMA (a) and LA (b) for needles with increasing ages (0: current year needle). Grey circles are LMA values of needles 2007 to 2003 from the 2007 twig sampling (Dataset 1). Black circles are traits values of the 2007 needles sampled in 2007 and in 2009 (Table 1). White symbols were LMA observed for two characteristics twigs (Squares: Dtop=1m, Dext=0.5m, elevation=1300m; Triangles: Dtop=5m, Dext=2m, elevation=1300m), and the corresponding asymptotic equation (dashed) for LMA and linear regressions for LA.

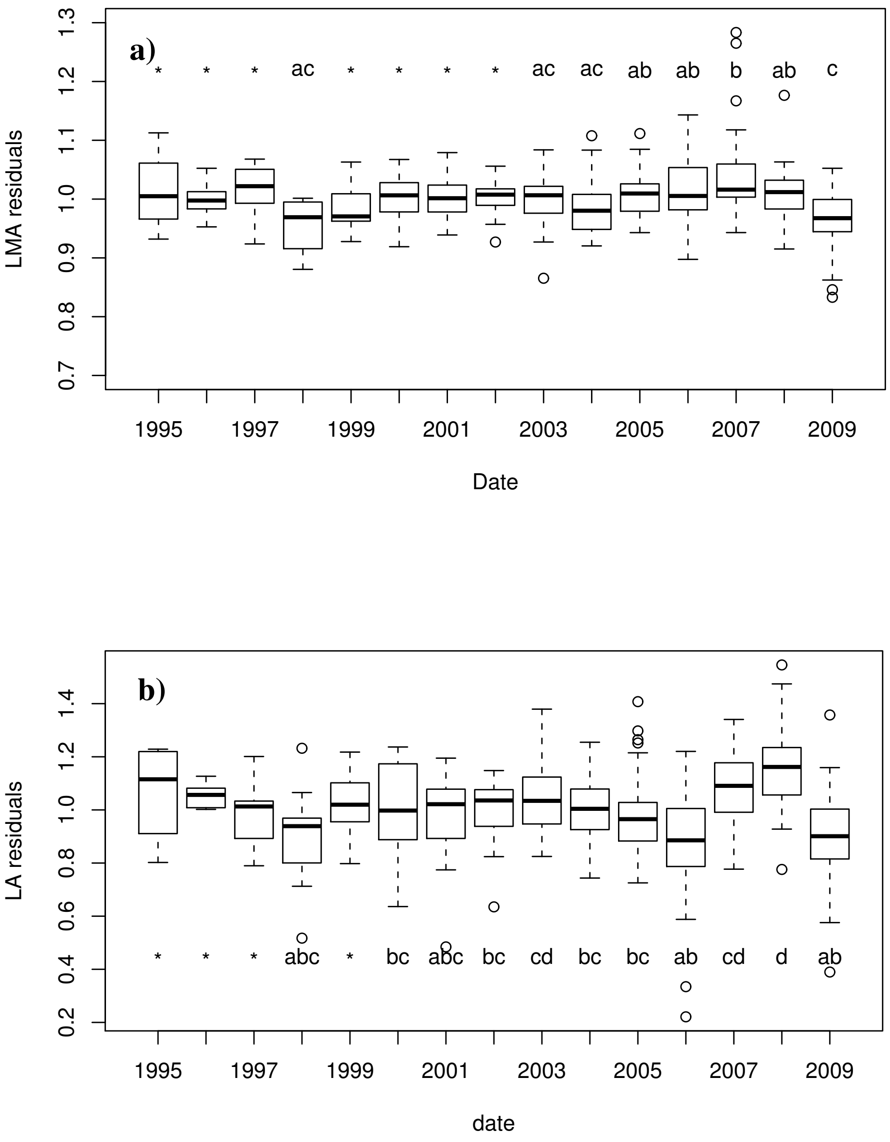

Figure 3: Impact of the year of needle production on LMA (a) and LA (b) after removing aging effect respectively using asymptotic and linear models. Different letters showed significant differences between dates, Stars indicates that means are not different from the others (Up: * = abc; Bottom: * = abcd).

Tables

	2007	2009	% change
Nb needle / cm	23.7 ± 6.0	20.4 ± 5.4	-13.9 % ^{NS}
LA (cm²)	0.21 ± 0.07	0.29 ± 0.06	+35.5 % ***
LM (10^{-3}g)	6.2 ± 2.3	10.3 ± 2.6	+66.1 % ***
LMA (g/m²)	288.6 ± 34.6	348.2 ± 39.0	+20.6 % ***

Table 1: Impact of needle aging of two years on several traits of 2007 needles.

	LMA (g/cm²)		LA (10^{-3} cm²)	
All needles (N=354)	**Estimate [95% IC]** (linear mixed model)	**Proportion of deviance explained** (%) (linear model)	**Estimate [95% IC]** (linear mixed model)	**Proportion of deviance explained** (%) (linear model)
Intercept	128.2 [-35 ; 299]		-45.7 [-357 ; 272]	
Dtop	-9.8 [-27.4 ; -8.5]	17.0	-8.8 [-11.6 ; -5.9]	2.6
Dext	-19.1[-27.4; -10.3]	0.1	7.2[-14.9 ; 26.2]	0.0
Elevation	0.1 [-0.1; 0.3]	1.5	0.1 [-0.2 ; 0.4]	13.6
Needle age	11.3 [10.5 ; 12.1]	53.1	7.5 [5.2 ; 9.5]	10.5
Tree dbh	2.3 [-2.2 ; 6.6]	1.4	6.9 [-1.9 ; 14.7]	0.0
Residuals		26.9		73.3

Table 2: Estimates of the linear mixed models and proportion of the deviance explained by linear models fitted to LMA and LA data of adult trees and ontogenic, architectural and environmental variables, considering all needles' years. LA is provided in 10^{-3} cm² in order to simplify estimates writing

Variables	a	b	c
Elevation	-0.04 ^{NS}	0.01 ^{NS}	$3.6.10^{-4}$ **
Distance to tree top (Dtop)	-2.96 ^{NS}	-5.42 **	-0.01 **
Horizontal distance to crown limit (Dext)	5.23 ^{NS}	-2.94 ^{NS}	-0.057 *

Table 3: Estimates of the generalized linear models between each asymptotic equation parameters and environmental variables.

	LMA (g/cm²)		LA (10^{-3} cm²)	
2008-2009 needles (N=390)	**Estimate [95% IC]** (linear mixed model)	**Proportion of deviance explained** (%) (linear model)	**Estimate [95% IC]** (linear mixed model)	**Proportion of deviance explained** (%) (linear model)
Intercept	90.6 [-45 ; 224]		**-143.9 [-294 ; -2.8]**	
Dtop	**-8.2 [-9.4 ; -7.0]**	34.4	**-5.4 [-8.0 ; -3.0]**	3.4
Dext	**-25.5 [-36.1 ; -15.3]**	2.0	-20.7 [-43.8 ; 0.8]	0.0
Elevation	0.1 [-0.0 ; 0.2]	8.4	**0.2 [0.1 ; 0.3]**	13.7
Needle age	**35.1 [29.3 ; 41.4]**	18.8	**65.4 [52.2 ; 78.8]**	25.4
Tree dbh	1.9 [-1.7 ; 5.4]	1.2	3.4 [-0.5; 7.2]	1.6
Residuals		35.2		55.9

Table 4: Estimates of the linear mixed models and proportion of the deviance explained by linear models fitted to LMA and LA data of adult trees and ontogenic, architectural and environmental variables, considering only 2008 and 2009 needles. LA is provided in 10^{-3} cm² in order to simplify estimates writing. The significant effects at 5% of the mixed model are bolded.

		LMA (g/cm^2)		LA (10^{-3} cm^2)	
Scale	**Variable**	**Estimate [95% IC]** (mixed model)	**Proportion of deviance explained** (%) (fixed model)	**Estimate [95% IC]** (mixed model)	**Proportion of deviance explained** (%) (fixed model)
	Intercept	**158.1 [123.3; 191.1]**		**129.1 [19.6; 237.0]**	
Env.	Elevation (m)	**-0.05 [-0.07; -0.02]**	2.7	-0.01 [-0.9; 0.07]	0.01
	Light environment (%)	**0.6 [0.5; 0.8]**	9.6	0.03 [-0.6; 0.6]	0.001
Ind.	Tree age (y)	0.1 [-0.2; 0.3]	0.04	0.1 [-0. 8; 1.0]	0.01
	Tree height (m)	**-10.8 [-20.7; -2.0]**	1.7	19.0 [-15.4; 44.9]	0.08
	Tree base diameter (cm)	**18.8 [14.5; 23.5]**	15.7	**23.7 [10.5; 39.3]**	6.4
Axis	Ramification Order	**-7.9 [-11.0; -4.3]**	1.8	8.6 [-0.8; 18.3]	0.6
	Type (PW/IW)	**-10.3 [-13.9; -6.5]**	2.9	**-45.4 [-54.7; -33.4]**	10.0
A.S.	Needle Age (0/1)	**34.7 [31.1; 38.5]**	31.5	**33.0 [22.5; 43.9]**	5.6
	Residuals		34.2		77.2

Table 5: Estimates of the linear mixed models and proportion of the deviance explained by linear models fitted to LMA and LA data of juvenile trees and ontogenic, architectural and environmental variables for 2008 and 2009 needles. LA is provided in 10^{-3} cm^2 in order to simplify estimates writing. A.S. means Annual Shoots. The significant effects at 5% of the mixed model are bolded.

Supplementary materials

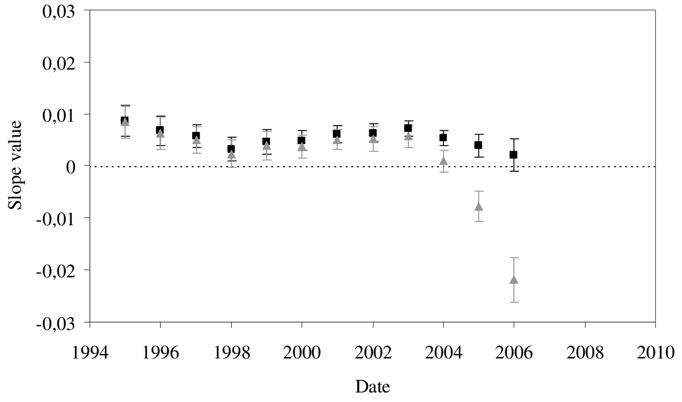

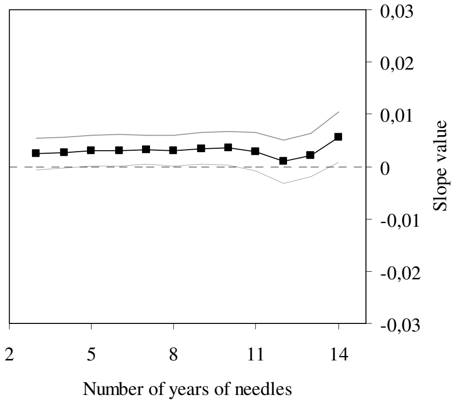

Figure S1a (Left): Evolution of the slope value of the linear relationship between needle aging and area (cm²/needle) according to the year of the older needle of the twig. Slopes were averaged for all the trees by taking into account 2009 needles (Black squares) or not (grey triangles).

Figure S1b (Right): Effect of the number of needles years used to assess aging effect on LA (mean value in black, confidence interval in grey). Values were significantly different from zero for 5 to 10 years and 14 years ($p<0.05$)

Annexe 7

Modélisation du fonctionnement des sapins du Mont Ventoux

Davi H, Cailleret M

INRA URFM, 84914 Avignon

CASTANEA est un modèle croissance forestière qui simule l'impact des conditions environnementales sur la plupart des fonctions de l'arbre : la photosynthèse à partir de l'interception lumineuse, la respiration, et l'allocation du carbone, ainsi que les différents flux hydriques (interception des pluies, transpiration, évaporation du sol…). Il représente la parcelle sous la forme d'un arbre moyen. La canopée est divisée en plusieurs couches d'indice foliaire (LAI) afin de prendre en compte l'impact des variations lumineuses et de l'évolution des propriétés biochimiques des feuilles au sein de la canopée. L'arbre moyen est divisée en cinq compartiments : les racines fines, les grosses racines, le tronc, les branches et les réserves carbonés. CASTANEA a été développé par l'Université de Paris-Sud par le laboratoire Ecologie Systématique et Evolution (Dufrêne *et al.* 2005 ; Davi *et al.* 2005), et a été sans cesse amélioré depuis (Delpierre 2009).

Dans le cadre des travaux effectués durant cette thèse, CASTANEA a été adapté au sapin pectiné du Mont Ventoux à partir de la version existante sur l'Epicéa (Delpierre 2009), et y en intégrant les différents paramètres écophysiologiques (photosynthèse, renouvellement des aiguilles…), dendrométriques et édaphiques mesurés sur nos sites (cf Chapitre 3 et Tab 1).

Le modèle a tout d'abord été utilisé pour analyser le potentiel de production avec l'altitude selon une gamme de réserves utiles (30, 50, 100, 200 mm) à partir du climat passé (1968-2010) et présent (2000-2010). Comme nous l'avons observé en analysant les données de croissance sur un gradient altitudinal (Annexe 1), le modèle reproduit un optimum aux altitudes intermédiaires pour une faible réserve utile (50 mm ; Fig 1). Cependant, cet optimum se décale à basse altitude dès 100 mm de réserve utile. D'autre part, le modèle prédit le déplacement de cet optimum vers les hautes altitudes lorsque la période d'intérêt est 2000-2010 (Fig 1), ce qui conforte les résultats obtenus dans l'Annexe 1.

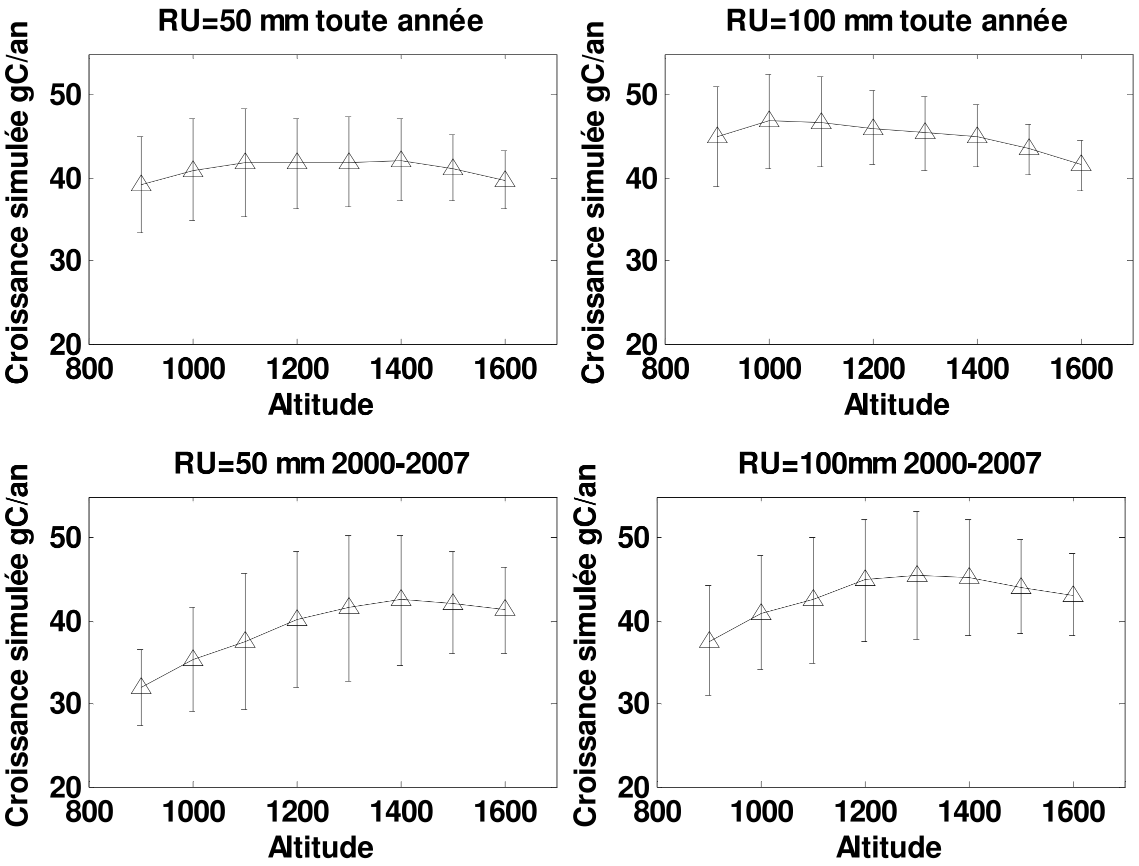

Fig 1 : Accroissement simulé de la biomasse (gC/an) de sapins au Mont Ventoux en fonction du climat (haut : climat 1964-2007 ; bas : climat 2000-2007) et de la réserve utile du sol (RU= 50 ou 100mm).

L'analyse temporelle de l'évolution de l'accroissement de la biomasse vivante simulée est assez bien corrélée avec celle de la surface de cerne mesurée (Fig 2 ; $R^2=0.41$). La meilleure corrélation est obtenue lorsque la réserve utile du sol utilisée pour la simulation est faible (30mm) et lorsque le BAI moyen est calculé à partir des arbres situés sur sol résistif. Les baisses de croissance des années sèches 1974, 1976 et 1989 sont bien simulées, ainsi que la baisse de croissance depuis 2000. Cependant les arrières-effet d'une sécheresse ne sont pas très bien reproduits (par exemple après 1989).

En ciblant des variables importantes comme la dynamique interannuelle de la respiration, de la photosynthèse, du rapport entre les deux, et du LAI, l'analyse temporelle donne des indications sur le processus de dépérissement et de mortalité des sapins (Fig 3). Il semble que le rapport GPP/respiration soit un bon indice ; quand il chute en dessous de 1.1, la surface foliaire ne revient pas à l'équilibre (moindre production d'aiguilles) et le processus de résilience paraît compromis. Le modèle prédit un décrochage du LAI (Fig 3) à faible altitude (900 m) et faible Réserve Utile (30 mm) qui est surtout du à une explosion de la respiration en 2003 à cause des fortes températures, couplée à une photosynthèse faible à cause des sécheresses successives.

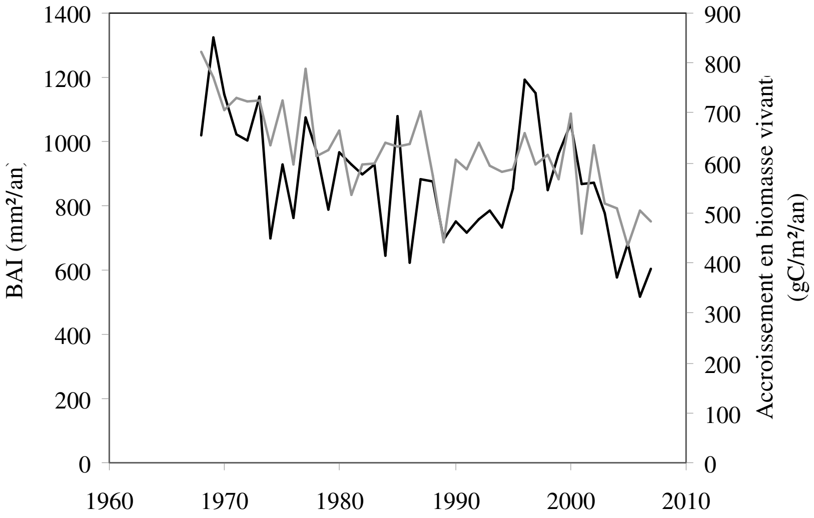

Fig 2: Evolution de l'accroissement radial moyen (BAI ; mm²/an) observé pour les arbres poussant sur un sol à forte résistivité électrique en surface (ER3 et ER4) (noir) au Mont Ventoux, et de l'accroissement en biomasse vivante (gC/m²/an) simulé à 1200m d'altitude, pour un sol de 30mm de Réserve Utile (gris).

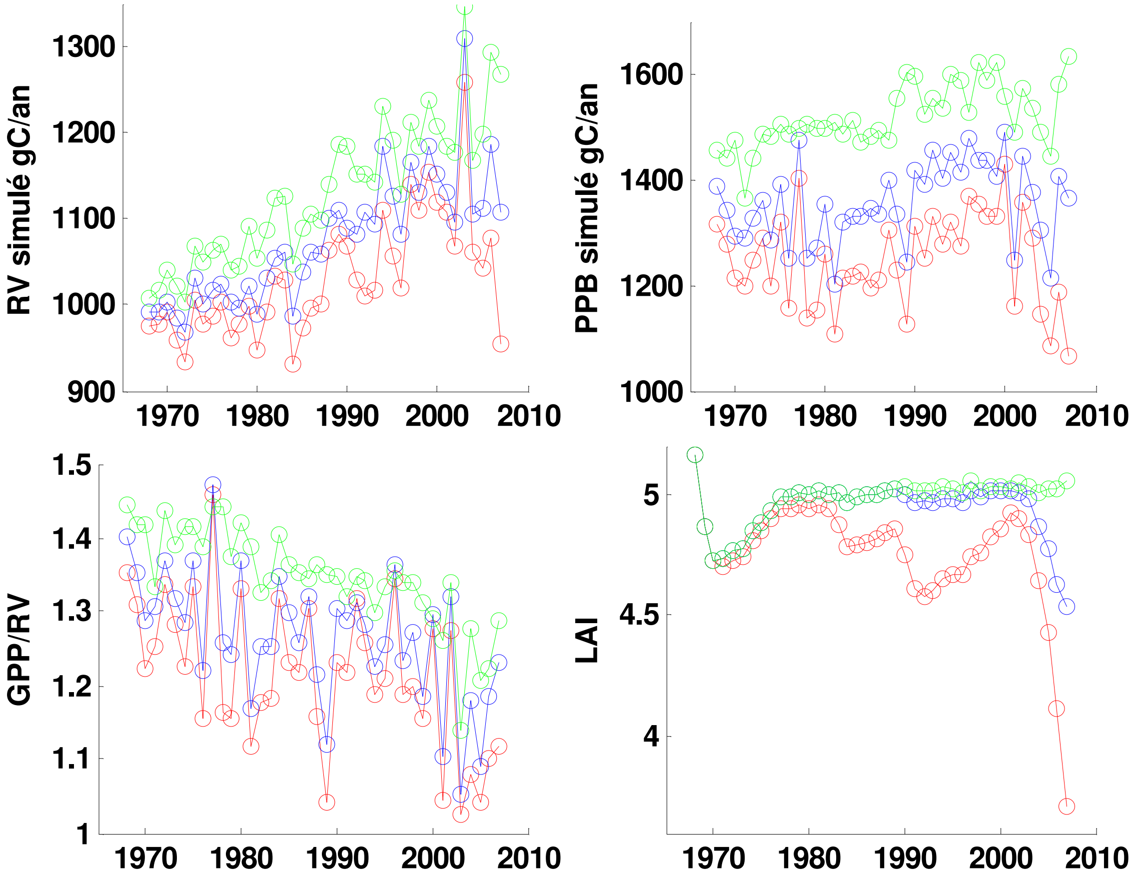

Fig 3: Simulation de l'évolution de la respiration (RV), de la photosynthèse (PPB ou GPP), du rapport entre photosynthèse et respiration, et du LAI pour 3 sols à réserve utile différente situés à 900m d'altitude (vert : RU=200mm ; bleu : RU=50mm ; rouge RU=30mm).

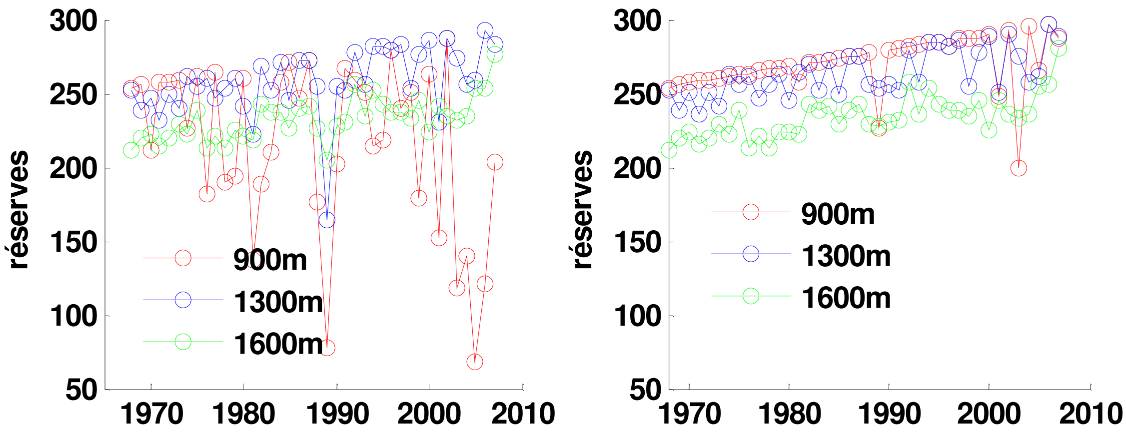

Fig 4 : Dynamique des réserves carbonés à trois altitudes pour une ré »serve utile de 50mm (à gauche) et de 100 mm (à droite).

Le décrochage se traduit aussi par une chute du niveau des réserves dans l'arbre. Le modèle peut a aussi permettre de déterminer la part relative de la réserve utile et celle de la baisse en altitude dans le niveau de stress hydrique perçu par les arbres (indice cumulée chaque année des réductions de photosynthèse due au stress). Une analyse de variance entre ce niveau de stress simulé et l'effet altitude d'une part, et réserve utile d'autre part indique que 10% du stress hydrique est expliqué par l'altitude et 90% par la réserve utile (entre 30 et 200 mm) (Tableau 2). La diminution du gradient de RU utilisé ne change qualitativement pas les résultats (données non montrées).

Tableau 2 : Analyse de variance de l'effet altitude et de la réserve utile sur le niveau de stress hydrique annuel simulé.

'Source'	Sum Sq.	d.f.	'Mean Sq.'	'F'	'Prob>F'
Altitude	74829	7	10690	57.76	0
Réserve utile	2.923e+005	3	97433	526.45	0
'Error'	2.3486e+005	1269	185.07		
'Total'	6.0199e+005	1279			

Ces résultats préliminaires ne prennent pas en compte les effets directs des sécheresses sur l'embolie des vaisseaux du xylème ou sur la chute d'aiguilles directement induite par la sécheresse. De plus, CASTANEA n'est pas réellement adapté à l'analyse du processus de dépérissement puisqu'il fonctionne en arbre moyen. Une version en modèle arbre centré devra aussi être utilisée pour les simulations ultérieures. D'autre part, le fait que les arbres ayant poussé sur des sols superficiellement favorables ont une plus grande vulnérabilité n'est pas reproduit dans ce cas là car la dynamique de croissance racinaire n'est pas finement modélisée. Néanmoins, ces résultats indiquent que même à basse altitude le Sapin pourrait se maintenir sur des conditions édaphiques très favorables.

Tableau 1 : Liste des paramètres de CASTANEA et leur valeur sur le Ventoux (site Dvx5)**.**

Symbole	Description	Unités	Valeur	Référence
Rayonnement et structure du couvert				
Long	Longitude	Degré	44.18	
Lat	Latitude	Degré	-5.28	
ρ_{PAR}	Réflectance foliaire pour le PAR	sans dimension	0.09	Ibrom (2006)
τ_{PAR}	Transmittance foliaire pour le PAR	sans dimension	0.045	
ρ_{glo}	Réflectance foliaire pour le PIR	sans dimension	0.33	Ibrom (2006)
τ_{glo}	Transmittance foliaire pour le PIR	sans dimension	0.225	
α_L	Angle foliaire moyen	°	40	Falge (1997)
LMA_{sunmax}	Masse surfacique des feuilles de lumière	$g_{dm}\ m^{-2}$	323	Moyenne Ventoux (2007)
k_{LMA}	Coef. d'extinction du LMA dans le couvert	sans dimension	0.07	Epicea Tharandt
L_{max}	Indice foliaire maximum	$m_{leaf}^{2}\ m_{soil}^{-2}$	5.67	Mesures Dvx5
Agreg	Facteur d'agrégation		0.39	Mesures transect en courbe de niveau
Carbone				
Photosynthèse de la feuille et du couvert				
α_{Na}	Dépendance entre le V_{Cmax} et l'azote surfacique	$\mu mol_{CO_2}\ g_N^{-1}s^{-1}$	20	Ventoux 2008
β	Ratio entre V_{Cmax} et V_{Jmax}	sans dimension	3.2	Ventoux 2008
α	Rendement quantique	mol electrons (mol quanta)$^{-1}$	0.3	Ibrom (2006)
θ	Le degré de courbature de la relation entre le taux de transport d'électrons et la lumière	sans dimension	0.7	fixé
g_0	Ordonnée à l'origine de la relation de Ball et al. (1987)	$mol_{H_2O}\ m^{-2}\ s^{-1}$	0.001	fixé
g_{1max}	Pente de la relation de Ball et al. (1987) (val. max)	sans dimension	12	Ventoux 2008
Respiration d'entretien				
$Q_{10\ stem}$	Effet température pour les troncs	sans dimension	.13	Ceschia thesis
$Q_{10\ branches}$	Effet température pour les branches	sans dimension	.25	Ceschia thesis
$Q_{10\ coarse\ roots}$	Effet température pour les grosses racines	sans dimension	.9	Burton 2002
$Q_{10\ fine\ roots}$	Effet température pour les fines racines	sans dimension	.44	Stockfors 1997
$Q_{10\ leaves}$	Effet température pour les feuilles	sans dimension	.44	Stockfors 1997
T_{MR}	Température de base pour la respiration d'entretien	°C	5	Damesin et al. (2002)
$N_{mleaves}$	Azote foliaire	$mg_N\ g_{dm}$	10.5	Ventoux 2007
$N_{mbranches}$	Azote dans les branches	$mg_N\ g_{dm}$	1.38	Tharandt Epicéa
$N_{mtrunks}$	Azote dans le tronc	$mg_N\ g_{dm}$	0.94	Tharandt Epicéa
$N_{mcoarseroots}$	Azote dans les grosses racines	$mg_N\ g_{dm}$	0.94	fixé
$N_{mfineroots}$	Azote dans les fines racines	$mg_N\ g_{dm}$	7.00	Mund 1996

MRN	Dépendance de la respiration à l'azote	$mol_{CO2}\ g_N^{-1}\ h^{-1}$	$.5\ 10^{-4}$	Ryan (1991)
ros	Densité du bois	Kg/m3	03	Decoux et al

Symbole	Description	Unités	Valeur	Référence
Phénologie: débourrement, croissance et chute des feuilles				
N_{Start1}	Date de début de la somme des températures Pour le débourrement	Jour	40	Ventoux (2007-2010)
T_2	Température de base pour le débourrement	°C	1	Ventoux (2007-2010)
F_{critBB}	Seuil critique entraînant le débourrement	°C	500	Ventoux (2007-2010)
T_3	base temperature for leaf growth	°C	0	fixé
LA_{max}	Surface foliaire maximale	m^2	2.1^e-4	Ventoux (2007)
Allocation				
$TO_{fineroots}$	Taux de renouvellement des racines fines	$jour^{-1}$	1/365	Bauhus & Bartsch (1996)
P_{branch}	Proportion de branches	sans dimension	0.15	Tharandt Epicéa
$P_{alive\ branch}$	Proportion de cellules vivantes dans les branches	sans dimension	0.70	
$P_{alive\ trunk}$	Proportion de cellules vivantes dans les troncs	sans dimension	0.42	Ventoux
Respiration de croissance				
CR_{leaves}	Coût de construction des feuilles	$gC\ gC^{-1}\ _{organe}$	1.21	calcul from Niinemets 1997
CR_{wood}	Coût de construction du bois	$gC\ gC^{-1}\ _{organe}$	1.18	Stockfors & Linder 1998
$CR_{fine\ roots}$	Coût de construction des fines racines	$gC\ gC^{-1}\ _{organe}$	1.28	Agren and Axelsson (1980)

Eau

Précipitation et interception				
RA_{bark}	Capacité de rétention d'eau du bois	$mm_{H_2O}\ m^{-2}$	0.37	estimé
RA_{leaf}	Capacité de rétention d'eau des feuilles	$mm_{H_2O}\ m^{-2}$	0.13	estimé
C_{ia}	Coef. d'interception brute (pente)	sans dimension	0.85	Calculé
C_{ib}	Coef. d'interception brute (ordonnée à l'origine)	$m^2\ m^{-2}$	1.5	Calculé epicéa